ANL-HEP-TR-92-50

HIGH ENERGY PHYSICS DIVISION SEMIANNUAL REPORT OF RESEARCH ACTIVITIES

January 1, 1992 – June 30, 1992

ARGONNE NATIONAL LABORATORY
Argonne, Illinois
Operated by THE UNIVERSITY OF CHICAGO for the
U.S. DEPARTMENT OF ENERGY
under Contract W-31-109-Eng-38

Argonne National Laboratory, with facilities in the states of Illinois and Idaho, is owned by the United States government, and operated by The University of Chicago under the provisions of a contract with the Department of Energy.

DISCLAIMER

This report was prepared as an account of work sponsored by an agency of the United States Government. Neither the United States Government nor any agency thereof, nor any of their employees, makes any warranty, express or implied, or assumes any legal liability or responsibility for the accuracy, completeness, or usefulness of any information, apparatus, product, or process disclosed, or represents that its use would not infringe privately owned rights. Reference herein to any specific commercial product, process, or service by trade name, trademark, manufacturer, or otherwise, does not necessarily constitute or imply its endorsement, recommendation, or favoring by the United States Government or any agency thereof. The views and opinions of authors expressed herein do not necessarily state or reflect those of the United States Government or any agency thereof.

Reproduced from the best available copy.

Available to DOE and DOE contractors from the
Office of Scientific and Technical Information
P.O. Box 62
Oak Ridge, TN 37831
Prices available from (615) 576-8401

Available to the public from the
National Technical Information Service
U.S. Department of Commerce
5285 Port Royal Road
Springfield, VA 22161

ANL-HEP-TR-92-50

Argonne National Laboratory
9700 South Cass Avenue
Argonne, Illinois 60439

HIGH ENERGY PHYSICS DIVISION SEMIANNUAL REPORT OF RESEARCH ACTIVITIES

January 1, 1992 - June 30, 1992

Prepared from information gathered and edited by
the Committee for Publications and Information:

Members: P. Schoessow
P. Moonier
R. Talaga
R. Wagner

November 1992

Table of Contents

		Page
	Abstract	1
I.	*Experimental Program*	2
	A. Physics Results	2
	B. Experiments Taking Data	25
	C. Experiments in Preparation Phase	26
II.	*Theoretical Program*	38
III.	*Experimental Facilities Research*	50
	A Mechanical Support	50
	B. Electronic Support	60
	C. Computer Support	64
IV.	*Accelerator Research and Development*	65
	A. Advanced Accelerator Test Facility (AATF) Program	65
	B. Progress on the Argonne Wakefield Accelerator (AWA)	65
	C. Accelerator Physics	71
V.	*SSC Detector Research and Development*	73
	A. Overview of ANL SSC Related R&D Programs	73
	B. Compensating Scintillator Plate Calorimeter R&D	74
	C. SDC Data Systems R&D	83
VI.	*Publications*	86
VII.	*Colloquia and Conference Talks*	93
VIII.	*High Energy Physics Community Activities*	97
IX.	*High Energy Physics Research Personnel*	99

Abstract

This report describes the research conducted in the High Energy Physics Division of Argonne National Laboratory during the period of January 1, 1992 - June 30, 1992. Topics covered here include experimental and theoretical particle physics, advanced accelerator physics, detector development, and experimental facilities research. Lists of division publications and colloquia are included.

I. EXPERIMENTAL PROGRAM

A. Physics Results

1. Collider Detector at Fermilab

The CDF experiment recorded the first $\bar{p}p$ collisions of 1992 around 6:30 a.m. on May 12. Since that date, an integrated luminosity of several 10's of nb^{-1} has been written to tape, primarily for debugging purposes, including on the order of 100 $W \rightarrow$ lepton events. Although serious hardware problems need to be addressed, the basic detector, including calorimetry, central tracking, and major detector upgrades (the new silicon vertex detector, muon chambers, and central preshower detector) appear to perform well.

Analysis has continued with the 1988-1989 data, including new results on b-physics. We comment here on new cross section measurements using the J/ψ and ψ' data, and searches for the B-baryon. The inclusive differential cross sections for production of J/ψ and ψ' have been measured, and are shown in Figs. 1 and 2. The event samples consist of 845 J/ψ's and 33 ψ', with $|\eta| < 0.5$ and $p_T > 6$ GeV/c. Theoretically, the main source of ψ''s at high p_T is expected to be decays of B-hadrons, while the sources of J/ψ's include B decays, χ decays, and direct production. For the B-decays, we can predict the shapes of the J/ψ and ψ' p_T spectra, by convolving the b-quark p_T spectrum with the $b \rightarrow B$ fragmentation distribution (measured in e^+e^- experiments) and the $B \rightarrow J/\psi, \psi'$ decay distribution (measured at CLEO and ARGUS). If we use the next-to-leading order predictions for the b-quark p_T spectrum, as derived by Nason, Ellis, and Dawson, we obtain the dashed curve in Fig. 1 and the solid curve in Fig. 2, for the J/ψ and ψ' p_T spectra, respectively.

In order to interpret the J/ψ spectrum of Fig. 1, we need to take into account the non-B-decay sources of J/ψ production. We accomplish this using the following two constraints. First, the shape of the p_T spectrum associated with the $\chi \rightarrow J/\psi$ decays and the direct J/ψ production from $c\bar{c}$ pairs can be estimated by NLO theory; we use the calculations published by Glover, Martin, and Stirling. Second, the integrated cross section for $\chi \rightarrow J/\psi + \gamma$ has been measured using the same CDF data set; this measurement, taking into account production of χ's via B-decays, indicates that $65 \pm 17\%$ of J/ψ's in our kinematic range ($p_T > 6$, $|\eta| < 0.5$) come from B-decays, and 35% come from χ decay and direct production. The dashed curve in Fig. 1 is the B-decay contribution, normalized to make up 65% of the observed yield, and the solid curve is the sum of B-decay and non-B-decay sources, normalized to the total observed yield. The

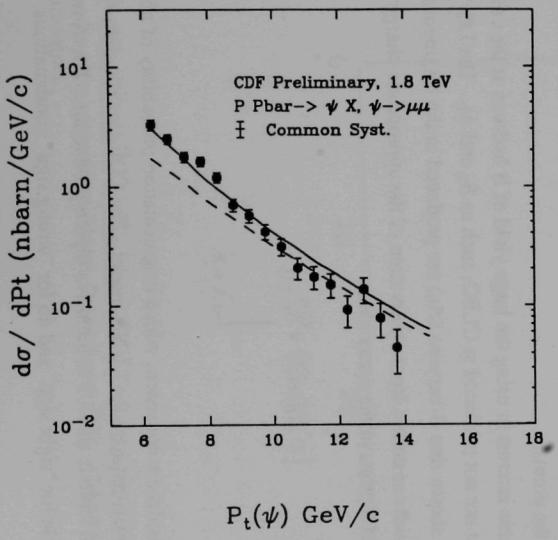

Fig. 1. Inclusive differential cross section for production of J/ψ. The dashed curve is derived from the Nason, Ellis and Dawson prediction for b-quarks, normalized to 65% of the observed yield. The solid line is the sum of B-decay and non-B-decay sources, normalized to 100%.

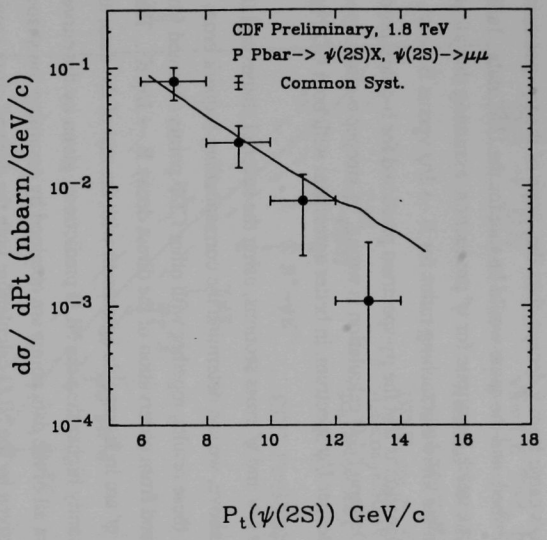

Fig. 2. Inclusive differential cross section for production of ψ'. The curve is derived from the Nason, Ellis and Dawson prediction for b-quarks.

data show a significantly softer p_T spectrum than the model. The same effect was observed at 630 GeV by the UA1 experiment. There are several possible interpretations of this discrepancy. One is that the mix of B-decay and non-B-decay contributions is incorrect. If all of the J/ψ's came from χ decays, then the shape of the p_T spectrum in Fig. 1 would be well described, and the same would be true for the UA1 data. In this scenario we would expect a much lower rate for ψ' production, assuming that all ψ's come from B's, and given the known branching ratios for $B \rightarrow J/\psi$ versus $B \rightarrow \psi'$. A second, more likely, explanation is that the p_T-spectrum predicted for b-quark production in the Nason, Ellis, and Dawson NLO calculation is wrong. A steeper b-quark spectrum would naturally yield a steeper J/ψ spectrum, in better agreement with both CDF and UA1 data.

By integrating the J/ψ and ψ' cross sections, using the spectral shapes and the B-decay fraction described above, we can determine the corresponding b-quark cross sections. Figure 3 shows these results, together with other CDF points obtained from inclusive electron yields and from observation of the direct decay $B \rightarrow J/\psi K^-$. The three points shown for J/ψ and ψ' are in reasonable agreement with the rest of the data, and all cross sections are significantly higher than the NLO predictions, given by the curves in Fig. 3. We emphasize that all of the data points are obtained by assuming the shape of the b-quark p_T spectrum given by the NLO calculation; both the derived cross section in Fig. 3, and the p_T spectra for J/ψ and ψ' production discussed above, suggest that the actual b-quark spectrum may be softer than this calculation, in turn introducing (small) correlated errors in all of the points.

There is considerable interest in using the large yield of B hadrons at the collider to study species of B's that are not produced at CLEO, such as B_s and Λ_b. The LEP experiments have already shown that B-baryons (Λ_b) are produced in the fragmentation of b-quarks. The main evidence comes from observation of the appropriate charge correlation between Λs and leptons in the decay chain

$$\Lambda_b \rightarrow l^- \nu \Lambda_c$$
$$\Big\downarrow \rightarrow \Lambda + X.$$

The OPAL and ALEPH results are consistent with a fragmentation probability of about 10% for b-quark $\rightarrow \Lambda_b$, consistent with the LUND model. The CDF electron data show a similar correlation between leptons and Λ's in inclusive lepton production. The Λ mass spectrum is shown in Fig. 4a for "right sign" and 4b for "wrong sign" combinations.

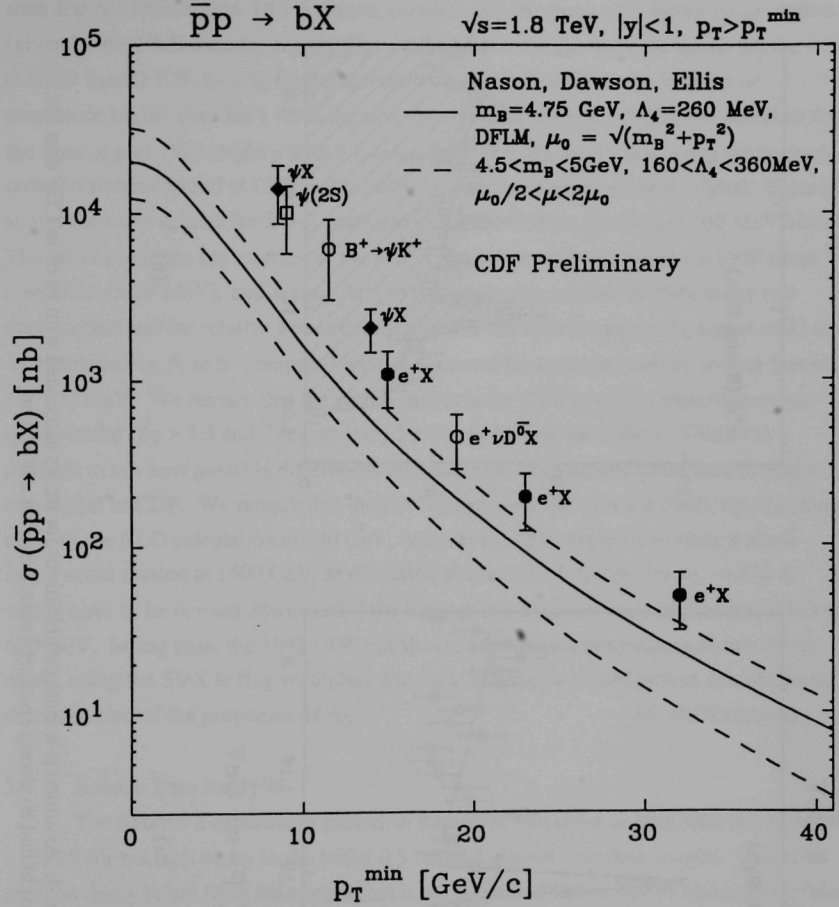

Fig. 3. Cross section for b production with $p_T > p_T$ min. as a function of p_T min. The curves show the range from Nason, Dawson and Ellis. The points are various CDF measurements.

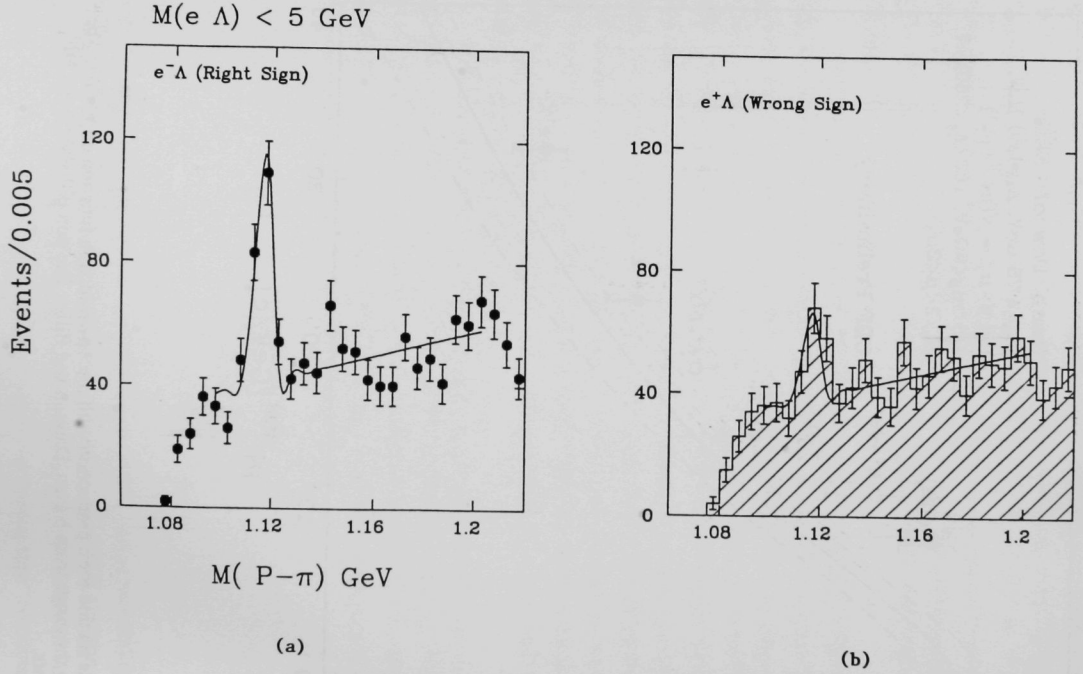

Fig. 4. Assumed p-π mass combinations for tracks associated with an $e^{\pm}$ in CDF data for a) right and b) wrong ep charge correlation for a b-baryon.

There is a clear excess of right sign Λ-e^- events, and we may conclude that Λ baryons are produced at CDF.

Recently the UA1 experiment published evidence for production of Λ_b in the final state $J/\psi\ \Lambda$. Their signal, 16 ± 5 events, coupled with the assumed b-quark cross section (given by the NLO calculation), implies a BR of 1.8% for $\Lambda_b \rightarrow J/\psi\ \Lambda$, assuming the (LUND based) 10% $b \rightarrow \Lambda_b$ fragmentation probability. This is about an order of magnitude higher than BR's for B mesons to decay into J/ψ K,K*. CDF has searched for the same signal. We obtain a 90% c.l. upper limit of 0.4% on this BR, using the b-quark cross section measured at CDF, calibrated with the observed $B \rightarrow J/\psi\ K^-$ signal. Figure 5 shows the mass spectra for J/ψ-Λ combinations from CDF in 20, 40, and 100 MeV bins. The arrows indicate the location of the UA1 signal. For example, given the CDF mass resolution ($\pm$ 20 MeV), and scaling the UA1 signal by the number of J/ψ's in the two experiments and the relative detection efficiencies, we would expect a Λ_b signal of 73 ± 41 events in Fig. 5, to be compared with an observed background level of around 5 events per 100 MeV. We remark that the p_T thresholds in the CDF and UA1 experiments are quite similar ($p_T > 5.5$ and 7 respectively for the Λ_b in UA1 and CDF). Thus, it is difficult to see how possible differences in production mechanisms could lead to absence of a signal in CDF. We remark that the UA1 experiment assumes a b-quark cross section close to the NLO calculation at 630 GeV, whereas the CDF experiment finds a much larger cross section at 1800 GeV, as discussed above. The UA1 BR for $\Lambda_b \rightarrow J/\psi\ \Lambda$ would have to be revised downward if the b-quark cross section were higher than NLO at 630 GeV. In any case, the 1992 CDF run should allow direct observation of this decay mode, using the SVX to flag secondary J/ψ decays, and this should permit unambiguous determination of the properties of Λ_b. (A. B. Wicklund)

2. Soudan Data Analysis

The Soudan 2 experiment passed an important milestone in May with the completion of a search for nucleon decay in the initial 0.5 fiducial kiloton year data sample. This first nucleon decay result from the experiment is the subject of University of Minnesota graduate student Dave Schmid's Ph.D. thesis. The analysis takes advantage of the excellent particle identification properties of Soudan 2 to search for decay modes involving a K^+ meson and a lepton: $p \rightarrow \nu K^+$, $n \rightarrow e^- K^+$, and $n \rightarrow \mu^- K^+$. The fine-grained tracking and dE/dx capabilities of the detector allow these modes to be identified with very low background from other processes. Candidate events are selected on the basis of overall topology, K^+ range and dE/dx, and μ^+ range and decay. Algorithms for the identification of e^- showers and μ^- tracks were

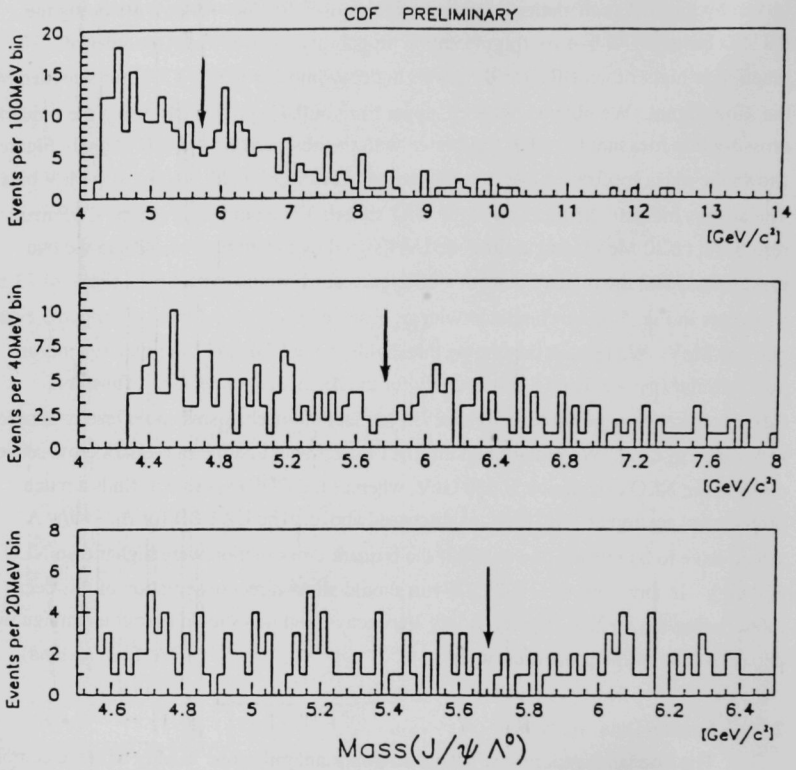

Fig. 5. Mass spectra for J/ψ-Λ combinations in 20, 40 and 100 MeV bins. The arrow indicates the position of the UA1 signal.

developed using Monte Carlo simulations and data from the ISIS test beam calibration of a Soudan 2 module.

Four different event recognition methods were developed, one using cuts on measured quantities, two using likelihood methods, and a neural network program. Monte Carlo and test beam events were used to optimize each algorithm, and to determine both its efficiency and the background from atmospheric neutrino interactions. The selection criteria for each method were varied to obtain a range of efficiencies and backgrounds: looser requirements gave high efficiency for nucleon decay along with relatively higher predicted backgrounds. Tighter requirements resulted in lower efficiency and lower backgrounds. Figure 6 shows the correlation between the lifetime over branching ratio limit and the expected background for the $p \rightarrow \nu K^+$ mode, for the case where no events are identified in the 0.5 fiducial kiloton year data sample. No candidate events were found for any of the three decay modes, yielding the following 90% confidence level lifetime limits and predicted background levels:

Mode	τ/BR (90% CL limit)	Background
$p \rightarrow \nu K+$	4.5×10^{30} year	0.10 events
$n \rightarrow e^- K^+$	7.5×10^{30} year	0.03 events
$n \rightarrow \mu^- K^+$	6.5×10^{30} year	0.04 events

Although more restrictive limits on these modes have already been established by other experiments, the low background levels indicate that Soudan 2 should be able to set competitive limits with its planned exposure of 5 fiducial kiloton years. Alternatively, this tenfold increase in exposure could result in the identification of nucleon decay events which would have been confused with the neutrino background in other experiments. The search for nucleon decay in other modes is under way, and work to improve event identification algorithms for the modes listed above is continuing.

A closely related activity is the study of atmospheric neutrino interaction events in the initial 0.5 fiducial kiloton year Soudan 2 data set. The measurement of the flux ratio of muon neutrinos to electron neutrinos is the topic of Argonne Laboratory graduate student Don Roback's Ph.D. thesis. The anomalously low ν_μ/ν_e ratio reported by water Cerenkov experiments has been interpreted as evidence for neutrino oscillations. Techniques for distinguishing between electron showers and muon tracks in Soudan 2 are already well developed for the nucleon decay search described above, and demonstrate clear advantages over water Cherenkov detectors. Identification of neutrino events in the Soudan 2 data sample is now nearly completed, and the study of systematic corrections and uncertainties which affect

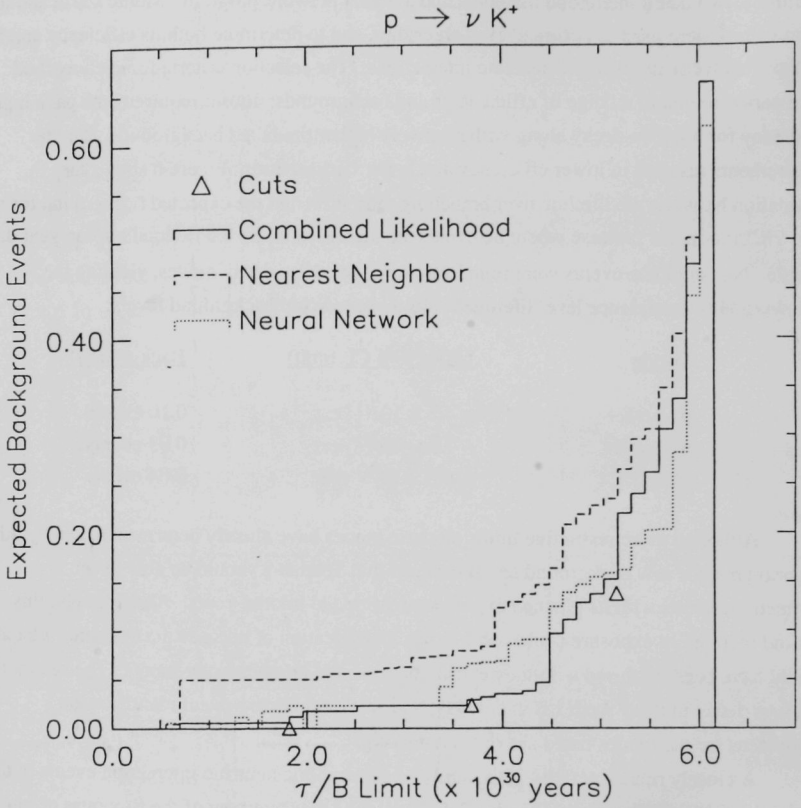

Fig. 6. Correlation between the lifetime-over-branching-ratio 90% confidence level limits and the neutrino background level, for nucleon decay in the mode $p \rightarrow \nu K^+$. Results from four different event identification methods are shown. The lifetime limits correspond to no candidate events in the 0.5 fiducial kiloton year data sample which was analyzed. The results quoted in the text were obtained from the neural network curve.

the ν_μ/ν_e ratio is in progress. Figures 7 and 8 show examples of typical quasi-elastic muon neutrino and electron neutrino scattering events recorded by Soudan 2.

The collaboration presented preliminary results from a Soudan 2 search for very high energy neutrinos at the Workshop on High Energy Neutrino Astrophysics in March. A number of astrophysical models predict that Active Galactic Nuclei (AGN's) contain black-hole power sources capable of producing detectable fluxes of 100 TeV neutrinos. Although the flux from any single AGN would be too small to detect, the integrated flux from all AGN's is predicted to be observable with several more years of Soudan 2 exposure.

Very high energy neutrinos are identified in Soudan 2 by observation of the muons which they produce in the rock surrounding the detector. These very high energy muons are identified by requiring catastrophic interactions along their tracks, with more than 40 GeV measured in the detector. Background from ordinary cosmic ray muons is reduced by selecting horizontal muon tracks, with zenith angles greater than 60^o. Approximately 85% of 100 TeV muons are expected to undergo interactions depositing more than 40 GeV in Soudan 2. In the 1989-1991 Soudan 2 data sample, which contains 2.4 million cosmic ray muon tracks, no very high energy horizontal muon tracks were found, yielding a 90% confidence level flux limit for 100 TeV muons of 10^{-13} $cm^{-2}s^{-1}sr^{-1}$. Lower energy muons from AGN neutrinos are less likely to produce catastrophic interactions in Soudan 2, yielding less restrictive flux limits.

Preliminary Soudan 2 limits on the flux of high energy neutrinos from active galactic nuclei are shown in Fig. 9. Although these limits are close to the curve showing the initially predicted flux level, several new calculations presented at the Workshop indicated that the actual AGN neutrino flux is likely to be about 30 times lower than indicated by the curve in Fig. 9. Soudan 2 should reach this level of sensitivity in two or three years. While more data accumulates, analysis efforts will focus on the calculation of background levels and on the development of more efficient methods for the identification of very high energy muons.

An important milestone was passed with the submission to Physical Review D of the paper describing the results of the search for GUT magnetic monopole tracks in Soudan 2. The previous Semiannual Report contained a detailed description of this work, which was performed almost entirely by Argonne physicists. Argonne physicists also made significant contributions to the paper describing the surface-underground coincidence experiment, performed with the Soudan 1 detector and an above-ground surface array, which appeared in Physical Review D in March. The Proceedings of the Workshop on Long Baseline Neutrino Oscillations, which was held at Fermilab in November 1991, was edited by Argonne physicist Maury Goodman (who also chaired the Workshop organizing committee). These proceedings were published in June, and contained three papers by Argonne authors. Argonne physicists also wrote a number of internal PDK notes during the first half of 1992. (D. Ayres)

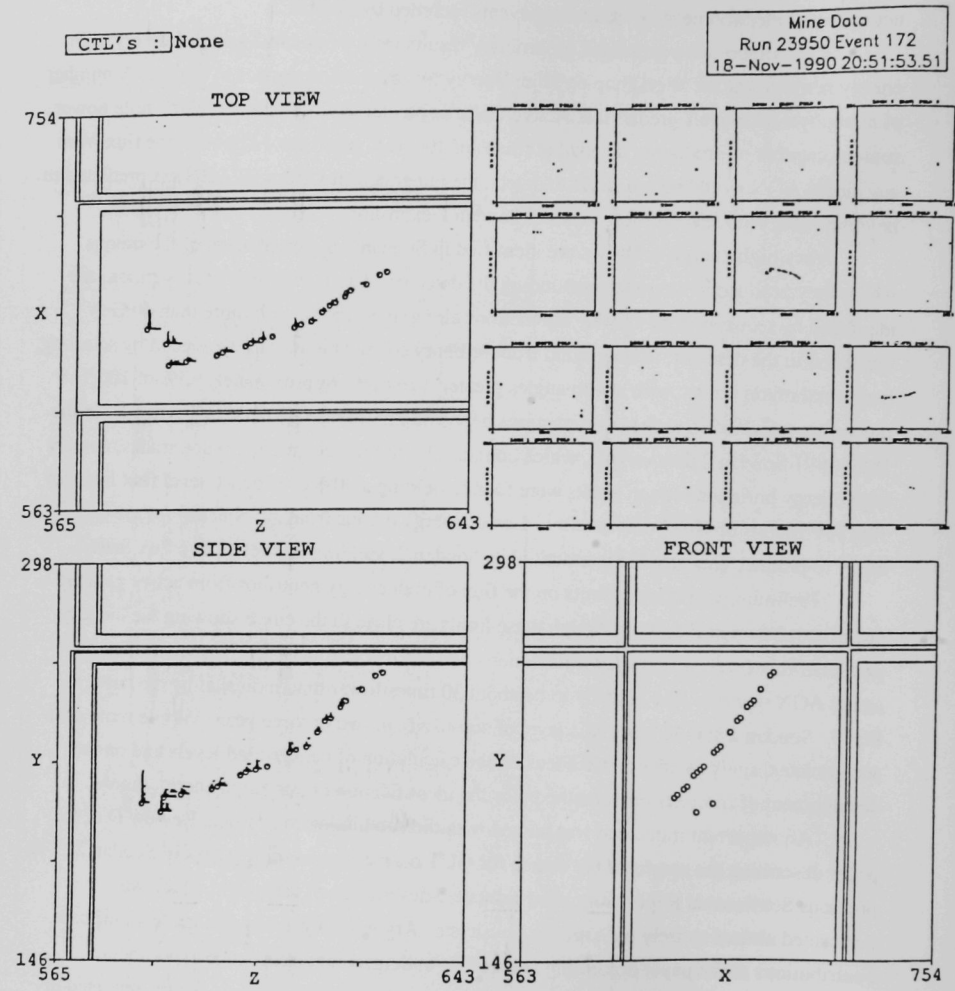

Fig. 7. Reconstruction of a muon neutrino quasi-elastic scattering event, $\bar{\nu}_\mu p \rightarrow \mu^+ n$, recorded by Soudan 2. The raw data are shown in the upper right quadrant. The closeup views show three orthogonal projections of the event; distance scales are in centimeters. The long smooth track is a positive muon, which stops and decays at the lower left in all three views. The decay positron is responsible for the two hits at the end of the track. Negative stopping muons are usually captured by iron nuclei in Soudan 2, and do not decay visibly. The muon in this event has a range of 90 cm, corresponding to a momentum of 350 MeV/c.

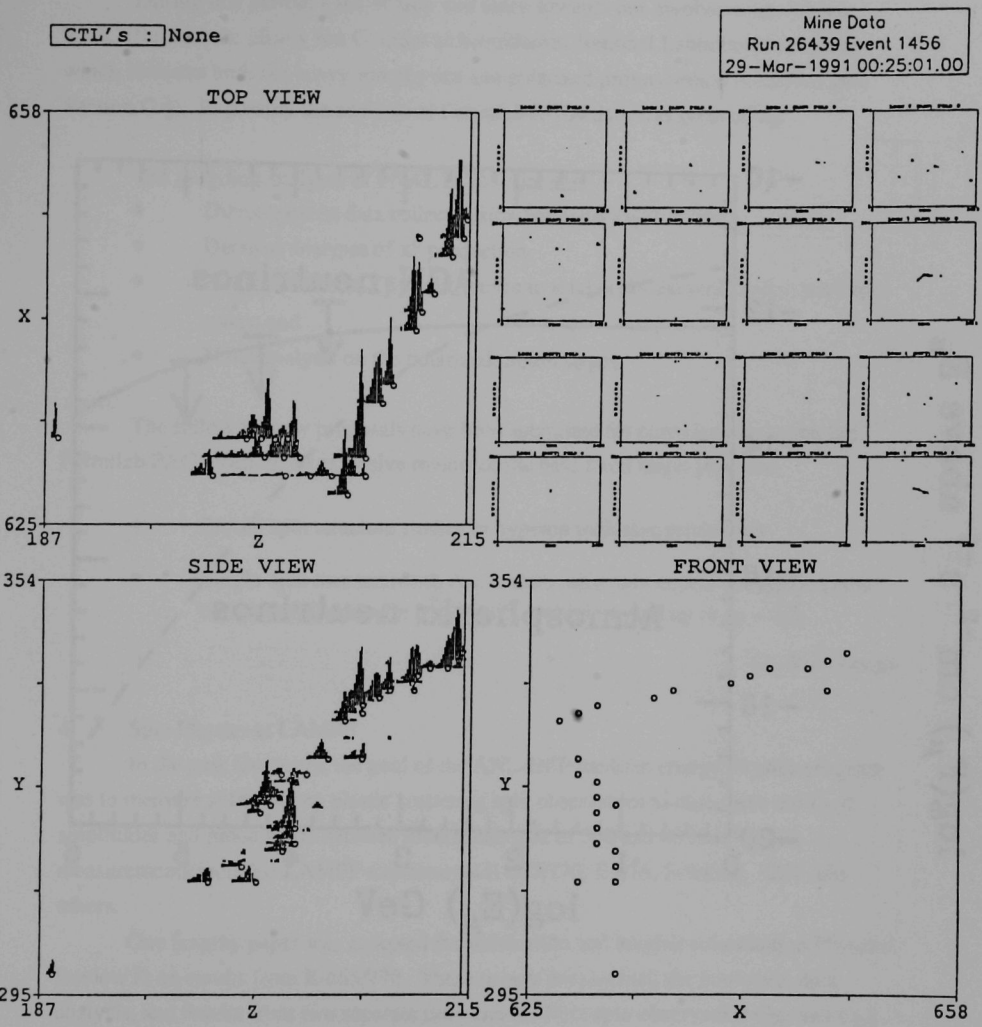

Fig. 8. Reconstruction of an electron neutrino quasi-elastic scattering event, $\nu_e n \rightarrow e^- p$, recorded by Soudan 2. The views are the same as in the previous figure. The long, straight, heavily ionizing track is the recoil proton, with a range of 22 cm (700 MeV/c). The electron shower is at the lower left in all three views, and has an energy of 180 MeV (based on the 13 hits recorded).

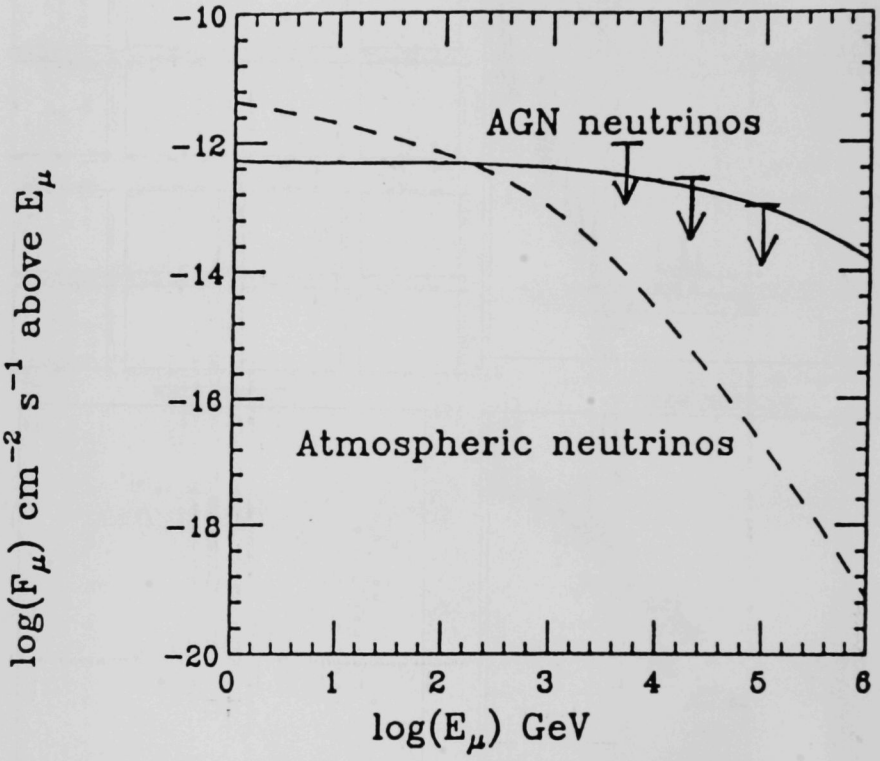

Fig. 9. Preliminary flux limits for very high energy muons in the Soudan 2 detector. The AGN curve shows the integrated flux predicted to be produced by neutrinos from active galactic nuclei interacting in the rock surrounding Soudan 2.

3. Polarized Proton Physics

During this period, a major step was taken towards our involvement with the RHIC (Relativistic Heavy Ion Collider at Brookhaven National Laboratory) program which includes both the heavy-ion physics and polarized proton-proton collisions (see Section C.4). In parallel the analysis of Fermilab E-704 data was proceeding.

The on-going analyses of FNAL E-704 data are:

- Direct-gamma data collected simultaneously with π° data,
- Detailed analyses of π° production,
- $\Delta\sigma_L(pp)$ and $\Delta\sigma_L$ ($\bar{p}p$), difference in total cross sections, and in pure spin states, and
- NMR analysis on the polarized proton target.

The following new proposals have been submitted for consideration at the fall Fermilab PAC meeting, an extensive review of the next fixed target program.

- Proton spin structure studies in hyperon inclusive production
- Single-spin measurement, A_N, to determine spin dependent quark-gluon correlation function in $p^{\uparrow}p \rightarrow \pi^\circ X$, at high p_T and up to $x_F \approx 0.3$.

(A. Yokosawa)

4. Spin Physics at LAMPF

In the past few years, the goal of the ANL-HEP medium energy physics program was to measure sufficient np elastic scattering spin observables to determine the I = 0 amplitudes and phase shifts between kinetic energies of 500 and 800 MeV. The measurements included LAMPF experiments E-665/770, E-876, E-960, E-1274, and others.

One lengthy paper was accepted for publication and another submitted to Physical Review D on results from E-665/770. These papers documented the hardware, data analysis, and results from two separate run periods. Pure spin observables C_{SS} and C_{LS} with a polarized neutron beam incident on a polarized proton target are shown in Fig. 10. The data correspond to c.m. angles between 25° and 80°, and beam kinetic energies of 484, 634, 720, and 788 MeV. A variety of phase shift predictions are shown for comparison. From these results and pp data, pure I = 0 spin observables, and observables corresponding to an interference of I = 0 and I = 1 amplitudes, can be derived; see Figs.

11 and 12. Fits to these results have been performed with Legendre polynomials. If only one partial wave is responsible for the observed variation with energy, then the data are consistent with changes in the $^3D_1$ wave. On the other hand, there are insufficient statistics to rule out other waves, nor can the case with energy variation in more than one partial wave be rejected. Analysis of the remaining E-770 data for np elastic scattering and of the E-665/770 data for the np $\rightarrow$ dπ° reaction is continuing.

A paper was accepted for publication and another submitted to Physical Review C on results from E-876/1234. These experiments scattered the polarized neutron beam from liquid hydrogen and deuterium targets, respectively. Outgoing protons were detected in a magnetic spectrometer and the spins measured with a carbon polarimeter. E-876 results included K_{SS}, K_{LS}, K_{SL}, and K_{LL} at 634 and 484 MeV over a wide angular range. The E-1234 data were finalized and are shown in the last progress reports. The experiments will continue this summer with measurements of the spin observable K_{NN} at several beam energies. Work to prepare the ANL-HEP neutron counters for the run was performed by an ANL physicist in June. It is not yet decided whether E-876 will continue next year. (H. Spinka)

5. Computational Physics

The computational physics effort continues to be devoted to numerical simulations of lattice field theories. This continues to be dominated by studies of lattice quantum chromodynamics(QCD), where QCD is defined on a discrete spacetime lattice to facilitate numerical simulations. Such lattice QCD simulations are aimed at measuring such non-perturbative phenomena as hadron masses and other low energy matrix elements, and at studying QCD at high temperatures, a study relevant to the early universe and relativistic heavy ion collisions. We are also applying lattice techniques to the study of the electrodynamics of the Abelian Higgs model which should help us understand the nature of the Higgs sector of the standard model.

We have been using the Intel Touchstone Delta computer at Caltech to calculate masses of the low lying hadrons in the quenched (valence quark) approximation. The high performance of the massively parallel Delta (9.5 Gflops for our assembler coded updating code) has enabled us to use large lattices ($32^3 \times 64$) and small quark masses (such that $M_\pi/M_N \sim .25$) with lattice couplings in the scaling regime ($6/g^2 = 6.5$), putting these calculations at the forefront of the field. The gauge fields are being generated using Monte Carlo (Metropolis and overrelaxation) techniques. The hadron propagators are

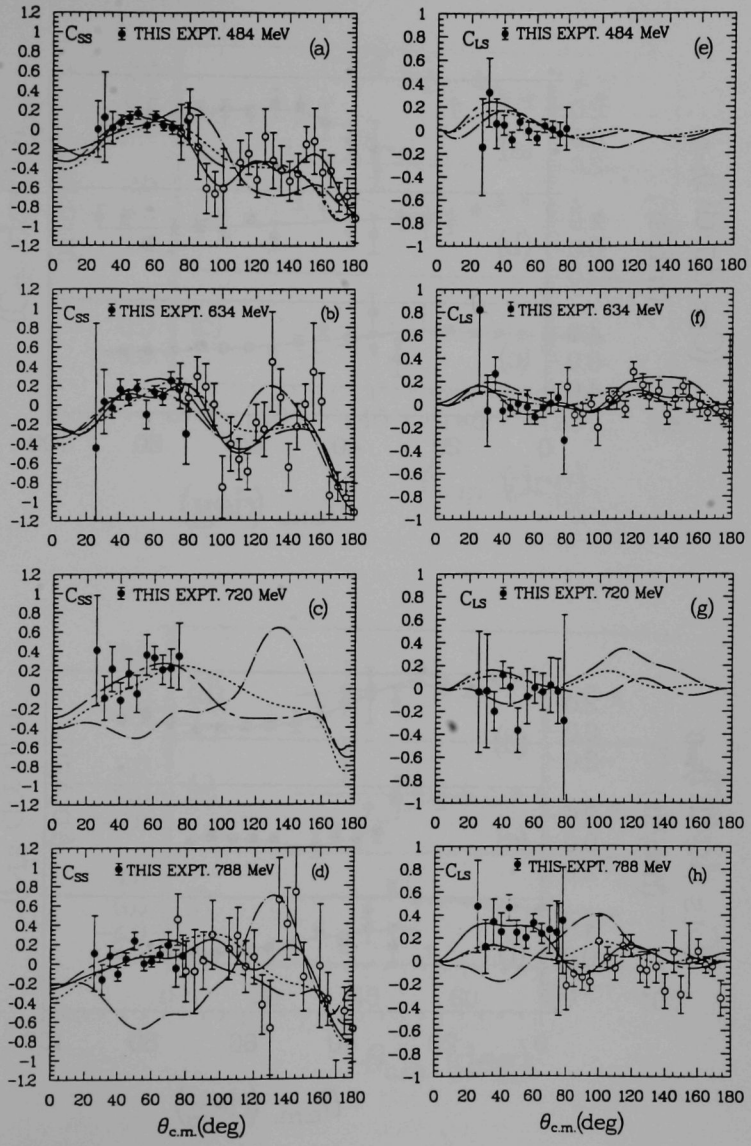

Fig. 10. Final results of the np elastic scattering spin observables C_{SS} and C_{LS} at 484, 634, 720, and 788 MeV as a function of c.m. angle. The solid circles are data from E-770 and the open circles from E-665. Solid lines are fits to the experimental data, and the other curves are phase shift predictions of Arndt et al. (chain-dash), Bugg (dash), and Hoshizaki et al. (chain-dot).

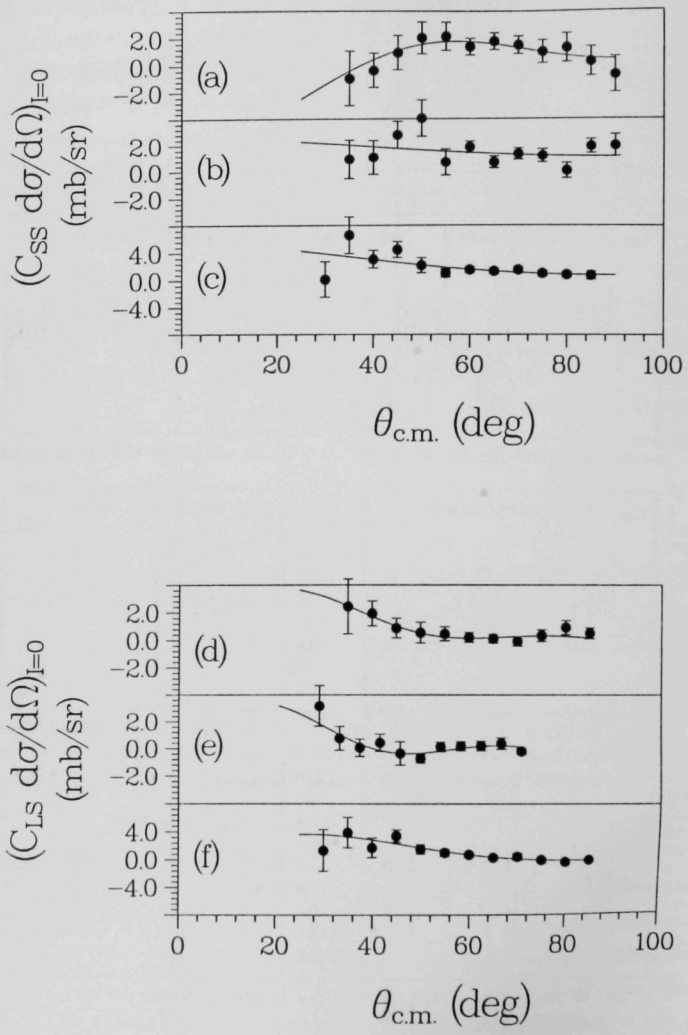

Fig. 11. Plots of pure I = 0 spin observables derived from E-665/770 measurements and from pp elastic scattering data. The curves are Legendre and associated Legendre polynomial fits to the data.

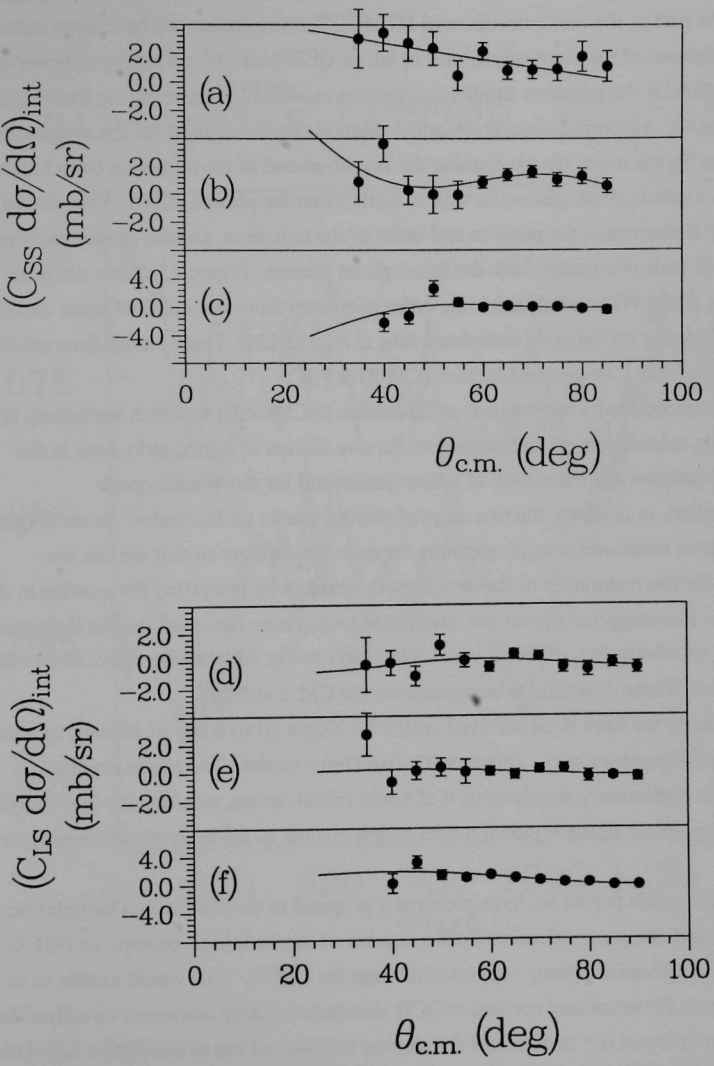

Fig. 12. Plots of spin observables that are an interference of I = 0 and I = 1 amplitudes derived from E-665/770 measurements and from pp elastic scattering data. The curves are Legendre and associated Legendre polynomial fits to the data.

extracted using quark propagators calculated using conjugate gradient methods. We are currently trying to extract reliable hadron masses from a limited set of these propagators.

As part of the multi-institutional HTMCGC collaboration we have been extending our simulations of the thermodynamics of lattice QCD on a $16^3 \times 8$ lattice to lower quark mass, (0.00625: the previous simulations were at m_q=0.0125) nearer to the true u and d quark masses. Hybrid molecular dynamics methods are being used for the simulations. As for the higher mass, we are probing the neighborhood of the transition from hadronic matter to a quark-gluon plasma as well as further into the plasma phase. This should enable us to determine the position and order of the transition, and the properties which distinguish hadronic matter from the quark gluon plasma. Figure 13 shows the time evolution of the Wilson/Polyakov line order parameter from hot and cold starts close to the transition for the recently completed runs at m_q=0.0125. These simulations are being performed on the Connection Machine (CM-2) at PSC.

A second multi-institutional collaboration (HCMCGC) to which we belong is just completing calculations of hadron masses for two flavors of light quarks both in the staggered fermion representation of lattice quarks and for the Wilson quark representation, to compare the two ways of putting quarks on the lattice. In the staggered case we have measured several operators for each meson state so that we can see evidence for the restoration of flavor symmetry (broken by latticizing the quarks) in the spectrum. For staggered quarks we have made preliminary runs with quarks light enough that the ρ can decay (m_q =0.005), but it is too early to say whether the effect of this decay will be seen. These simulations were made on the CM-2 at SCRI.

Finally we have been involved with John Kogut (University of Illinois) in a study of the electrodynamics of the compact Abelian Higgs model. The phase structure observed in preliminary simulations, if of a non-trivial nature, would mean that analyses of the Higgs sector of the standard model which assume its triviality would need to be redone.

During this period we have prepared a proposal to the NSF which includes both physicists and computer scientists from a number of institutions to become an NSF Grand Challenge Applications group supported through the HPCC. This would enable us to set up a structure for extending our lattice QCD simulations, using advanced visualization methods to interpret our results, and developing software of use to our lattice calculations and beyond. (D. Sinclair)

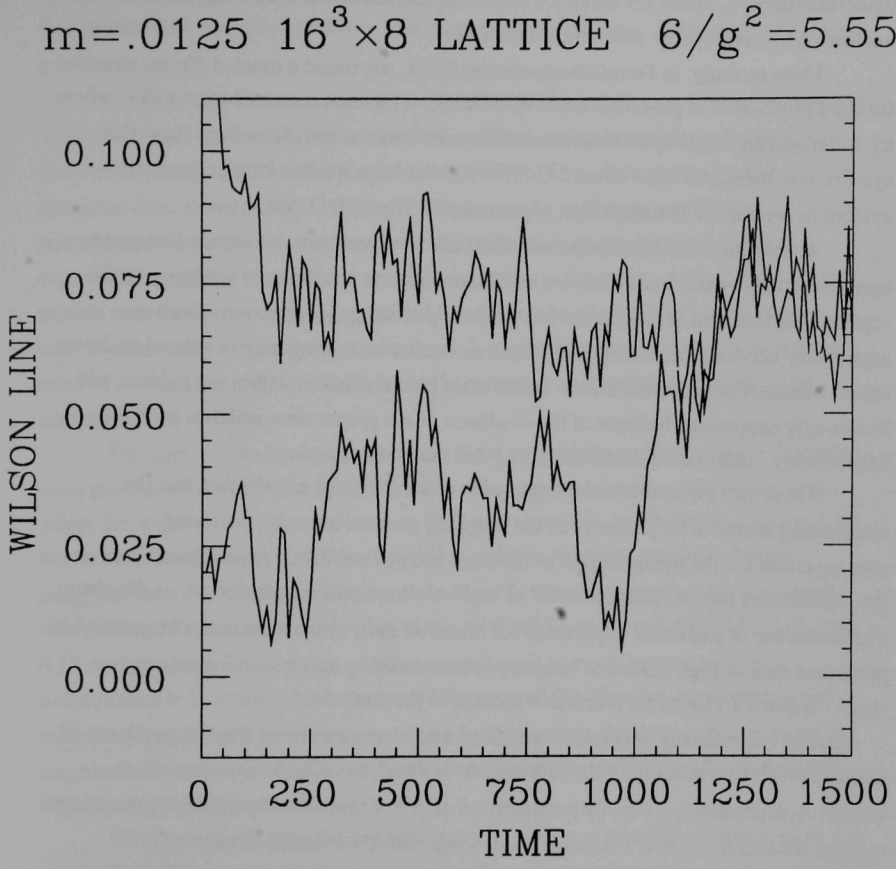

Fig. 13. Time evolution of the Wilson/Polyakov line order parameter from hot and cold starts close to the transition for the runs at $m_q = 0.0125$.

6. Nuclear Effects in Massive Dihadron Production

Experiments have shown that nuclear effects are quite small for Drell-Yan dilepton production in πA collisions at pion beam momenta of ~ 200 GeV/c. The measured k_T (rms transverse momentum) of the produced dilepton system from a deuterium target is about 1.3 GeV/c. For nuclear targets, it was found that the additional nuclear contribution to k_T was only 0.4 GeV/c.

More recently, in Fermilab experiment E609, we found a much different situation for dijet production in pA collisions at 400 GeV/c. The nuclear contribution to k_T, where k_T is defined analogously as the rms net transverse momentum of the final state dijet system, was measured to be about 2 GeV/c. Similar large nuclear k_T effects are also evident in the data of Fermilab dijet experiment E557 at 800 GeV/c.

A straightforward interpretation of the above experimental results is that parton hard scatterings within nuclei involve substantial nuclear scattering of outgoing hard-scattered partons, but very little nuclear scattering of the incident parton. Such an asymmetry between initial state and final state nuclear scattering may be related to the so-called Landau-Pomeranchuk effect: initial state gluon radiation within the nucleus will be strongly suppressed because of the smallness of the proper time which is available between any initial state nuclear scattering and the hard scattering.

These two phenomena, the large value of k_T (nuclear) and the fact that the rescattering seems to be primarily of the outgoing partons, have some striking consequences for the interpretation of the large body of published experimental data on the "anomalous nuclear enhancement" of cross-sections, particularly for pA → dihadrons. The issues are of particular importance for dihadron data, because there is a large body of published data of high statistical accuracy whose meaning may become much clearer when nuclear k_T effects are taken into account in the analysis.

Several experiments at Fermilab and Serpukhov have measured the A dependence of a differential cross section for the process pA → dihadrons +X. The nuclear cross-section A-dependence is usually parametrized as A^α, where $\alpha > 1$ is called an anomalous nuclear enhancement, $\alpha < 1$ is called shadowing, and $\alpha = 1$ would be expected for independent scattering from each of the nucleons as though they were free. The dihadron cross section is normally measured in a small region of the available phase space. The choice of this region is a crucial and delicate matter, as we shall describe.

First, it is necessary to recall that anomalous nuclear enhancement effects, which were originally discovered in large p_T inclusive pion production, have been generally interpreted as being caused mainly by nuclear scattering. Nuclear scattering of fast partons will tend to enhance the differential cross section in regions of low population

density in phase space. In particular, because the cross section is falling so rapidly with increasing p_T, nuclear scattering, which has effects similar to broadening the angular acceptance function of the detector, can lead to a substantial increase in the measured cross section at large p_T. In this way, nuclear scattering of either incident or scattered fast partons will naturally yield $\alpha > 1$ for single particle or single jet production at large p_T.

The fact that nuclear scattering will tend to preferentially populate regions of low density in phase space also means that there will be a depopulation for regions of high density. This depopulation can also be a large effect. This is illustrated by Fig. 14, the measured dijet azimuthal opening angle distribution for hydrogen and Pb targets. Both data sets are normalized to the same area. Note that among the dijet and dihadron experiments, E609 is the only one with full azimuthal acceptance. A dijet Pb/H cross section ratio measurement which required that the jets be exactly 180^o apart in azimuth would yield a ratio which is about a factor of 2 lower than the true dijet cross-section ratio. To obtain the correct ratio, it is clearly necessary to integrate over all relative azimuths of the two jets.

For dijet or dihadron measurements, if the azimuthal acceptance of the detector were narrow (as for example in the Fermilab dihadron experiment of McCarthy et al., where the width of the $\Delta\phi$ acceptance at 180^o was about 5^o), a substantial correction to the measured value of α would be required in order to represent the cross section integrated over the entire azimuthal peak in Fig. 14. For this example, this correction would raise the observed dipion value of $\alpha = 1.00 \pm 0.05$ to about $1.13 \pm .05$. Although 0.13 does not seem to be a huge additive correction, it is much larger than the uncertainties in α which have been quoted for most of the dihadron experiments, and represents a factor of 2 in cross section for a heavy nucleus. Furthermore, it is equal in magnitude to the full anomalous nuclear enhancement effect as originally observed in high p_T single pion production.

We also note that the limited acceptance of a dijet or dihadron experiment in Δp_T can lead to a further upward correction for α. The essential physics ingredients are those mentioned above: in the absence of k_T or experimental resolution effects, the two jets of the dijet would have the exact correlations $p_T(1) = p_T(2)$, and $\phi(1) = \phi(2) + 180^o$. Of course $\theta(1)$ and $\theta(2)$ are only broadly correlated, because of the wide distribution in longitudinal momentum of the initial state partons. Unless the experimental acceptance in both $\Delta\phi$ and Δp_T are sufficiently broad to accept the entire correlation function for the nuclear target case, the measured value of α will be smaller than the true value.

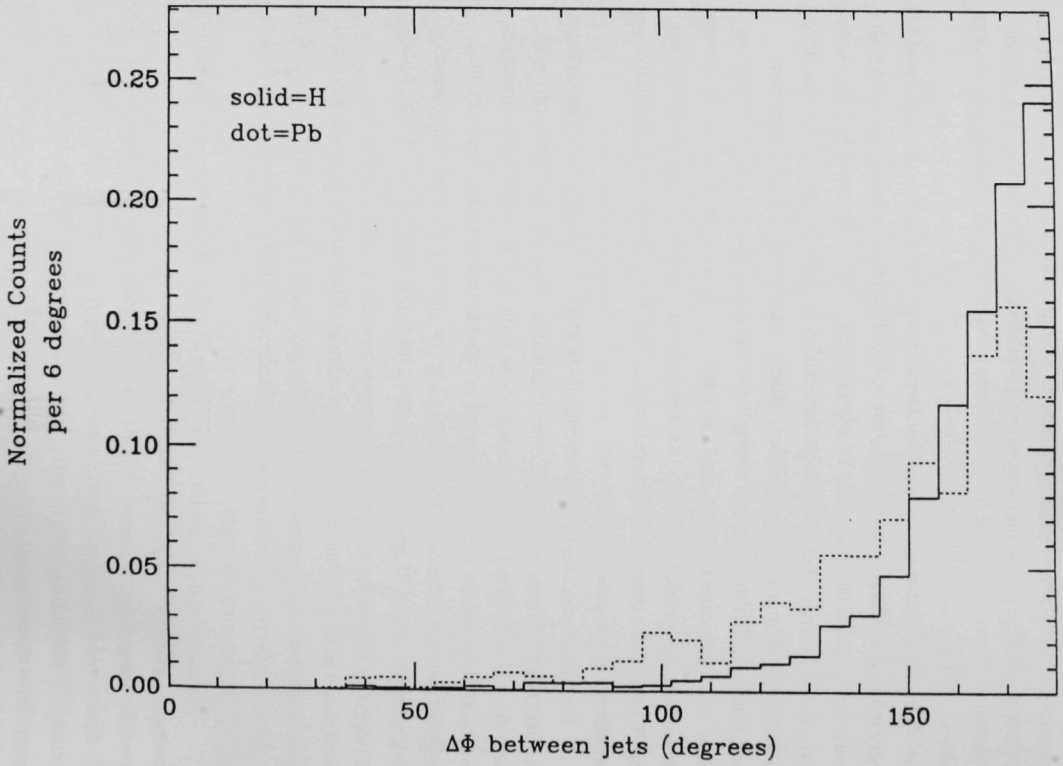

Fig. 14. Experimental data from E609 on the distribution of azimuthal opening angle for dijet events from H and Pb targets, with p_{beam} = 400 GeV/c, θ(cm) ≈ 90°, and p_T ≈ 5 GeV/c. Both distributions are normalized to unit area.

In summary, we have interpreted recent dijet data as indicating that nuclear scattering in hard parton-parton scattering events is substantial and is experienced mainly by the final state outgoing partons. This scattering then has large effects upon the dijet and dihadron correlations, and leads to significant corrections for some of the existing dihadron measurements . Final state nuclear scattering is expected to yield $\alpha > 1$ for dijet or dihadron experiments. We also suggest that much of the physics can be summarized in $k_{T\phi}$ (nuclear), which can be measured quite accurately and directly.

(T. Fields)

B. Experiments Taking Data

1. Soudan 2

The Soudan 2 experiment operated smoothly during the first half of 1992 and recorded data for 146 days of livetime, giving a duty cycle of 80%. This brought the total Soudan 2 exposure to 980 days, or 1.05 fiducial kiloton years for contained events. The detector is operated for physics data primarily during night and weekend periods when installation work is not in progress and the underground laboratory is unoccupied. The anode-cathode edge trigger, which was devised for neutrino interactions and nucleon decay, has high efficiency for cosmic-ray muon tracks as well. The data from all triggered events is processed by track reconstruction programs and the analysis results are recorded on 8-mm magnetic tape cassettes for distribution to the collaborating institutions.

In addition to data from the underground Soudan 2 detector, data from the 40 m^2 surface array are recorded for every event in order to measure the energies of cosmic ray air showers which produce underground muons. Of course, only a small fraction of the air showers which produce muons in Soudan 2 are oriented in such a way as to strike the small surface array. The surface array measurement of shower energies for multiple muon events is used in studies of the nuclear composition of cosmic ray primaries. About 28,000 events with surface-underground coincidence data have been recorded during first year of surface array operation. (D. Ayres)

2. Spin Physics at SATURNE

Recently, a nucleon-nucleon scattering program was begun at Saclay, France with a goal to extend the LAMPF I = 0 measurements to higher energies and to investigate the origin of energy-dependent structure in various pp spin observables near 2100 MeV.

The multiwire proportional chamber (MWPC) and various associated hardware shipped to Saclay last October was installed, cabled and tested during the past six months. After considerable work, the information from this MWPC was read into the experimental data acquisition computer. Some minor problems remain that should be easily solved before the next experimental run in November 1992.

Considerable effort was devoted to improving the operation of the polarized target for these experiments. The polarizing magnet power supply was modified by the addition of a transductor and a two quadrant regulator, to permit more stable operation and a faster polarizing time. Additional modifications are planned for the holding-field magnet power supply and a completely new NMR measurement system will be built to determine the target polarization more accurately.

Finally, a new data acquisition computer and operating system will be used for the next experiment. Argonne physicists have been working to become familiar with the hardware and will be deeply involved in developing the on-line software. (H. Spinka)

C. Experiments in Preparation Phase

1. Collider Detector at Fermilab

The checkout period for the current collider run began with the detector roll-in during March. The first luminosity appeared in May. The luminosity and the reliability of both the accelerator and the CDF detector have since been slowly improving. The silicon vertex detector has come on well. The muon upgrade is working well with the exception of a trigger rate problem with the muon extension. The new vertex drift chambers have been integrated into the system, but a substantial number of modules have had high voltage problems and a long access will be needed for repairs. The modified electronics for lower gas gain in the inner three superlayers of the central tracking chamber have noise problems which require hardware and software modifications. The new Silicon Graphics Level 3 trigger is working well and the new Level 1/2 hardware is progressing as planned with the possible exception of the new fast tracker. The overall data acquisition system and those detectors with few or no modifications are gradually being brought up to nominal performance.

The new central preradiator system from Argonne is installed and functional as shown in Figure 15. The strip chambers and crack chambers are reasonably functional although the level of broadcast noise being picked up is higher than previously observed. One quadrant of one strip chamber has a high voltage problem which we hope to fix during the coming long access. The various calorimeter wire chambers are using high voltage feedback to stabilize gain. A gas monitor system for our Ar/CO_2 systems has been installed and is being debugged. Gary Houk and others from the Pennsylvania group have been working with us on making all the central EM PMTs operational and performing calibrations.

The active patch panels for the strip chamber/preradiator level 2 trigger have been checked out. The Fastbus card has been fabricated and plans for testing it are beginning to be implemented. At the University of Chicago, the new front end wire readout cards are being tested. Another design iteration to reduce noise may be needed. The overall system needs to be tested in sufficient time so all the front end cards can be ordered. These would then be installed during the linac upgrade shutdown, tentatively set to begin next March. The design bunch spacing for eventual multibunch running has been settled at 128 ns. (L. Nodulman)

2. Soudan Detector Installation

Fifteen 5-ton modules were constructed at the Argonne module factory during the first six months of 1992, bringing the total number of U.S. modules completed to 137. Eight modules were shipped to the mine site from the Argonne module factory, bringing the total number of modules underground to 200 (860 tons). It is planned to construct the last eighteen modules needed to complete the 960 ton Soudan 2 detector by the end of 1992.

One new halfwall was added to the Soudan 2 detector during the first half of 1992. (A halfwall is a subassembly of eight 5-ton modules, stacked four across and two high.) This increased the operating mass from 688 to 722 tons. Figure 16 is a photograph of the 688 ton Soudan 2 detector taken in March. In addition to new halfwall construction, two halfwalls were rebuilt to replace older modules with nonuniform wireplane response and poor gas seals. These modules were overhauled and several were reinstalled in the detector during the period when new modules were unavailable due to the contaminated bandolier problem. A number of anode high voltage splitters, which allow top and bottom modules to operate at different, optimum wireplane voltages, were installed while the detector was open for module replacement.

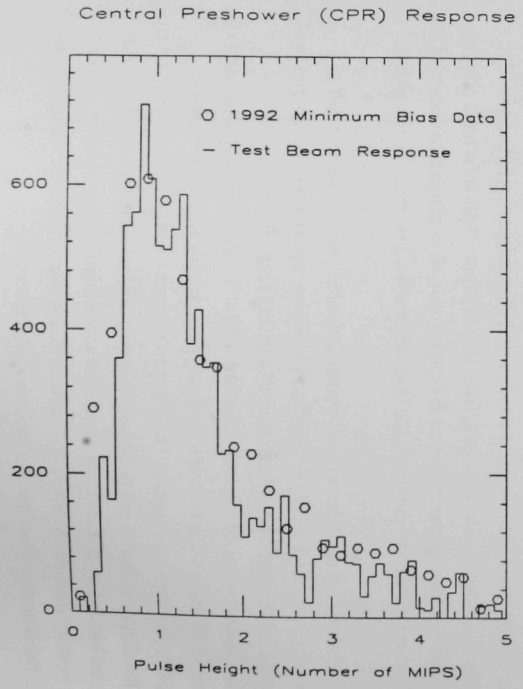

Fig. 15a. Pulse height in minimum bias events reproduces testbeam results for minimum ionization.

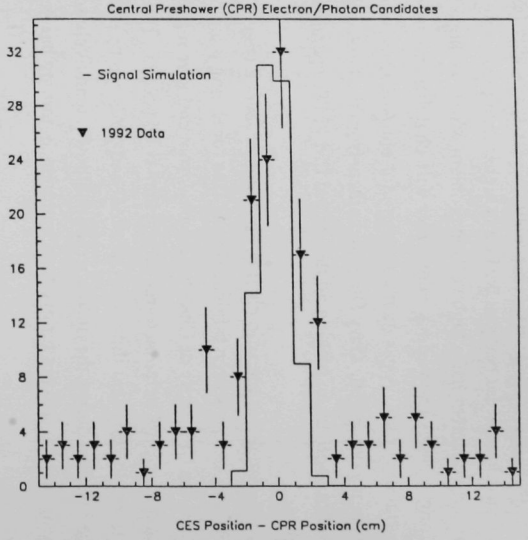

Fig. 15b. Azimuthal position as measured by the preradiator wires aligns with the strip chamber wire measurement.

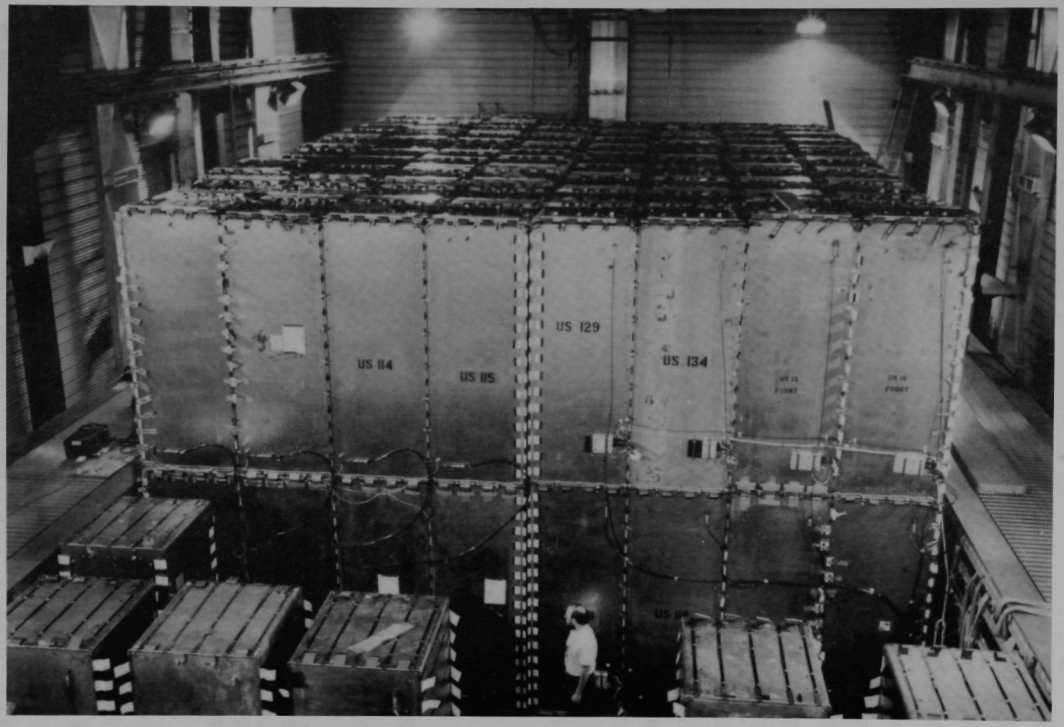

Fig. 16. Photograph of the 688 ton Soudan 2 detector, taken in March 1992. The aluminum active shield proportional tube manifolds can be seen in the background, covering the walls of the cavity. The individual 4.3-ton calorimeter modules in the foreground are undergoing performance testing prior to installation. (Photograph by Tomas Kafka, Tufts University.)

In January the heat treatment of 5-ton modules constructed with "poisoned" bandolier began at the Soudan mine site. The heating fixtures were built at Argonne during the summer of 1991 and used to decontaminate six modules before being shipped to Soudan. Modules are insulated and the steel stacks are held at 50° C for two to four weeks (depending on the level of contamination), while heated air is blown through the stack. A total of twenty modules have now been heat treated at Soudan. A number of these decontaminated modules have been used in new or rebuilt detector halfwalls and have performed well. At the Argonne module factory, the bandolier for new modules is now heated in an oven for 3 days at 70° C, in order to remove most of the methylene chloride contamination before stacking.

Argonne physicists and engineers continued to make substantial contributions to the installation and operation of the detector during 1992. Major activities included the setup and monitoring of the module heat treatment facility, study of detector and electronics performance, coordination of module assembly, and improvements in several electronics systems. (D. Ayres)

3. ZEUS Detector at HERA

a) HERA Status

HERA began operation just prior to the Easter break and established single bunch electron beam operation. Operation of the proton injection and storage at 40 GeV began after the break and the milestones below were achieved up to June 30:

• Technical commissioning of the HERA electron ring	April 1.
• HERA proton operation	April 23.
• HERA proton ring reached its design energy of 820 GeV	May 15.
• e-p operations	May 26.
• First luminosity operation in 1 x 1 bunch mode	May 30-31.
• First 10 x 10 bunch operation	June 6.
• Luminosity operation with 10 x 10 bunches	June 28.

HERA operation was shared between machine development and data taking during the period through June 30. However, the data taking was extremely limited due to a number of HERA problems. Machine operation will continue until August 3 at which point access will be granted to the H1 and ZEUS experiments until August 17. Machine operation will then continue at least through the end of October and time will be shared between machine development for badly needed hardware, such as the multi-bunch feedback system, and data taking.

b) ZEUS Operations

A number of important tasks were completed in the period January through March. First, the procedure of wrapping the cylindrical surface of all photomultipliers (PMT) in the BCAL was finished. The aim of this operation was to eliminate charge buildup on the surface of the PMT which results in sparking to ground and eventually to destruction of the PMT base. Measurements of the base failure rate recorded by the end of June were reduced from 1 base/module/week as of December 1991 to about 0.3 bases/module/week, presumably as a result of the wrapping.

Installation of the interim calorimeter first level trigger (CFLT) was completed by the Wisconsin group. This trigger divides the calorimeter up into a number of regions such that within each region all electromagnetic and hadronic cells have a particular energy threshold chosen to match their environment. Thus in the rear calorimeter, the cells around the beam pipe have high energy thresholds to eliminate triggering on beam gas which tends to be localized there. This interim trigger was introduced because the design and construction of the trigger adder cards and construction of the trigger encoder cards was behind schedule, and the trigger processor was not available. The full trigger is not now expected to be installed until the winter shutdown beginning in November although a section of it may be installed earlier if the opportunity arises.

The H1 and ZEUS detectors were moved into their interaction regions at the end of March and access was restricted for machine operation soon after that. ZEUS operation then concentrated on integrating the various detector components into the three levels of trigger using the cosmic ray data, also used to study detector performance. At the same time, the run control and data acquisition systems underwent steady improvement.

Commissioning the detector took place under the direction of four run-coordinators:

B. Foster	Bristol University
R. Nania	University of Bologna
R. Talaga	Argonne
R. Walczak	University of Warsaw

and a four person shift operation schedule was started.

By May 28 26.6 GeV electron beams at about 10 μA and 820 GeV proton beams at 33 μA had been established. On May 31 e-p collisions in the ZEUS interaction region at $L \approx 2 \times 10^{27} cm^{-1} sec^{-1}$ were observed and the first deep inelastic events ($Q^2 \approx 5$ GeV^2) were seen. By June 29 luminosity operation was achieved on a fairly regular basis, often

with 1-2 fills/day. Very good data analysis turnaround was achieved from the first, with reconstructed data available within a few hours after data taking.

The ZEUS detector will operate its tracking systems in an incomplete state until the March 1993 running begins. The rear and forward tracking detectors will not have electronic readout and the central tracker will only read out superlayers 1, 3 and 5 of 9 total. The vertex detector was installed and operating in March but developed a cooling water leak in June which could not be repaired until the August shutdown. As a result only limited regions of the vertex detector could be operated for short times. This was sufficient to demonstrate, using cosmic rays, that the component will work well once this problem is fixed.

The uranium calorimetry operated well through June 30 although several problems were encountered. There were two accesses during this period which allowed the number of dead BCAL channels due to PMT base failures to be maintained at less than 1%. One problem which developed with the analog pipeline chips will not be fixed until the August shutdown but only affects a small number of channels. Some of the switched capacitor storage arrays develop a bad capacitor cell. All of the pipeline and buffer chips of the calorimeter will be replaced in the winter shutdown. The redesign by the Fraunhofer Institute will remedy this and other known pipeline problems. By the end of June, algorithms were developed using the reconstructed times from the forward and rear calorimeter cells around the beampipe to achieve a significant reduction in beam gas background. The time resolution from energy deposition above 1 GeV in a cell is ~ 1.5 ns, approaching the ultimate limit of about 0.2 ns. This is one advantage of scintillator calorimetry, as shown in Fig. 17 where the difference between the times from the forward and rear calorimeter cells around the beam pipe is plotted versus the rear calorimeter time. The real e-p events are clustered around (0,0) ns while the beam gas events appear around (12, -12) ns.

A problem with the BCAL found during the first detector test with solenoidal field in September 1991 was studied in detail during June. The magnetic shielding of the PMT is not sufficient to eliminate all the field effect on the PMT gain, observed in the variation of the ratio of uranium noise current from field on to field off. The aim is to remove hysteresis effects and it is necessary to define a standard procedure by which the final magnetic field configuration is reached so as to achieve this. A series of detailed measurements of the response to the laser injected light signal and of the UNO current under various field conditions and also with the forward and rear calorimeters in both the open (40 cm separation around the beam line) and closed positions, were taken. Since the response to the laser signal only involves changes in PMT gain due to the magnetic field

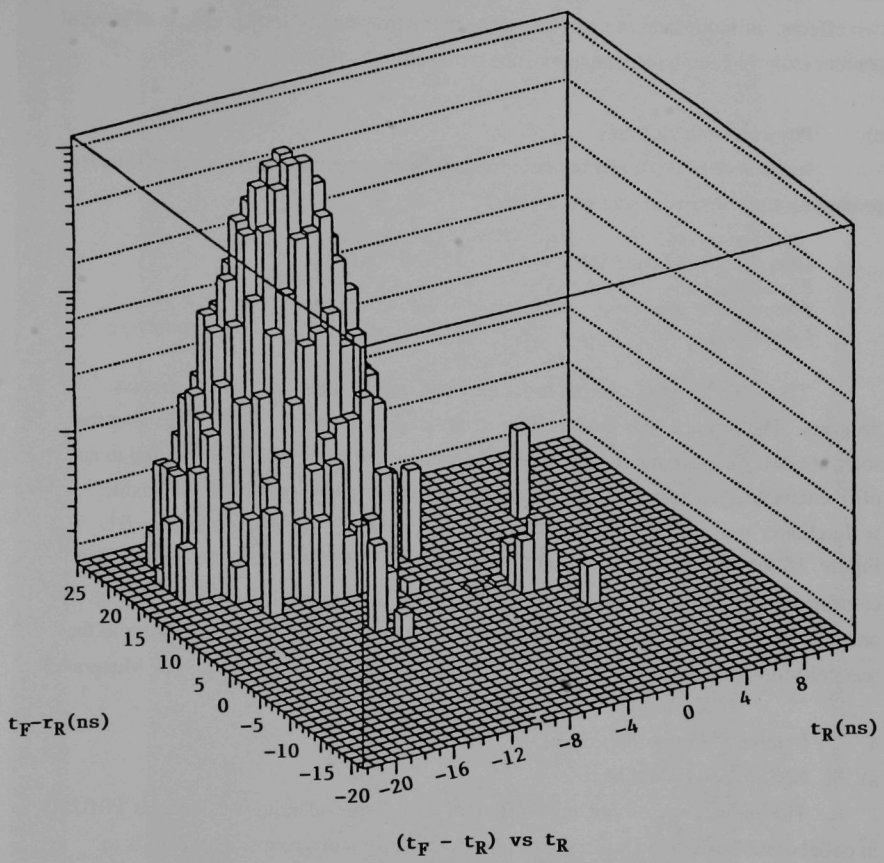

Fig. 17. Separation of real e-p collisions from beam-gas interactions using timing information from the forward and rear calorimeters. The real e-p data cluster around (0,0) nsec on the (t_F - t_R) versus t_R Leggo plot.

while the UNO response involves both the field effect on the PMT gain and also the well known increase in scintillator light due to magnetic field, it is possible to factorize these two effects. Initial results of analyzing these data show that hysteresis effects of several percent magnitude in gain change must be removed.

c) Physics Analysis Plans

In December 1991, physics coordinators were designated to organize efforts for producing early results in selected topics:

Deep Inelastic Scattering	M. Derrick (Argonne)
Exotic Physics	F. Sciulli (Columbia)
Photoproduction	A. Levy (Tel Aviv)
Low-x Physics	J. Whitmore (Penn State University)

The working groups began in January and held regular meetings to discuss progress. The physics coordinators were in close contact with the people directing the software development and those responsible for detector operation. This has led to an offline data analysis system which is expected to make reconstructed data available within hours of data taking. The first luminosity run in ZEUS occurred on May 31. Figure. 18 shows a reconstructed photoproduction event in the r-z and r-ϕ views. The calorimeter reconstruction program finds two jets in the forward calorimeter. In Fig. 19 one sees the first deep inelastic event found, with a clear 26 GeV electron cluster in the rear calorimeter. (B. Musgrave)

4. Polarized Proton Physics

a) BNL E-880 Experiment

The engineering design and drafting of the 4.7 ton solenoid was made at TRIUMF in collaboration with the University of Indiana and Argonne groups. Our plan is to complete the magnet by the end of this calendar year.

An absolute polarization measurement is necessary to clearly demonstrate that no polarization is lost during acceleration. The Argonne group is responsible for the design and construction of the internal polarimeter in the AGS. An energy loss spectrometer in recoil arm is likely to be built in the near future. The polarimeter target mechanism is currently under study.

The E-880 experiment will run sometime in 1993.

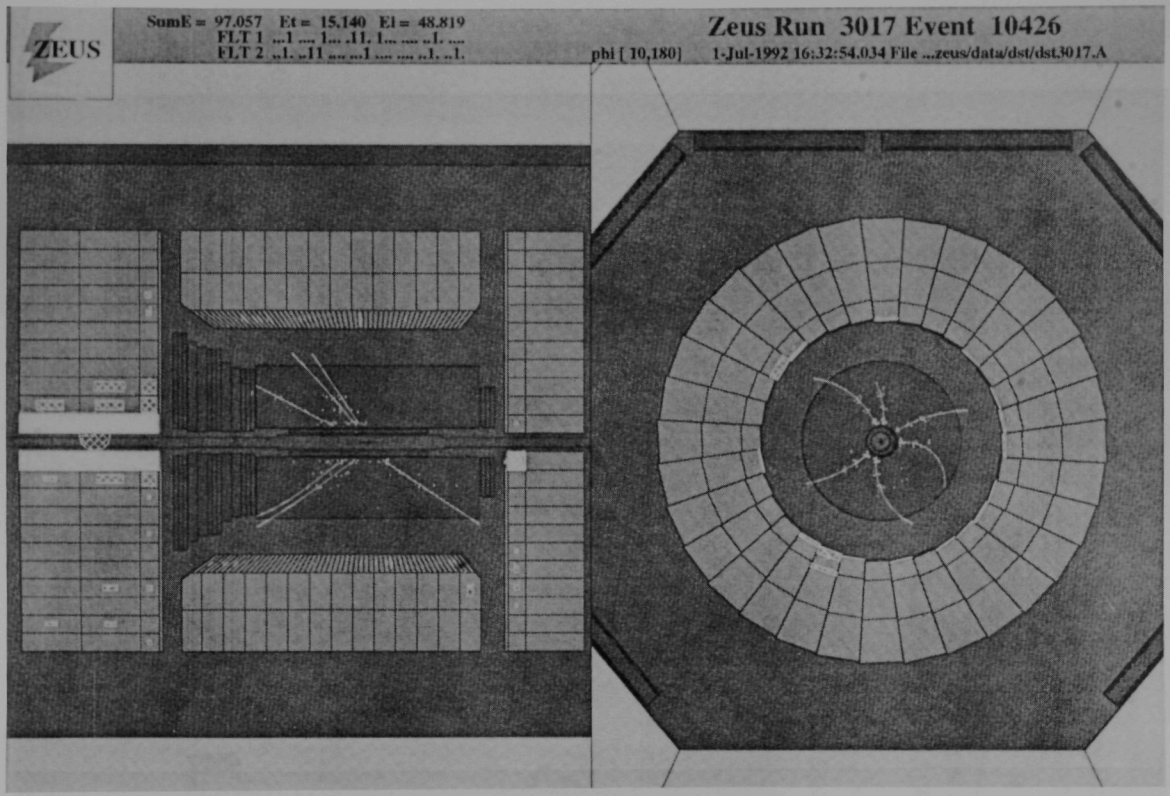

Fig. 18. Photoproduction event from an early ZEUS luminosity run.

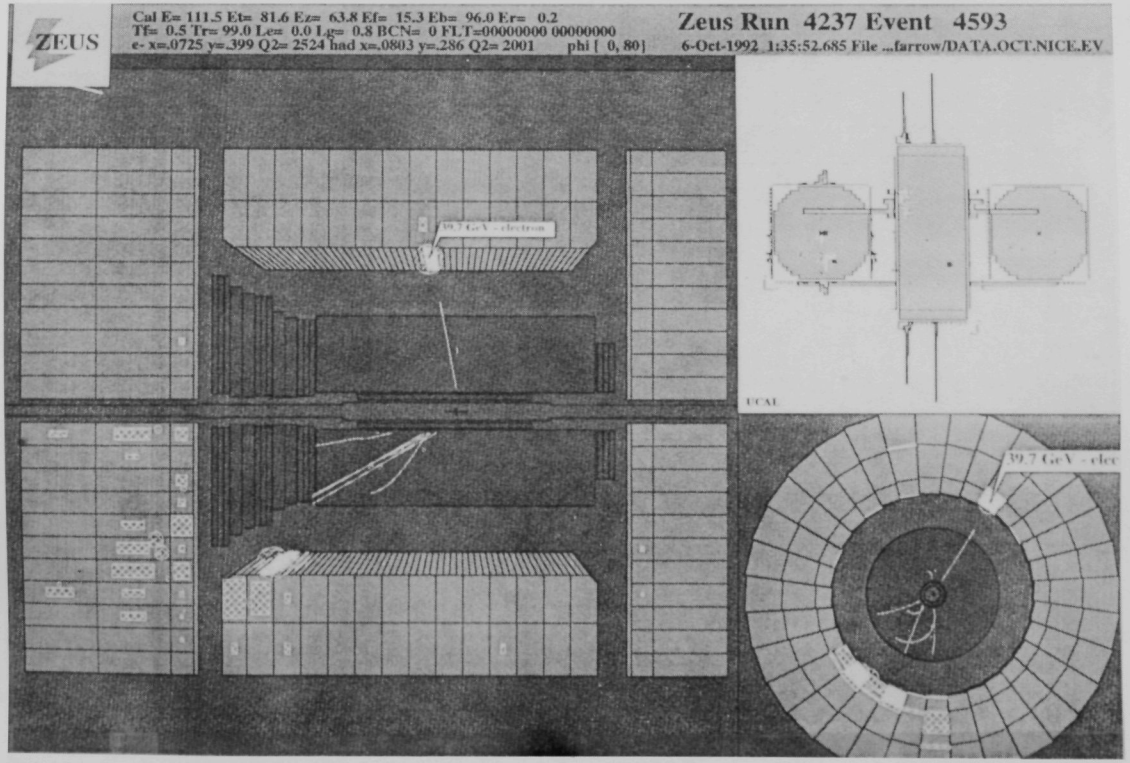

Fig. 19. One of the first deep inelastic neutral current events to be seen in ZEUS.

b) Experiments at RHIC

i) Heavy Ion Physics - Search for Signatures of Quark-Gluon Plasma

Since there is no single accepted signature for the QGP, it is essential to use a flexible detection system at RHIC that can simultaneously measure many experimental observables. For this purpose, two detectors (PHENIX and STAR) are being constructed.

ii) Polarized pp Collisions by RHIC Spin Collaboration (RSC)

The Argonne group recently joined the STAR group. We committed both to the polarized proton physics capabilities that RHIC can provide and to the heavy ion physics for which STAR has been approved.

The STAR detector utilizes a time projection chamber to measure hadron production over a large solid angle. Other important components of STAR include an EM calorimeter and shower maximum strip detector. With these components supplied by the RSC, STAR would offer ample opportunities to carry out spin physics. In fact it is important to recognize that these components significantly add to the heavy-ion physics capabilities. One may, for example, find a signature for the QGP in high p_T events.

The physics issues for polarized colliders include:

- Parton helicity distributions in a polarized proton
- Quark transversity distribution in a polarized proton
- QCD tests
- Single helicity asymmetry (parity-violating interaction) - new physics
- W production, Drell-Yan process

We intend to investigate the spin structure of the proton (issues raised by the CERN experiments--spin of the proton carried by the valence quarks, gluons, strange quarks, or orbital angular momentum), tests of various perturbative QCD predictions, parity violating interaction, and ultimately supersymmetry and compositeness.

(A. Yokosawa)

II. THEORETICAL PROGRAM

Indirect Dilepton Signatures in TeV e^+e^- and e^-e^- Collisions

One of the clearest signatures for the existence of new physics beyond the Standard Model would be the experimental observation of new particles which carry exotic quantum numbers. One possibility is the presence of spin-0 or spin-1 fields carrying two units of lepton number, called dileptons, which are expected to have masses not very different from the scale of the electroweak interactions.

In a recent paper, [ANL-HEP-PR-92-02, Phys. Rev. D, in press], T. Rizzo examined the indirect signatures for the existence of spin-1 dileptons in both e^+e^- and e^-e^- collisions at TeV energies. In addition to the mass of the dilepton (M), the only unknown parameter in such a model is the scaled strength of the gauge coupling of the dilepton to lepton pairs in comparison to electromagnetism (κ). For both the $e^+e^- \to e^+e^-$ and $e^-e^- \to e^-e^-$ processes, a search region can be defined in the M-κ plane (for a given integrated luminosity and machine center of mass energy, $\sqrt{s}$), for which ranges of these parameters will be excluded. Rizzo finds that the e^+e^- reaction is more sensitive to the existence of dileptons than is e^-e^-; specifically, for $\sqrt{s}$=500 (1000, 2000) GeV and an integrated luminosity of 25 (100, 400) fb^{-1}, dilepton masses less than 9-10$\sqrt{s}$ could be excluded for κ=1 which is approximately the value anticipated from the Frampton et al. model.

Phenomenology of Explicit R-Parity Breaking in E_6 Models

The minimal version of the SUSY Standard Model allows for the existence of new operators in the superpotential that can violate R-parity and either Baryon or Lepton number. In more elaborate SUSY models, such as those which arise from superstring-inspired E_6 scenarios, the possibility of R-parity violation can lead to a complicated interplay of various sources of new physics due to the presence of both exotic particles and new gauge degrees of freedom. T. Rizzo [ANL-HEP-PR-92-25, submitted to Phys. Rev. D] explored in detail the phenomenology of such models. In the usual R-parity-conserving version of E_6, the superpotential consists of at most 11 trilinear terms while in the R-parity-violating case 14 additional trilinear and 7 new super-renormalizable bilinear terms may also appear. In almost all cases, these additional operators involve exotic particle superfields. The existence of new gauge interactions is found to be capable of forbidding a large fraction of these new terms depending on the nature of the additional symmetry. For example, if the Standard Model gauge sector is enlarged to that of the Left-Right Symmetric Model, all R-parity violating terms involving only the superfields

of the Standard Model are forbidden. Many of the extended gauge symmetries which can exist in these E_6 models were shown by Rizzo to forbid *all* R-parity violating terms.

In cases where at least some of the new R-parity violating operators were allowed to exist, new production and decay channels for E_6 exotics were obtained. The phenomenological implications of these new interactions were explored for the Tevatron, SSC/LHC, HERA, and e^+e^-colliders in the TeV energy range. An additional prediction of these models is that the LSP can be unstable only over cosmologically interesting time periods, thus maintaining the relevance of the usual SUSY signal of missing energy at colliders.

Prompt Photon Production

Ed Berger and Jianwei Qiu (Iowa Sate University) have continued their investigations of prompt photon production in hadron collisions. They are preparing three new papers that should be issued within the coming months. In the first, they present a complete treatment of the *inclusive* prompt photon cross section in next-to-leading order QCD. This work will be of immediate use at fixed target energies and in other situations in which photon isolation is not required. At the time this first paper is issued, Berger and Qiu will make available a complete, efficient numerical program for the calculation of inclusive prompt photon yields. Their second paper will concentrate on quark and gluon fragmentation into photons and report the results of their next-to-leading order QCD analysis of fragmentation, using data from LEP to constrain the non-perturbative aspects of fragmentation. Their third paper will report a comprehensive analysis of *isolated* prompt proton production at hadron collider energies, incorporating the new fragmentation functions obtained from their study of the LEP data. Berger and Qiu intend to offer a practical numerical program that will allow users to calculate the isolated cross section at various energies, values of transverse momentum p_T, and choices of the isolation parameters.

Generalized Two Scalar Doublet Models

I.G. Knowles, C.D. Froggatt (Glasgow), and R.G. Moorhouse (Glasgow) have further pursued their project on models containing two scalar doublets. The most general such extension of the standard model, respecting the technical requirement of natural flavor conservation, has been constructed and a complete set of its Feynman rules explicitly specified [Nuclear Physics B, in press]. Using the infra-red fixed points of the hard couplings' renormalization group equations, robust (that is minimally dependent on speculative new physics at high energy scales) predictions for particle masses were

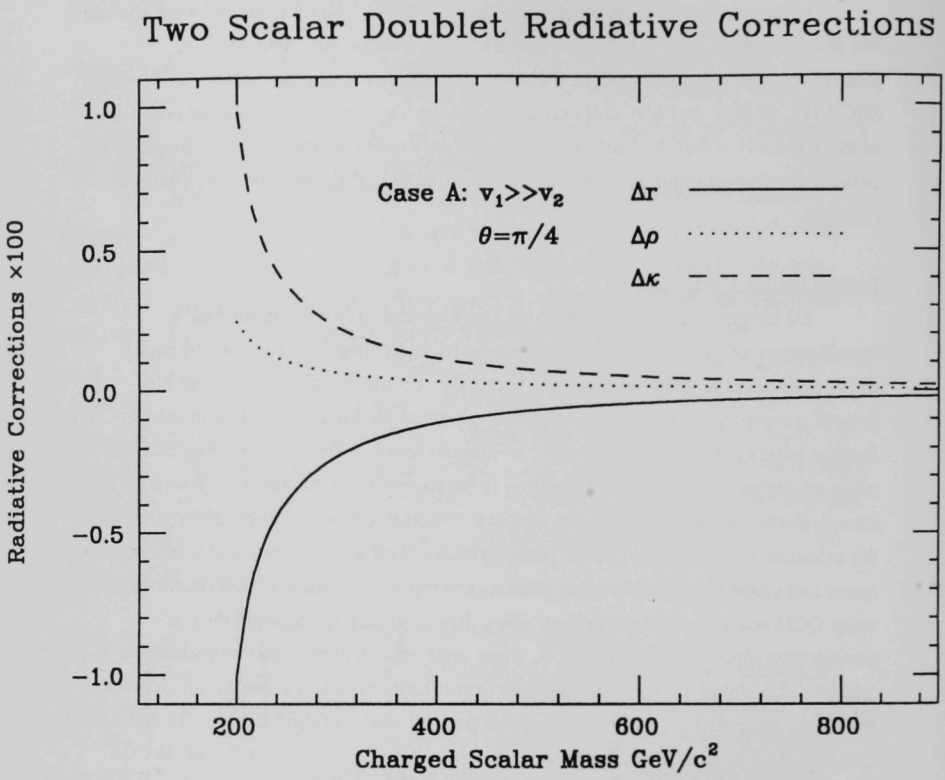

Fig. 20. The radiative corrections to Δr, $\Delta \rho$ and $\Delta \kappa$ obtained by Knowles et al. from a fixed point mass spectrum (using a large ratio of scalar field vacuum expectation values, $v_1 \gg v_2$, and maximal CP violation, $\theta = \pi / 4$) as a function of the potential's free soft parameter. The additional scalars' contributions are seen to vanish so that the extended model's scalars' are equivalent to a minimal Higgs particle, mass 241 GeV / c^2.

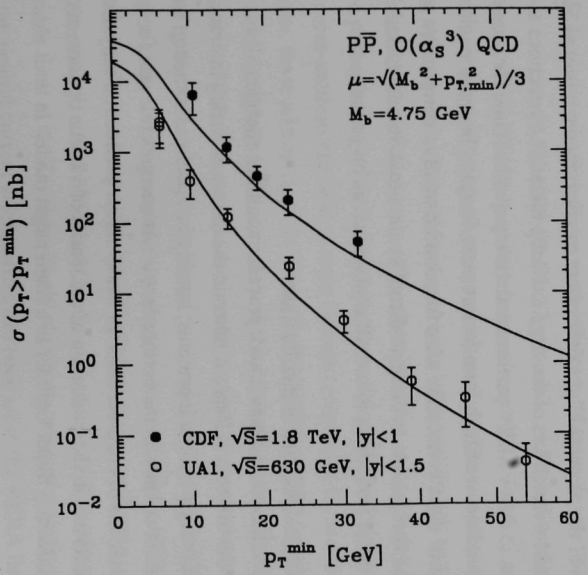

Fig. 21. The curves show the results of the fit obtained by Berger, Meng, and Tung to the CDF and UA1 data on bottom quark production. They are obtained from convoluting the $O(\alpha_s^3)$ QCD hard scattering cross section with new parton densities determined from a combined fit to deep inelastic lepton scattering data and bottom quark production data.

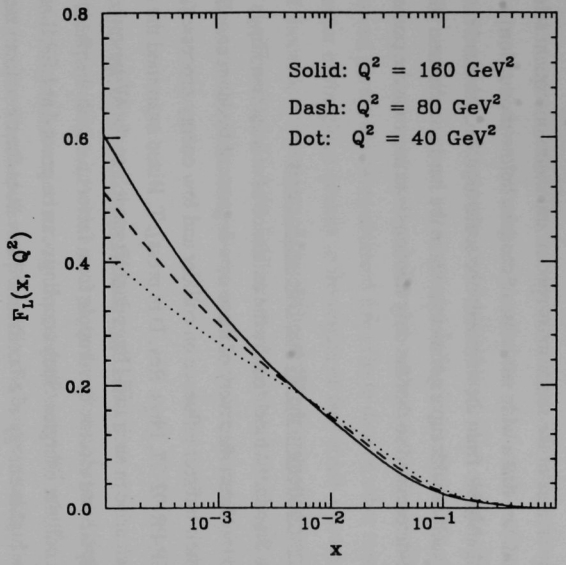

Fig. 22. Next-to-leading order QCD calculations by E. Berger and R. Meng of the longitudinal structure function , F_L, at values of the four-momentum transfer Q accessible at HERA.

calculated; in particular, two top quark mass values were obtained: 220 and 163 GeV / c^2. Interestingly, studies of the scalar mass spectra and their consequent 1-loop radiative corrections indicate that a wide sub-class of models, below production thresholds, are indistinguishable from the minimal, one scalar doublet, standard model. This occurs in models such as with supersymmetry, where the hard couplings in the scalar potential are pre-determined so that the only freedom is to increase the potential's soft parameters.

Two-Higgs Doublet Contributions to the W Anomalous Moments

Many extensions of the Standard Model require the existence of at least two Higgs doublets. In addition to the direct discovery of these new degrees of freedom at colliders, one can also examine their indirect influence on collider and low energy processes. In a recent paper [ANL-HEP-PR-92-27, Phys. Rev. D in press], T. Rizzo examined the one-loop contributions which arise in such two-Higgs doublet models to the W-boson anomalous magnetic dipole and electric quadrupole form factors for both the photon and Z couplings relevant at collider energies. Such couplings can be probed at LEP II and the SSC as well as at future higher energy e^+e^- colliders. The values for these form factors were generally found to be substantially different from their static, $q^2 = 0$, values. In order to reduce the number of free parameters in the calculation, it was assumed that the masses and couplings of the physical Higgs fields were as given by the minimal SUSY model, but also included were effects of the large one-loop radiative corrections to these tree-level relations due to heavy SUSY partners and the top quark. While the model parameter and q^2-dependencies of both form factors were found to be quite significant, the corresponding size of these corrections were found to be small in comparison to unity. They were shown to be comparable to those predicted by the usual Standard Model loop corrections but could differ from these in overall sign as well as magnitude.

Heavy Quark Production at Hadron Collider Energies

Heavy flavor production is a benchmark process at collider energies. It is interesting because of the theoretical issues it raises in the theory of strong interactions and because of the discovery potential it presents, notably in searches for the top quark and in studies of CP noninvariance in the bottom sector. At energies relevant for future hadron colliders, calculations of cross sections for heavy flavor production may assist in the design of experiments and in the evaluation of the merits of various options, such as the use of the Superconducting Super Collider in a fixed target mode. In

ANL-HEP-92-11, [published in Phys. Rev. D46, 169 (1992)] Ed Berger and Ruibin Meng present calculations of inclusive cross sections for the production of bottom quarks in proton-proton and proton-antiproton collisions as a function of energy, transverse momentum, rapidity, and pseudo-rapidity for values of $\sqrt{s}$ ranging from 100 GeV to 40 TeV. The computations are based on next-to-leading order matrix elements from perturbative quantum chromodynamics and on the most recently published sets of two-loop evolved parton densities obtained from fits to data on other reactions . Variations of the behavior of the gluon density in the region of very small x provide an estimate of the range of theoretical uncertainty. At SSC energies, results are presented for both the collider configuration $\sqrt{s}$ = 40 TeV and the fixed-target option $\sqrt{s}$ = 200 GeV. Included in the paper are calculations of charm quark inclusive cross sections at $\sqrt{s}$ = 200 GeV and 1.8 TeV.

New Probes for Extended Gauge Structures at HERA

HERA provides us with a new probe for physics beyond the Standard Model. In particular, the possible existence of new gauge bosons, W' and Z', can be examined via their influence on Standard Model processes, the usual technique being to examine the data for deviations in a number of neutral current asymmetries. Such analyses have, up to now, indicated that the indirect limits obtainable at HERA on the masses of Z' and W' would in most cases be inferior to the direct production limits obtainable from the Tevatron. T. Rizzo [ANL-HEP-PR-92-37, submitted to Phys. Rev. D] examined the limits obtainable from HERA on the masses of possible W' and Z' gauge bosons in models where both are present and a mass relationship between the two particles operates. When such a mass relation exists, the effects of the W' and Z' are no longer independent. In this case, the neutral current asymmetries no longer yield the most sensitive probe; whereas Rizzo found that the ratio of the neutral current to charged current cross-sections can lead to mass bounds comparable to, and in some cases even superior to, those arising from the Tevatron. This analysis takes advantage of the observation, first made by Doncheski and Hewett for the case of indirect signals for leptoquarks at HERA, that when both neutral as well as charged current channels are modified by the *same* new physics, superior limits can be obtained by constructing an observable using data from both channels. For example, with a HERA luminosity of 200 pb^{-1} and unpolarized beams, the limit obtainable using the R ratio on the mass of the Z' arising from the 'Unified' Model of Georgi et al. is 800 GeV, while to obtain a comparable limit at the Tevatron would require an integrated luminosity above 500 pb^{-1}. If only the neutral current asymmetries had been used, the HERA limit would have been

only 520 GeV even for fully polarized beams. Similar results were also found for other extended electroweak models.

Signals for Virtual Leptoquark Exchange at HERA

Doncheski (Univ. of Wisconsin) and Hewett have studied [ANL-HEP-PR-92-28, Z. Phys. C, in press] the effects of virtual leptoquarks on charged current and neutral current processes at the $e-p$ collider HERA. They present the areas of parameter space that can be excluded at HERA by searching for deviations from Standard Model expectations. It is found that measurements of the standard neutral current asymmetries using polarized beams, of the charge asymmetries, or of the neutral current and charge current total cross sections, are either plagued by systematic uncertainties or are simply not very sensitive to the indirect effects of leptoquarks. The best results are obtained by examining the ratio of neutral current to charged current cross sections, $R = \sigma_{NC} / \sigma_{CC}$ where, with 200 pb^{-1} of integrated luminosity for unpolarized e^- and e^+ beams, HERA can search for leptoquarks with masses up to ~ 800 GeV, with leptoquark coupling strengths of order α_{em}.

Field Theory at Non-zero Temperature

The prospect of producing the observed baryon number asymmetry of the universe at the electroweak phase transition has recently produced excitement in the field. Despite the fact that the classical Lagrangian of the standard model is exactly invariant under baryon and lepton number transformations, the quantum theory is anomalous. Thus, while perturbative processes cannot produce or destroy baryon number, non-perturbative effects (exponentially small at zero temperature) can be unsuppressed at high temperature; and, given the right conditions (being out of thermal equilibrium, existence of CP violation), the early universe electroweak phase transition itself may have produced a baryon number asymmetry. There has been intense activity on explicit calculations to establish the validity of this hypothesis in the standard model. In particular, Vokos has been studying the problem of infrared divergences which appear in finite-temperature field theory: Proper handling of the divergences is essential in identifying the region of validity of the perturbative calculations. This requires that several infinite classes of diagrams have to be resummed. In turn, their dominant behavior is identified and substituted in the one-loop results. In this light, the vacuum polarization tensors (self-energies) of the vector bosons (scalars) play a crucial role.

In collaboration with Ashok Das and Paulo Bedaque (University of Rochester), Vokos is preparing a paper [ANL-HEP-PR-92-51], where the subtleties of the

interchangeability of the limits $p^0 \to 0$, and $\vec{p} \to 0$ (with p^μ the four-momentum of the external particles) are clarified. These limits have dynamical interpretations in the theory.

In a separate collaboration, Vokos, G. Boyd (Chicago), D. Brahm (Caltech), and S. Hsu (Harvard), are constructing the effective action in the standard model at finite temperature. Among the most important byproducts of their work [ANL-HEP-PR-92-52], is the exact momentum-dependence of the polarization tensors of the massive vector bosons and the Higgs, together with improvements in the bounce and sphaleron solutions.

Probing New Gauge Boson Couplings via Three-Body Decays

The possibility of using rare, 3-body decays of a new neutral gauge boson, Z_2, to probe its gauge couplings at hadron colliders has been investigated by Hewett and Rizzo [ANL-HEP-PR-92-33]. Specifically, the decays $Z_2 \to W\ell\nu$ and $Z_2 \to Z\nu\overline{\nu}$ have been studied, with the result that much knowledge of the Z_2 properties can be obtained from these processes. In particular, these decay modes can yield valuable information on the amount of $Z_1 - Z_2$ mixing, on the generation dependence of the Z_2 couplings, on the properties of the new generator associated with the Z_2, as well as being used to distinguish between possible extended models. The analogous 3-body decays into a new, heavy charged gauge boson, $Z_2 \to W_2^{\pm}\ell^{\mp}\nu$, are also investigated in models where this can occur.

The Effects of Detector Descoping and Neutral Boson Mixing on New Gauge Boson Physics at the SSC

Hewett and Rizzo have examined [ANL-HEP-PR-92-34] how the abilities of an SDC-like detector to discover and identify the origin of a new neutral gauge boson are affected by $Z_1 - Z_2$ mixing and by variations in detector parameters, such as lepton pair mass resolution, particle identification efficiency, and rapidity coverage. Also investigated is the sensitivity of these results to variations in structure function uncertainties and uncertainties in the machine integrated luminosity. Such considerations are of importance when dealing with the issues of detector descoping and design. The results show that upgrades in the detector parameters over the SDC default values do not yield substantial improvements in Z_2 model differentiation, but a severe descoping could cause appreciable deterioration in the discovery and model identification ability. The results also show that the incorporation of $Z_1 - Z_2$ mixing does not significantly change the resulting determination of the Z_2 couplings.

Gluon Density at Intermediate Values of x

In next-to-leading order $O(\alpha_s^3)$ quantum chromodynamics, gluon-gluon interactions are the dominant mechanism for the production of bottom quarks at CERN and Fermilab hadron collider energies at values of momentum transfer currently accessible. There is a notable discrepancy between the Fermilab CDF data and existing $O(\alpha_s^3)$ theoretical calculations. Beginning with the recognition that the theoretical predictions are strongly sensitive to the magnitude and shape of the gluon density, Ed Berger and Ruibin Meng, in collaboration with Wu-Ki Tung (IIT), undertook to see if the bottom quark production data could be used to determine a new gluon density. In [ANL-HEP-92-32, Rapid Communication of Phys. Rev. D, in press] they show that these data, in conjunction with data from deep inelastic lepton scattering, can be used to determine a new gluon density whose shape differs substantially from that derived from previous fits to data. The new fit to the CERN UA1 and Fermilab CDF bottom quark production data is shown in Fig.21. Based on their analysis, Berger, Meng, and Tung have produced a new set of parton densities whose other implications they will continue to investigate. There are important consequences of the new parton densities for calculations of jet production and prompt photon production at collider energies, and for the longitudinal structure function, F_L, at HERA. Shown in Fig. 22 are calculations of the longitudinal structure function based on the new set of parton densities, for three values of the four momentum transfer Q.

Z - Photon Pair Production, Radiative Z Decays, and Anomalous Couplings

There is only limited experimental knowledge about the self-interactions of the photon, W, and Z gauge bosons. Within the Standard Model, these interactions are entirely fixed by the gauge structure of the model. Experiments at hadron colliders may provide important data concerning these couplings. A few years ago, Ulrich Baur and Ed Berger investigated limits that the CDF and D0 experiments at Fermilab might place on anomalous couplings at the $WW\gamma$ vertex, based on assumed data samples of 100 pb^{-1} [Phys. Rev. D41, 1476 (1990)]. The first direct measurement of the $WW\gamma$ vertex was reported recently by the CERN UA1 collaboration from their study of the process $p\bar{p} \to e^{\pm} \nu \gamma X$. Another process that is expected to be studied soon at the Tevatron is $p\bar{p} \to Z\gamma X$. During the past six months, Baur and Berger have been examining what new information may be gleaned from such data. The principal production mechanism is provided by $q\bar{q}$ annihilation, very similar to the mechanism Berger and collaborators have studied in the past for $\gamma\gamma$ production. At tree level in the Standard Model, there is no $ZZ\gamma$ or $Z\gamma\gamma$ vertex that may contribute to $q\bar{q} \to Z\gamma$, but there may be anomalous

couplings. Baur and Berger have examined the most general set of possible couplings, as they did for the $WW\gamma$ case a few years ago. In terms of making contact with experiment, they concentrate on cases in which the Z decays as $Z \rightarrow e^+e^-$, $\mu^+\mu^-$, or $\nu\bar{\nu}$. To fully represent the $e^+e^-\gamma$ and $\mu^+\mu^-\gamma$ final states, their analysis includes contributions from radiative Z decays. In the calculation, they take into account all diagrams, with the most general $ZZ\gamma$ and $Z\gamma\gamma$ vertices, and subsequent Z decays. The research is in progress, and a paper is planned for later in the year.

Light Quarks and Small-x Physics

Theoretical discussion of the small x behavior of parton distributions is currently dominated by questions of the applicability of the Lipatov equation, the meaning of the perturbative Pomeron, etc. The Lipatov equation is satisfied by a subset of the general set of reggeon diagrams that describe the Regge limit in gauge theories. In a paper [ANL-HEP-PR-92-40] presented at the Workshop on Deep Inelastic Scattering held at Teupitz, Germany, Alan White discusses the significance of the low transverse momentum part of the Lipatov equation, and of general reggeon diagrams, for the QCD soft Pomeron. The paper then goes on to argue that light quarks provide reggeon interactions that are essential for understanding confinement in the Regge limit together with the related emergence of a (soft) Pomeron with the right physical properties from the low transverse momentum region of reggeon diagrams. Finally, the implications for small x parton distributions are considered - including the phenomenological issue of the separation of perturbative, or "hard Pomeron" effects from "non-perturbative" soft Pomeron effects.

Photonic Decay of the Z as a Probe for New Heavy Particles

In a contribution [ANL-HEP-CP-92-9] to the Workshop on Photon Radiation from Quarks, T. Rizzo examined the possibility that a high luminosity version of LEP may indirectly reveal the existence of new, very massive particles via the presence of an excess of events with isolated photons in hadronic Z decay. While the production and decay of intermediate states associated with such new particles does, in fact, generate excess events in kinematic regions not well populated by Standard Model backgrounds, the corresponding event rates were found to be generally too small for all of the various scenarios examined even if very high integrated luminosities were to become available. The specific models examined include (i) spin-0 or spin-1 excitations of the Z and (ii) "excited" quarks, both of which may occur in composite model approaches.

Probing New Gauge Boson Couplings at Hadron Supercolliders

If a new neutral gauge boson Z' were discovered at the SSC/LHC, the determination of its various couplings would be necessary in order to know from which extended electroweak model it originated; this task would be quite difficult for realistic detectors such as the SDC and GEM. This problem has continued to attract growing attention over the past 1-2 years. Rizzo has recently reviewed the current status of this problem in an invited talk given at the Physics Beyond the Standard Model III Conference, which is summarized in a contribution [ANL-HEP-PR-92-47] to the proceedings. The first analysis of this type for a realistic detector scenario was performed by Hewett and Rizzo under the assumption that the Z' decays only to Standard Model particles. With this assumption, it was shown that (i) the new gauge bosons from various models would be relatively easy to distinguish, but (ii) that determining the Z' couplings themselves would be difficult. This analysis used the following input: the mass of the Z', its width, production cross section, and the forward-backward asymmetry for leptons. While the assumption of only SM decays is known to be applicable in some models, it is a general weakness of this approach. Subsequent analyses have thus concentrated on finding observables insensitive to this assumption.

Several sets of authors have examined 3- and 4- body Z' decay rates relative to the Drell-Yan channel and have found reasonable sensitivity to Z' couplings for masses less than 1-2 TeV. Some of these modes were shown to provide a unique window into the group structure of the extended gauge model. Anderson et al. re-examined the possibility of measuring the polarization of taus from Z' decay to probe the Z' couplings. Due to the large QCD and W^+W^- backgrounds, coupling sensitivity was only obtainable for relatively light Z' bosons. Fiandrino and Taxil have used polarized p-p interactions in order to explore Z' couplings in the Drell-Yan production mode. While this approach offers the cleanest signature even for a high mass Z', such an analysis is presently hampered by our poor knowledge of the polarized parton densities.

Quantum Algebras Inducing Supersymmetry

C. Zachos has followed up on his recent work [Mod. Phys. Lett. A7 (1992), 1595] which links the unconventional multicomponent wave function permutation structures of quantum algebras with supersymmetric behavior; he reported on these results at the XXIst International Conference on Differential Methods in Theoretical Physics, Tianjin, China [to appear in the proceedings]. R.B. Zhang (IAS, Canberra) was "inspired by [this] work" to work out the "essential" isomorphism between U_q(OSp(1|2n)) and U_{-q}(SO(2n+1)) restricted to tensorial representations.

It appears that q-deformations provide a smooth interpolation between bosons and fermions. Indirectly, it had been noted that deformer functionals of bosons suggest nilpotence (the Pauli exclusion principle), which remains the genuine hallmark of fermionic behavior---but this appeared to follow from mere anticommutativity of some wave functions in specific representations. For instance, in the deformed algebra $bb^\dagger - qb^\dagger b = 1$, deformation to conventional bosonic oscillators $A, A^\dagger$

$$b^\dagger = \sqrt{\left(q^N - 1\right)/\left((q-1)N\right)}\ A^\dagger$$

suggests a zero in the state $b^\dagger b^\dagger|0\rangle$ for $q = -1$, whence the exclusion principle.

But this is a far more general phenomenon, and representation-dependence may, in fact, be obviated [work in preparation]. Already at the algebraic level, the relation following from the above algebra: $bb^\dagger b^\dagger = q^2 b^\dagger b^\dagger b + (q+I)b^\dagger$ reduces to

$$bb^\dagger b^\dagger = b^\dagger b^\dagger b$$

for $q = -1$; so, acting on the vacuum state with $bbb^\dagger b^\dagger$ likewise yields $b^\dagger b^\dagger|0\rangle = 0$. However, this interpolation has not yet been achieved in complete generality, and, as a result, q-deformations still do not automatically blend graded and conventional bosonic algebras into the same one-parameter structure, and normally each has to be deformed separately---the noncommutative plane and quantum superplane are distinguishable. (Nevertheless, two parameter unifications are available). The implications of this transmutation are being pursued further. (C. Zachos)

III. EXPERIMENTAL FACILITIES RESEARCH

A. Mechanical Support

The Mechanical Support Group was involved with a number of projects during this reporting period. The largest percentage of the effort was devoted to Solenoidal Detector Collaboration (SDC) Detector R&D. Other projects included Soudan 2, and the Argonne Wakefield Accelerator. A small amount of effort was developed to the conceptual design of an electromagnetic calorimeter for the STAR detector at RHIC.

1. SDC

Argonne's involvement in SDC has been extensive from its inception, and we will continue to make significant contributions to its design and construction. SDC will be one of two detectors to be installed and operated when the SSC comes on line in the late 1990's.

The Argonne High Energy Physics Division has played a major role in the mechanical design of the central calorimeter. The conceptual design has passed through its final stages and progressed to the submission of the Technical Design Report published in April of 1992. Most of the baseline design concepts in this report in large part were generated by the Mechanical Support Group for the ANL High Energy Physics Division.

The details of this effort for this period are described below.

a) Test Castings for the Lead Electromagnetic Calorimeter (EMC)

To date three EMC test lead castings have been produced. Two were used in the test beam at Fermilab during the previous reporting period to produce test beam data, and the third was cast during this reporting period to test and confirm mechanical structure, lead alloys, and lead-to-structural support connections. This casting is shown in Fig. 23. As a precursor to this final 10-tower casting, Argonne, in conjunction with our industrial partner, Westinghouse Science and Technology Center (WSTC), produced a small (18-cell) casting to test casting processes and alloy dispersion. This small casting was then cut apart and tested to confirm alloying uniformity and yield strength. The tensile tests and hardness uniformity are illustrated in Figs. 24 and 25.

As a further test to investigate lead to bulkhead connections and end frame to lead terminations, three small single plate molds were designed and built. The mold and test setup are shown in Fig. 26.

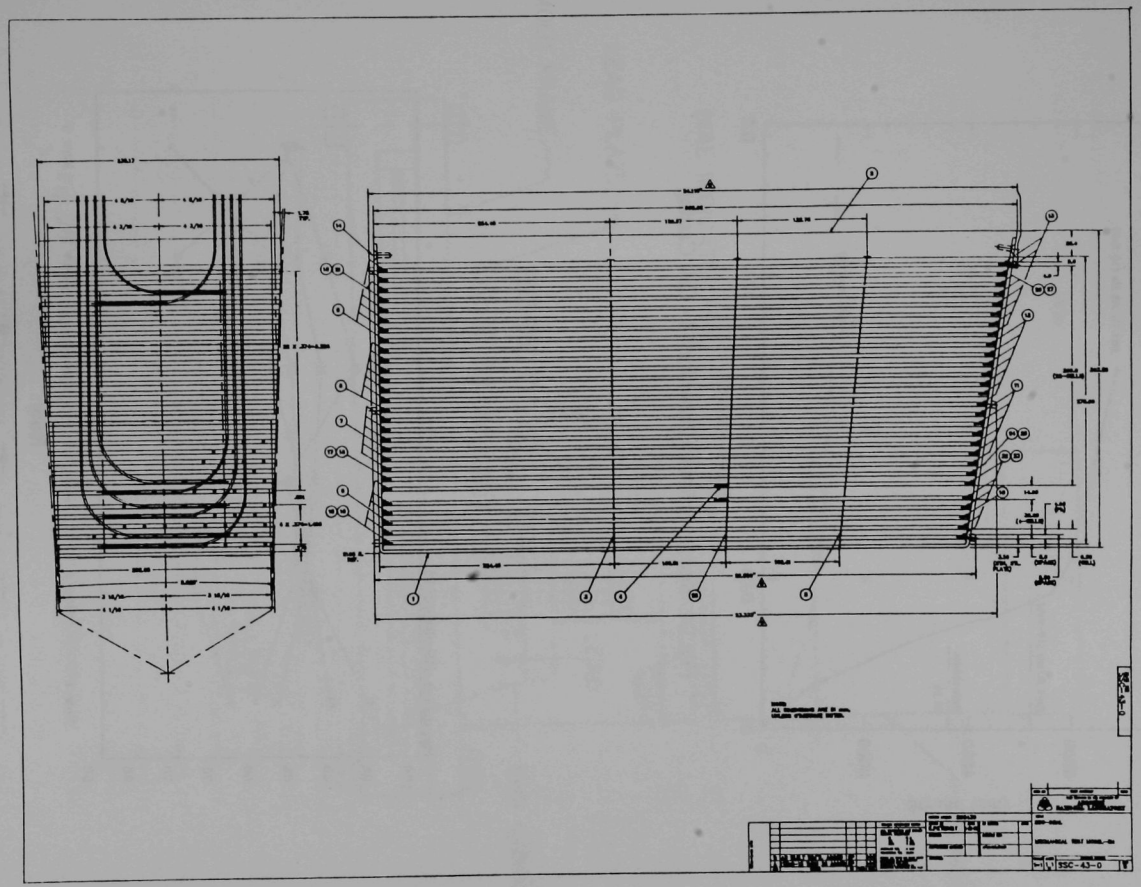

Fig. 23. SDC Mechanical Test Casting

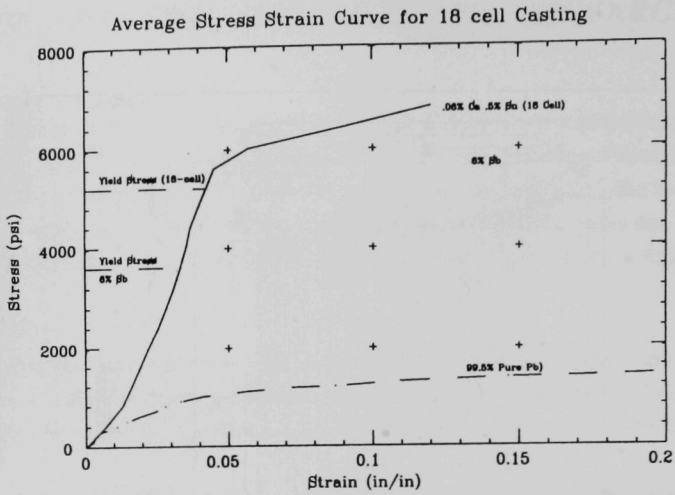

Fig. 24. Stress vs. Strain Curve for 18 - Cell Casting

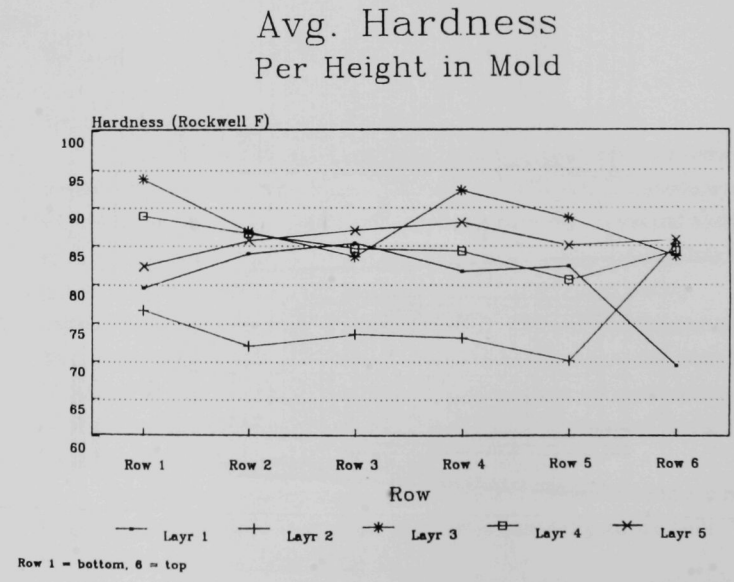

Fig. 25. Hardness of 18 - Cell Casting Samples

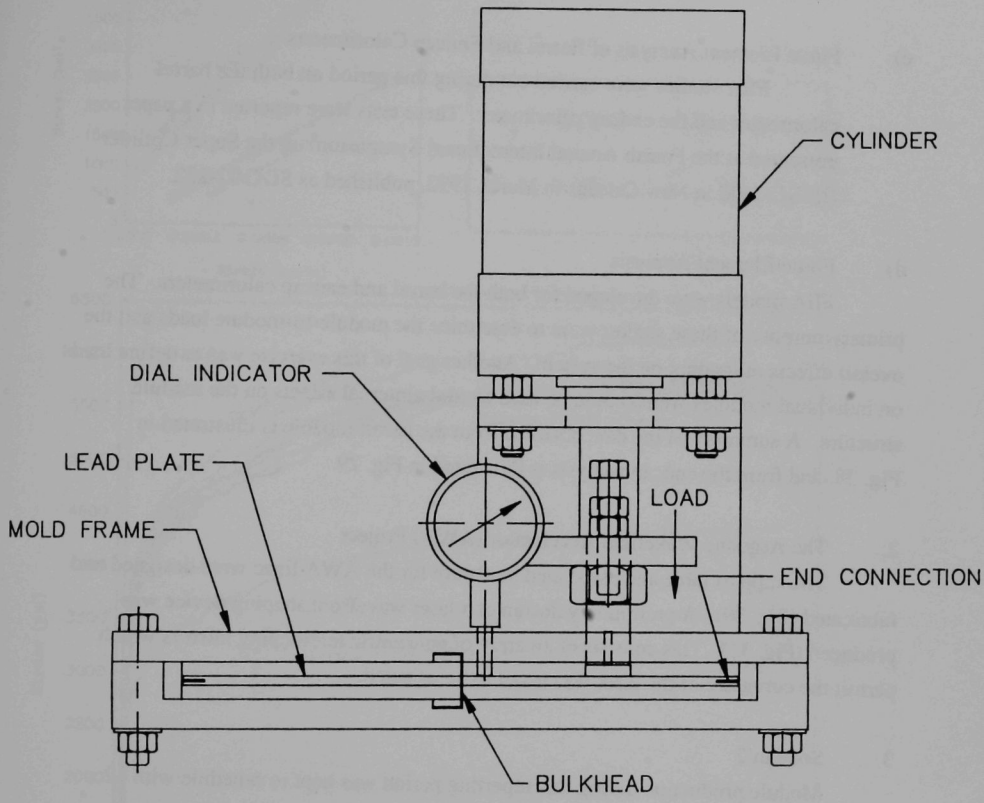

Fig. 26. Test Setup for Bulkhead to Lead Connections

b) Alloy Evaluation

Extensive testing of lead and Ca/Sn/Pb alloys was conducted to confirm yield stress and creep characteristics; a representative plot of results from these tests is presented in Fig. 27.

c) Finite Element Analysis of Barrel and Endcap Calorimeters

FEA studies were carried out during this period on both the barrel calorimeter and the endcap calorimeter. These tests were reported in a paper presented at the Fourth Annual International Symposium on the Super Collider (IISSC) held in New Orleans in March 1992, published as SDC 92-222.

d) Finite Element Analysis

FEA models were developed for both the barrel and endcap calorimeters. The primary purpose of these studies were to determine the module-to-module loads and the overall effects of loading on the system. Another goal of this exercise was to define loads on individual modules which could be used to study internal effects on the module structure. A summary of the data obtained from the barrel module is illustrated in Fig. 28, and from the endcap analysis is illustrated in Fig. 29.

2. The Argonne Wakefield Accelerator (AWA) Project

The support table and associated hardware for the AWA linac were designed and fabricated (Fig. 30). A preliminary design of a laser wavefront shaping device was produced (Fig. 31). This consists of an array of concentric telescoping mirrors which permit the curvature of the laser wavefront to be adjusted.

3. Soudan 2

Module production during this reporting period was kept to schedule with 12 modules produced, except for delays incurred as a result of poisoning of the gas by adhesives used in bandolier production. Extensive testing was necessary to define the problem, and many corrective measures were taken such as baking the bandolier, purging with many cycles of gas, and rehumidifying the bandolier prior to subjecting the modules to high voltage.

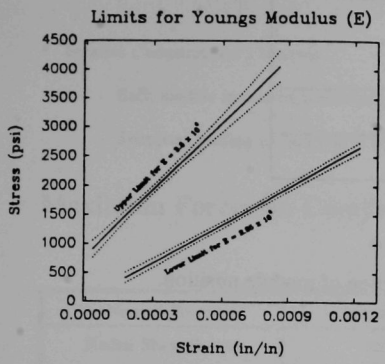

σ_y = 3,200 – 3,500 p.s.i

E = 3.05 x 10^6 p.s.i

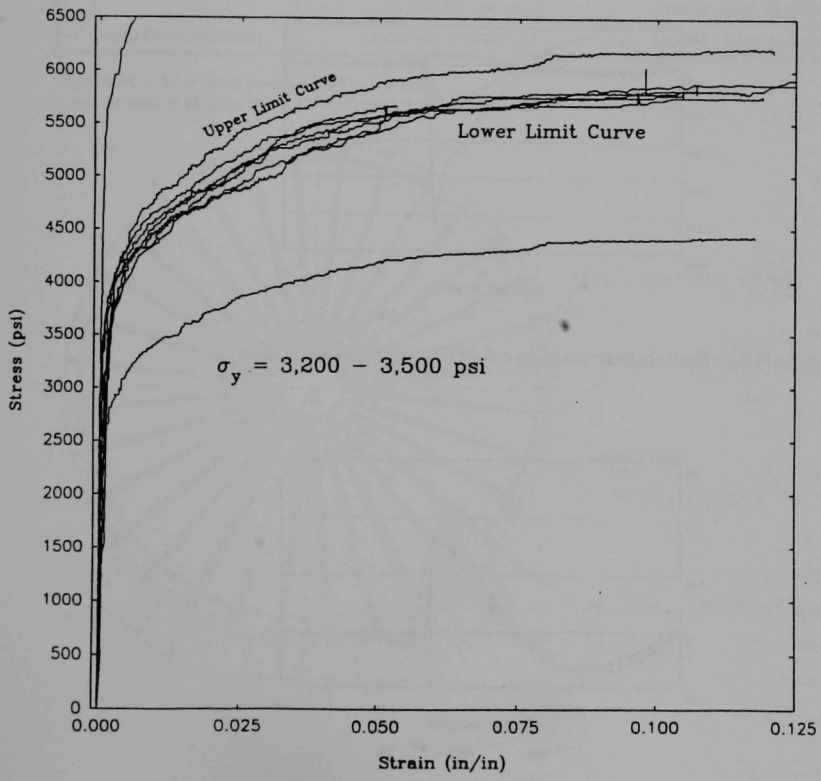

Fig. 27. Stress-Strain Curves for L50737 Lead Alloy
.06% Ca .5% Sn

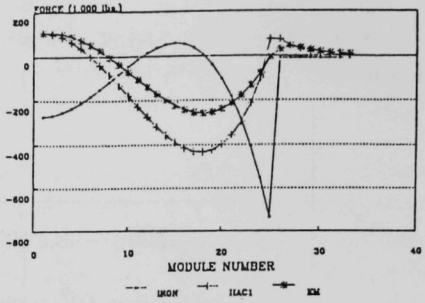

Forces normal to the surface as a function of module position.

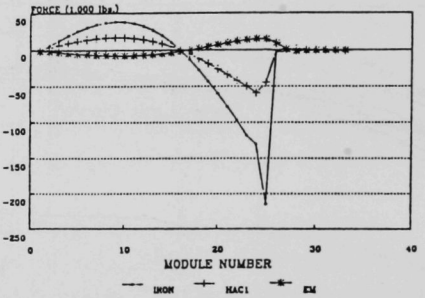

Radial shear force as a function of module position.

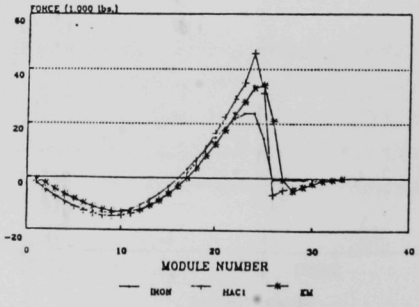

Beam direction shear forces as a function of module position.

Fig. 28. Barrel Calorimeter FEA Results

End Cap Finite Element Analysis

* Iterative ("construction") analysis
  - Each module is created individually and added into structure
  - Simulates loading as End Cap is being built

Maximum Forces on Completed Structure:

	Force (lbs.)	Location
Normal Forces	-125,000 lbs. (compression)	Module #10/11 Boundary
Radial Shear Forces	-126,000 lbs. (inward) 67,000 lbs (outward)	Module #12/13 Boundary Module #7/8 Boundary
Beam Direction Shear	-4,200 lbs. (towards I.P.)	Module #10/9 Boundary

Module #1 = 12 o'clock position, #17 = 6 o'clock
Supports start at Module #12

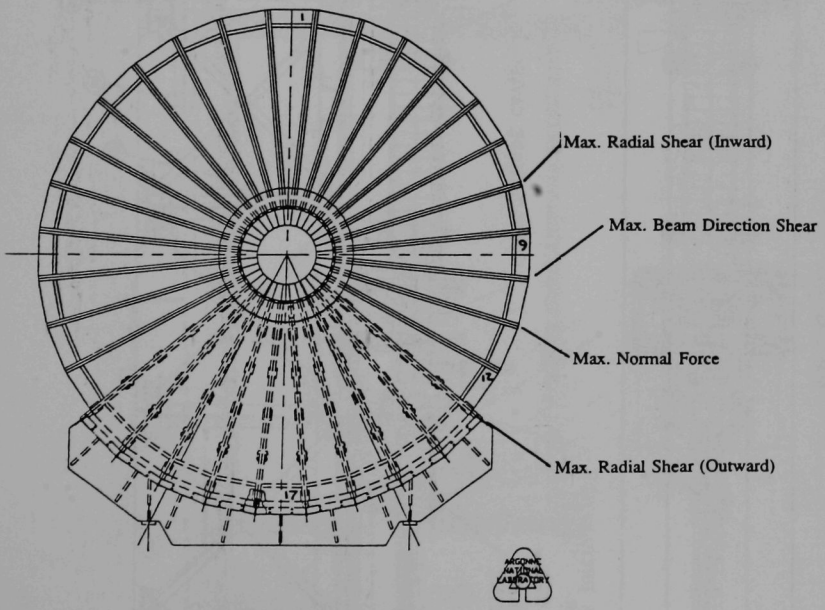

Fig. 29. Endcap Calorimeter FEA Results

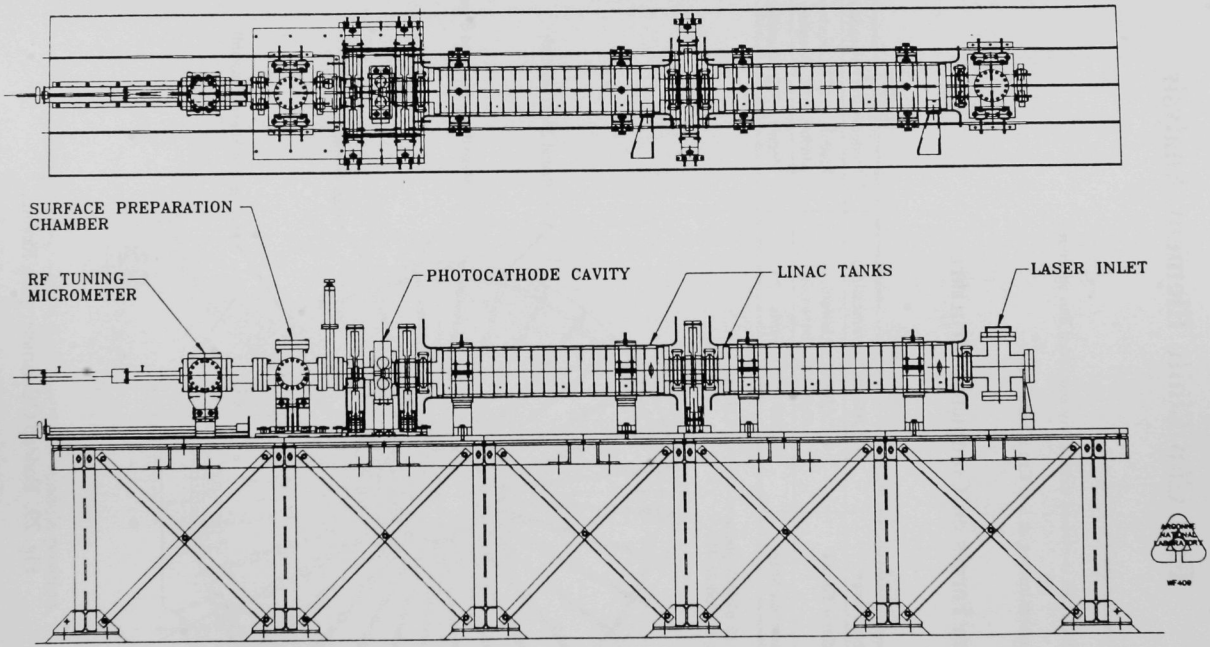

Fig. 30. AWA LINAC Components and Support System

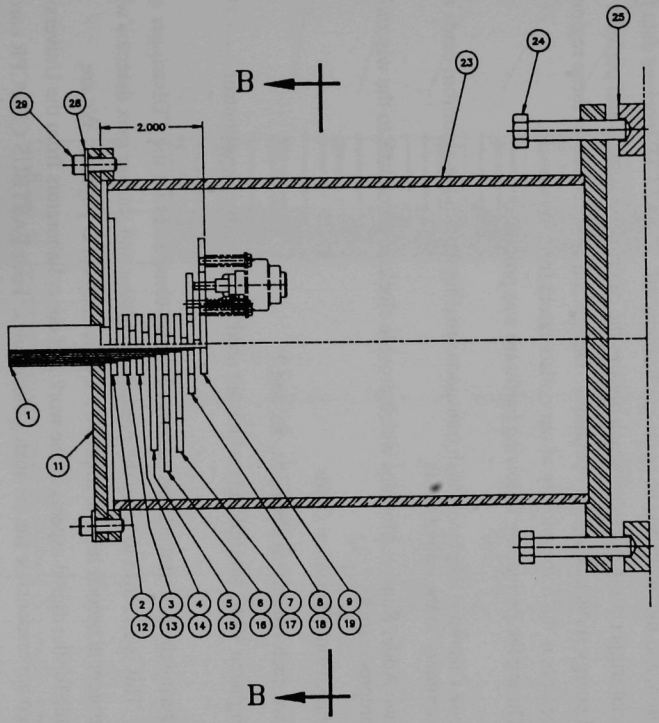

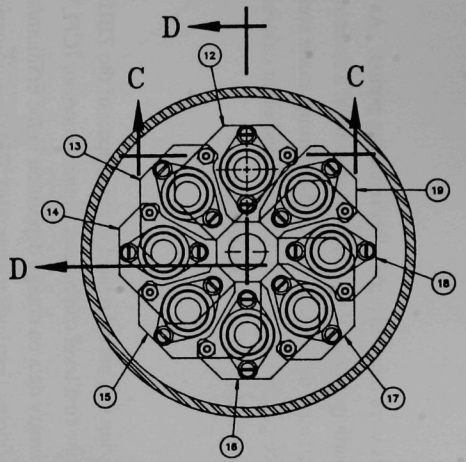

Fig. 31 AWA Laser Wavefront Shaping Mechanism

4. STAR

Two design projects were initiated during this reporting period. As part of the Argonne HEP Division's participation in the collaboration to build a detector for RHIC at Brookhaven National Laboratory, the Mechanical Support Group made some conceptual designs using the experience gained with SDC, CDF, HRS and other calorimeters. These conceptual design are represented in Figs. 32, 33, and 34.

(N. Hill)

B. Electronic Support

Our major effort during this period related to the support of the ZEUS calorimeter was in the development of the first level calorimeter trigger processor (CFLTP). The ZEUS CFLTP presents summary data on energy deposition in the uranium/scintillator sampling calorimeter to the global first-level trigger (GFLT). The summary data includes global and regional sums of electromagnetic and hadronic energy deposition, the number of isolated muons and isolated electrons, missing transverse energy, jet cluster information, and the likelihood of beam-gas background. The CFLTP receives data from 16 regional trigger pre-processors which digitize the calorimeter signals and perform regional energy sums and logical operations. Design and construction of these regional pre-processors is the responsibility of our collaborators from Wisconsin.

During the period, the following hardware was produced:

- one Custom Backplane which transports crossing data to the algorithm cards and summary to the output cards
- two Adder Support Modules which provide clocks and controls to the wisconsin preprocessors
- three Communication Cards
- two each Algorithm Cards, 5a, 5b, and 7
- eighteen VME Multiplexers which are used by DESY for slow control

During the period work has continued on our electronics for the CDF trigger upgrade. This is an effort to bring the preshower radiator and shower max detector wires into the trigger at second level to improve the efficiency for B physics. We are responsible for the digital aspects of the work and our collaborators from the University of Chicago are responsible for the analog electronics. Four FASTBUS CES/CPR cards were produced and are being tested. This card is manufactured in surface mount

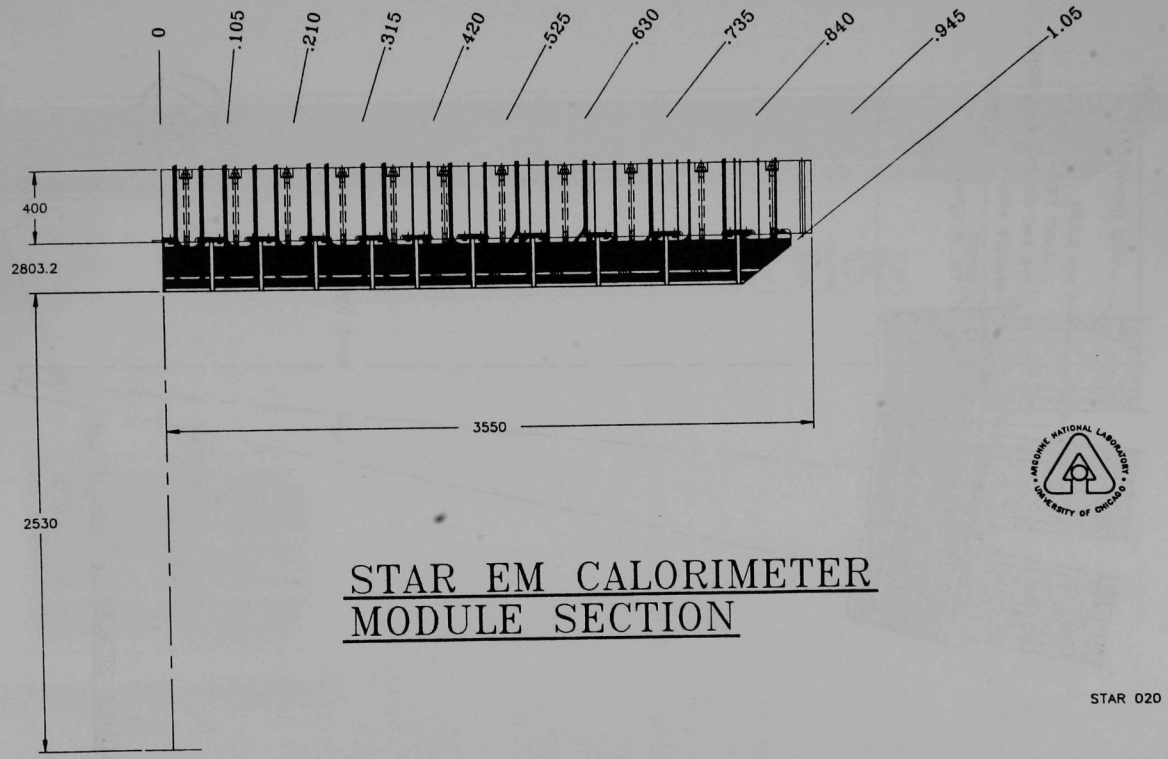

Fig. 32. Conceptual Design for the STAR EM Module

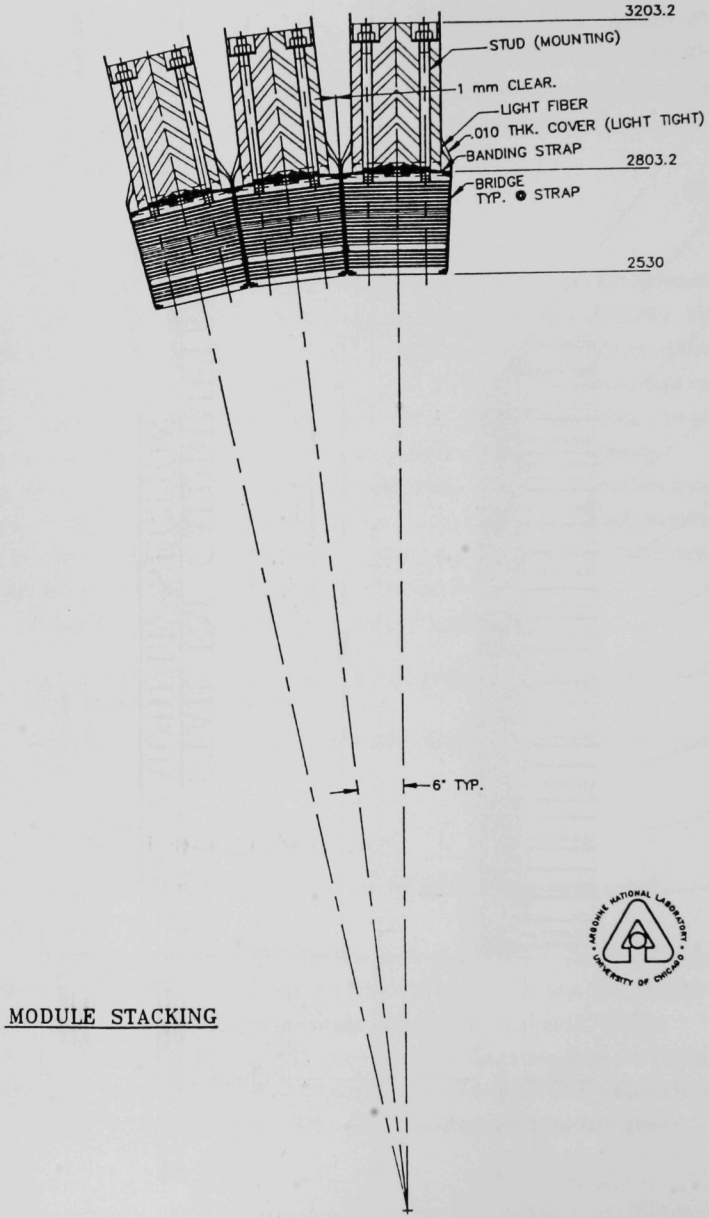

Fig. 33. Beam-Line View of STAR Modules (Conceptual)

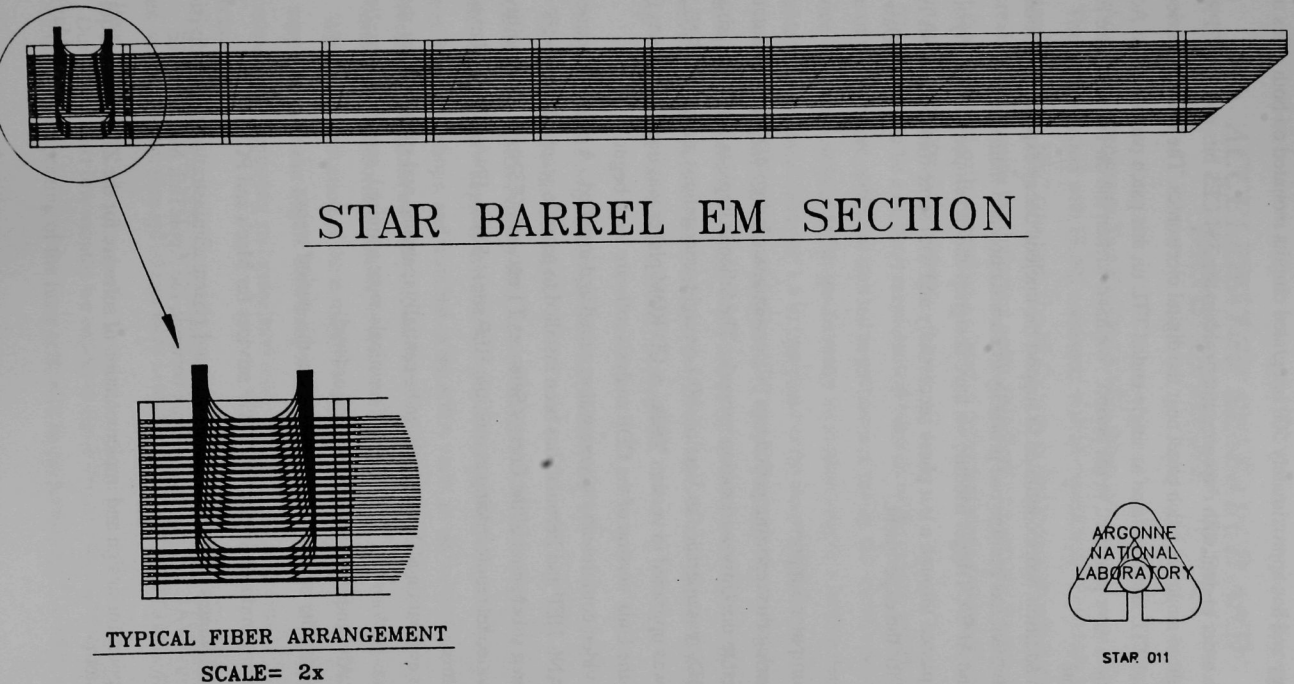

Fig. 34. Conceptual Fiber Routing Scheme for STAR EM Modules

technology and has approximately 500 integrated circuits mounted on both sides of the card.

In order to deal with the connector problem the 384 CES bits and 192 CPR bits are brought to an active patch panel near the digital electronics. The bits are carried as differential TTL and translated to single-ended TTL on this patch panel. Three Active Patch Panels were produced in the period. We have written the on-line software for data acquisition.

In addition, work continued to support the nucleon decay experiment, Soudan 2. Our involvment has become one primarily of construction and maintenance.

The APEX Trigger Module we have designed and developed for the Physics Division passed through a test phase successfully and with some minor revisions is being produced for the experiment. (J. Dawson)

C. Computer Support

During this reporting period two Silicon Graphics Indigo 4D/RPC workstations were added to the Unix workstation network. The Silicon Graphics Unix operating system IRIX was upgraded to Version 4.0.1 on eight workstations and the CERNLIB software was upgraded to version V92a. A CD ROM player was installed. Plans for installing the Unix version of the CDF analysis software were begun.

A video conferencing system was acquired and installed. A network connection between ANL HEP and Fermilab has been installed to provide access the the HEP video network on a subchannel of the Energy Sciences T1 network (ESNet). This facility provides video teleconferencing to multiple HEP sites: SSCL, FNAL, LBL, Harvard, and KEK (Japan).

An evaluation of X terminals, to be centrally managed and supported for the HEP division was performed. Three NCD X terminals were acquired, set up and installed on the HEP LAN, and three more have been ordered.

Among the other services provided in this period were:

- Testing and installation of TCP/IP services for Mac's and PC's .
- Continuing support for maintenance and system adminstration for the division central VAX cluster, the Sgi Unix network, the AppleTalk Mac's and the Pathworks PC's.
- Support for design and implementation of software for the ZEUS data acquisition system.

(E. May)

IV. ACCELERATOR RESEARCH AND DEVELOPMENT

A. Advanced Accelerator Test Facility (AATF) Program

The collaboration with SLAC continued with an experiment to measure wakes in a full-sized prototype NLC structure. The NLC cavity is designed to suppress multibunch beam breakup by detuning the deflecting wake, specifically by varying the gap and iris sizes of the individual cells to produce a spread of deflecting mode frequencies but a common accelerating mode frequency.

This proved to be a difficult measurement because of the overall length and small iris size of the structure, which in turn led to problems in tuning the witness beam through the device. Witness intensity at the spectrometer focal plane was low, with a maximum achievable driver-witness delay of 1.5 ns compared to the desired 3.0 ns.

Nevertheless, we did observe detuning of the deflecting wake in the structure. Interpretation of the results is further complicated by the effects of beam scraping insofar as the cavity design assumes identical coupling of the beam to all cells for optimal detuning. Analysis of the data is currently in progress.

B. Progress on the Argonne Wakefield Accelerator (AWA)

1. Construction Status Overview

During the period January thru June of 1992 the AWA drafting and construction proceeded rapidly. The support table for the gun and preaccelerator was designed, fabricated in central shops, and installed in the AWA vault. In addition, the copper for the preaccelerator was machined and polished in the optical shops to a mirror finish. The cavity fabrication is described further in section 4 below.

While the fabrication of these major components was underway, the drafting of minor support equipment began. This category includes magnet iron and supports, photocathode plug mounting and associated motion control hardware, and other linac support components.

The control room configuration was finalized, and the remaining electrical services were installed. Fire sprinklers were installed in the control and laser rooms and in the linac vault.

During the next few months we expect to finish the rf coupling cells to the preaccelerator. Final brazing of the linac cells will be performed by Pyromet. Cooling

water and electrical service will be installed during this time for the main solenoid magnets, as well as chillers to maintain photocathode gun and preaccelerator cavity temperatures. Designs for the radiation and laser safety systems for the linac tunnel are complete and will be installed by October.

2. Laser System

Commissioning of the laser system was performed during February and March. Both Coherent and Lamba Physik personnel were involved in this process. The measured performance of the each individual laser is given in the table below.

Laser	Output	Pulse length
Nd:YAG laser	25 W	100 ps
THG	1.5 W	70 ps
702 Dye laser	100 mW	1.5 ps
3-stage dye amplifier	300 μJ	1.5 ps
Final excimer amplifier	8 mJ	3 ps

Streak camera measurements show no apparent satellite pulses. The amplified spontanous emission is approximately 10%, measured 20 cm from the exit window. Timing jitter measurements were performed using both time and frequency domain techniques. The former consisted of a direct measurement of the waveform produced by the output of the 702 dye oscillator incident on an ultrafast photodiode (25 ps rise time) using a Tektronix sampling oscilloscope. This method yielded an upper limit on the timing jitter of 15 ps (peak to peak).

The frequency domain technique provides a more sensitive measurement of jitter. The photodiode signal is input to an rf spectrum analyzer (HP8569B). Assuming the timing jitter is essentially random, the Fourier transform of the imperfect mode-locked pulses indicates that the measured phase noise power spectrum is proportional to the squared harmonic number, but the amplitude noise spectrum is independent of harmonic number. Thus by choosing a sufficiently high harmonic mode, the measured noise will be dominated by the phase noise. By assuming all contributions to the noise spectrum are due to phase noise for a particular higher mode number (typically > 20 in practice), the upper limit of the rms timing jitter can be calculated. Figure 35 shows the frequency domain measurement for the 75th harmonic of the laser pulses. The timing jitter for this data is 2.5 ps rms, which is within our specifications.

The acceptance test of the laser system took place on April 17. The laser was run continously for a 6 hr period at rep rates as high as 35 Hz (30 Hz nominal). All performance specifications were met.

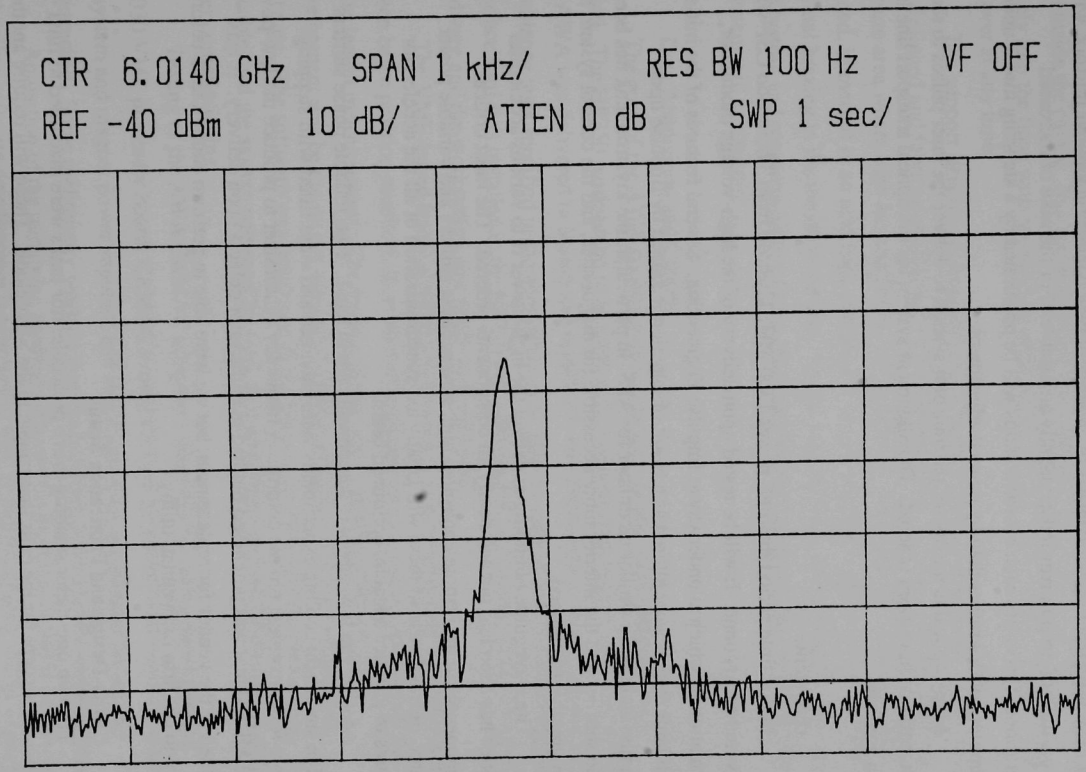

Fig 35. Measured phase noise spectrum for the AWA laser system.

The wavefront shaper has been designed and is being fabricated. It will provide a shaped laser wavefront to produce an initially curved electron bunch in the photocathode gun. The wavefront shaper consists of an array of nine concentric annular mirrors, with the position of each mirror independently adjustable. For the sake of increased operational flexibility each mirror annulus will be positioned by a stepping motor under computer control rather than by manual adjustment.

Many optical elements for the transport system to deliver the laser pulses to the photocathode have been ordered. The alignment system for the optical transport line has been studied.

3. rf System

In this time period the high-power 1300 MHz klystron from Thompson CSF was delivered to Argonne. It will be tested upon delivery of the high-voltage modulator, fabrication of which is underway at Impulse Engineering. Several features of the initial modulator design were altered as a result of experience gained by Impulse upon commissioning of a similar modulator for APS. In particular, the klystron tank has been made sturdier and the interior more accessible for diagnostics, and the control system has been greatly streamlined.

The waveguide plumbing to deliver the high-power rf to various accelerator cavities has been laid out and nearly all components ordered. The most critical components are the remote controlled high-power phase shifters and variable power splitter. Reliable use of these will greatly aid synchronization of all the accelerator cavities to produce a stable, optimized beam.

Most of the low-power rf components are in hand. Two reliable phase shifters used in stochastic cooling experiments were salvaged and were fitted with stepping-motors for convenient remote control. A frequency synthesizer to produce the low-power 1300 MHz signal was purchased but had manufacturer defects upon delivery. It was returned to the vendor for replacement, but we were able to perform enough tests before return to confirm its eventual utility.

4. Cavity Design and Fabrication Status

The two one-meter standing-wave preaccelerator tanks were machined to final dimensions, except for the cells that couple to the waveguide. These will require another month of testing and tuning before fabricating the cell/coupling iris/waveguide transition from a solid block of copper. It was determined that the rf input iris should be a long thin H-field coupler rather than a waveguide "full-height" E-field coupler. In a standing-wave

cavity linac section, the rf power builds to a high steady state level inside the cavity on the time scale Q/ω with large initial power reflection from the coupling iris, thus requiring a thin iris that allows the input power to hold back the large radiation pressure from inside the cavity. In a traveling-wave linac, the rf power must flow unimpeded directly into the linac with no build-up time, thus requiring a large iris that doesn't reflect rf power at any time.

The support structure to hold and align the linac tanks in the final brazing oven was designed and fabrication initiated. All the copper linac cells were polished near the aperture area where high electric fields will be present. The cells will be ultrasonically cleaned, immersed in an acid bath, rinsed, placed in a shipping crate, and sent to Pyromet for final brazing in the month of August. By the time the linac tanks return to Argonne, the klystron and modulator should be coming on line and commissioning of the complete rf system will commence.

5. Data Acquisition and Control

The core of the AWA control system was put in place during this reporting period. The HP750 workstation to be used as the main control computer for Phase-I of the AWA was delivered in March and installed in the AWA control room. All the acceptance tests specified in the acquisition plan were completed successfully. The VME interface card was installed in the HP750 and software for data transfer between VME hardware and the workstation was developed and tested.

The VME-based frame grabber will be used to aquire video data from phosphor screen beam position monitors, laser spot diagnostics, and the streak camera used for pulse length measurements. The frame grabber was installed and tested, and development was begun on the associated video acquisition, display, and analysis software. The software was developed to the point at which useful data taking was possible, and the system was used for laser spot uniformity measurements as part of the laser commissioning.

Testing of the AWA CAMAC subsystem was initiated, using the embedded 68030 VME processor board. CAMAC is used for here for control and monitoring of the rf system and magnet power supplies, and also controls the accelerator timing and sequencing. Some preliminary work on interupt handling in the system was also begun.

Aquisition of the remaining hardware (mostly CAMAC modules) is underway, and online software development is proceeding well. Control software will be available as needed for hardware system checkout.

6. Trigger Module

The master trigger circuit provides a signal that triggers the laser and rf systems to begin their firing sequences for the generation of an electron pulse. The master trigger pulse is synchronized to the 60 Hz wall power to reduce periodic noise that is often associated with heavily pulsed loads on the power line. The capability of selecting the optimal operating phase with respect to the line signal is also provided. Finally, the repetition rate of the accelerator is also selected using this circuit.

The entire circuit has been designed on a CAMAC card so it can be used as a standard CAMAC module. The user will be able to program this card either manually by front panel knobs on the module or by computer through the CAMAC dataway bus. Design of the module has been completed. Care was taken to ensure CAMAC compatibility. All logic for this circuit is implemented on a PLD (programmable logic device) thus making the circuit both extremely compact and extremely reliable.

7. Witness Gun Development

The use of using a dielectric loaded rf gun as a possible alternative to a multicell conventional cavity for witness beam generation at the AWA is currently under investigation. Initial studies done in the last 6 months appear promising. Based on the results of a numerical simulation, it appears that a 4-5 MeV beam out of the witness gun cavity can be obtained by supplying an 80 cm length gun with about 3 MW of power, with the final output beam energy depending on the assumptions one makes about the material properties of both the metal and dielectric.

Based on a Q of 15,000 for the copper and a loss tangent of 10^{-4} for the dielectric an overall Q value of 6,500 was predicted. Several bench measurements of a prototype dielectric cavity were made, using alumina as the dielectric. Measured Q values in the range from 6,000 to 8,000 were obtained. The quality of the copper and the alumina varied enough to account for this range of Q values.

From the test, we conclude that a carefully prepared cavity can have a Q near 8,000. Based on this intial result, a serious study of the feasibility and possible advantages of the dielectric witness gun option has begun, the next step being simulation of the beam dynamics in the gun using the PARMELA code.

C. Accelerator Physics

1. High Resolution Beam Profile Monitor Development

Efficient linear colliders require very small beams to produce high luminosities with reasonable input power, which limits the number of electrons that can be accelerated to high energies. Design studies for higher energy colliders have thus proposed beam spot sizes much smaller than the 1.7 μm spot produced at the Stanford Linear Collider: from 0.090 to less than 0.001 μm. Such a small beam spot, however, becomes a very challenging test of the design, construction and stability of all aspects of the accelerator, as well as a difficult measurement problem.

A proposal to develop a beam profile monitor using bremsstrahlung was approved by the DOE. This device is in principle capable of resolutions ~ .003 μm. A demonstration test using the beam from the injector linac at the Argonne Advanced Photon source is being planned. Contingent upon success of those tests, measurements of the 0.060 μm spot which will be produced at the SLAC Final Focus Test Beam will be undertaken.

The system, shown in Fig. 36, is basically a "pinhole" camera, using 1 - 50 GeV gammas, with the height of the beam determined by the width of the penumbra caused by a collimator edge. The design of the bremsstrahlung detector, which uses a pair converter and Cherenkov radiator to produce an optical image, is determined by the requirement that it should give good position information on high energy photons but be nearly blind to low energy bremsstrahlung and synchrotron radiation. Seismic motions must also be considered. The ultimate limits of the resolution of this system will probably be set by a combination of optical diffraction, mechanical limits and seismic stability.

(J. Simpson/P. Schoessow)

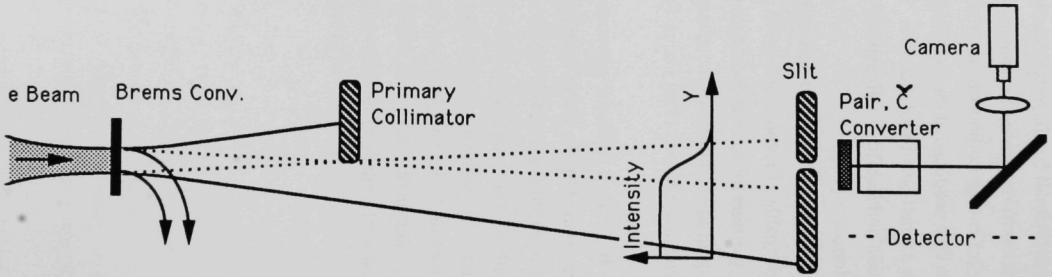

Fig. 36. High resolution beam monitor experiment schematic.

V. SSC DETECTOR RESEARCH AND DEVELOPMENT

A. Overview of ANL SSC Related R&D Programs

Apart from participation in some general committees, Argonne's work on the SSC program is now fully focused on activities related to the SDC detector. SDC activities can be separated into categories of management, calorimetry, and computing. The SDC Technical Design Report (TDR) was submitted to the SSC Laboratory on April 1. Argonne physicists played major roles in preparation of both the calorimetry and computing chapters.

In the management area, Argonne has members on the collaboration's Executive Board (L. Price) and Technical Board (L. Price and J. Proudfoot). Participation in the management work of the Executive Board has included chairing a subcommittee on management of SDC during the construction phase, which finished its work during this reporting period.

Calorimetry takes the majority of ANL effort on SDC and is expected to be the area where Argonne will contribute in a major way to the construction of SDC. A beam test of a portion of electromagnetic calorimeter, expected to be very close to the final design, was completed at FNAL at the end of CY 1991. This test used an integral lead casting and scintillator tiles with wavelength-shifting fiber readout as described in the TDR. Analysis of that data and use of the results in refinement of the design was a major activity during the first half of 1992. In parallel with that analysis, final work on the conceptual design of the calorimeter was completed and described for the TDR. Other R&D work related to calorimetry was ongoing and included simulations of many calorimeter configurations, especially those employed by us and others in the recent test beam run. Refinements and tests of the optical system, both optimizing light output and measuring radiation hardness also continued. L. Nodulman acted as overall editor of the Calorimeter chapter of the TDR and others at ANL wrote substantial parts of it.

Computing saw two types of activity. One was ongoing leadership and work in the computing group. A successful workshop was held in January at SSCL and defined three task forces which were organized over the next few months. L. Price edited the Computing chapter of the TDR and Argonne people wrote parts of it.

The other major activity related to the national High Performance Computing and Communications (HPCC) Initiative. Early funding had been provided to a collaboration of Argonne, University of Illinois at Chicago, and University of Maryland to investigate

solutions to the data storage and access problem of detectors at the SSC and related data-intensive scientific activities. In April, an expanded collaboration, including LBL and SSCL, was approved as a five-year project in the DOE HPCC program. The project was also included in a proposal from Argonne and many other institutions for a High Performance Computing Research Center, to include substantial leading-edge computing equipment and several research projects. (L. Price)

B. Compensating Scintillator Plate Calorimeter R&D

1. Introduction

The conclusion of the test beam program associated with this project occurred in early January. With this milestone reached, the emphasis has shifted to test module data analysis, final design details for casting a full length module, and R&D associated with specific design questions (scintillator tile geometry and radioactive source calibration). This design using cast lead absorber is the baseline design for the SDC barrel EM calorimeter. Further work on alternatives is being phased out.

2. Test Module Data Analysis

The main concern of the SDC calorimeter group has been the response uniformity and homogeneity of the cast lead electromagnetic calorimeter design. These issues have been the focus of the analysis in the period up to July 1992. The questions are twofold:
a) how much is the response degraded by cracks and uninstrumented support mass;
b) can a correction be developed to optimize the uniformity of the device.

Figure 37 shows the response of the calorimeter to 35 GeV electrons in a scan along the length of the module. The arrows indicate the positions of 0.5 mm thick stainless steel bulkheads, which form part of the absorber support frame. The loss of signal response is significant in these regions and is reflected in a significantly poorer resolution (Fig. 38a). The curve is a fit to the response using the impact point on the calorimeter as measured by the beam system (to resolution ~ 2 mm). When this fit is used to correct the observed signal, the resolution in the region of the bulkheads is much improved (Fig. 38b). The resolution distribution for the three central towers, in which there is full containment, is shown in Fig. 39 and shows the excellent uniformity attainable with this calorimeter.

A second issue which has been studied is the effect of the projective cracks between the tiles used to form pairs of ϕ towers in the test module. Their impact on the mechanical details for the full module design is on the tile size tolerances and on the bulkhead-bulkhead dimensional tolerance. Figure 40 shows the measured loss of signal

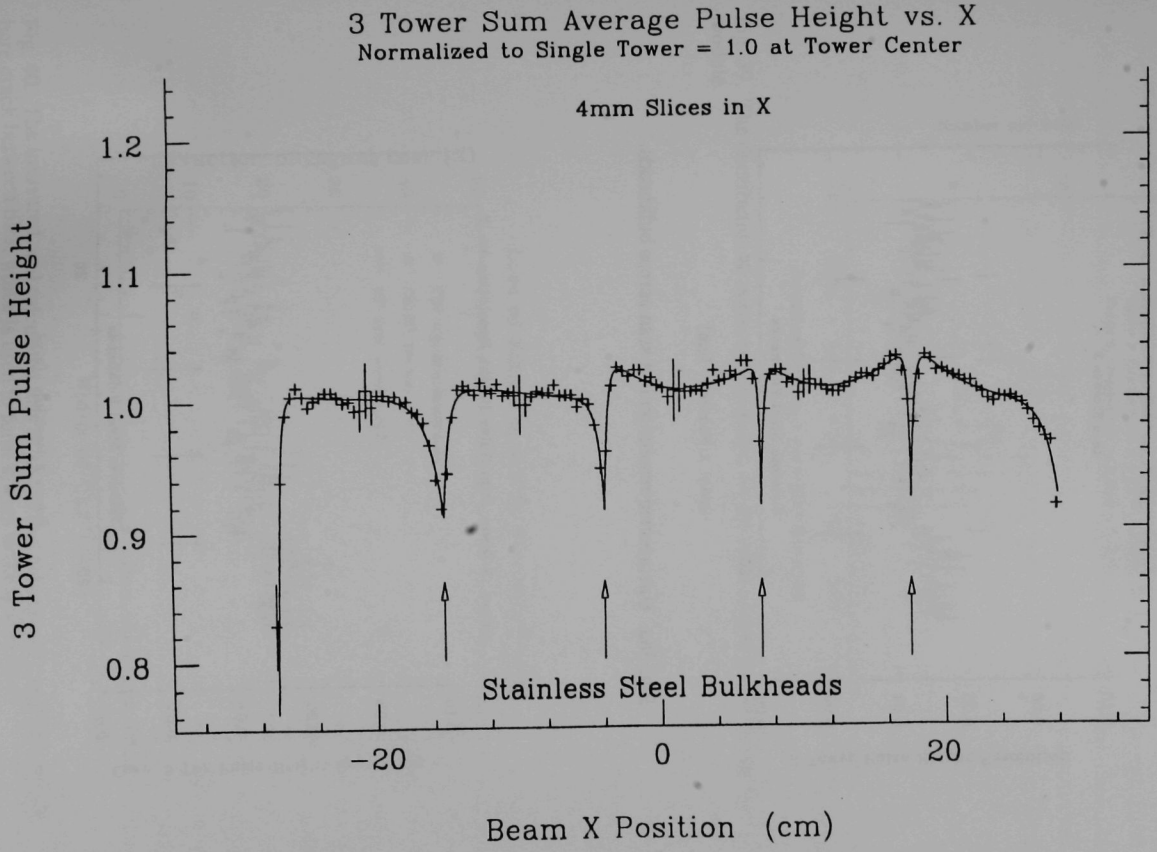
3 Tower Sum Average Pulse Height vs. X
Normalized to Single Tower = 1.0 at Tower Center
4mm Slices in X
3 Tower Sum Pulse Height
1.2
1.1
1.0
0.9
0.8
Stainless Steel Bulkheads
−20
0
20
Beam X Position (cm)

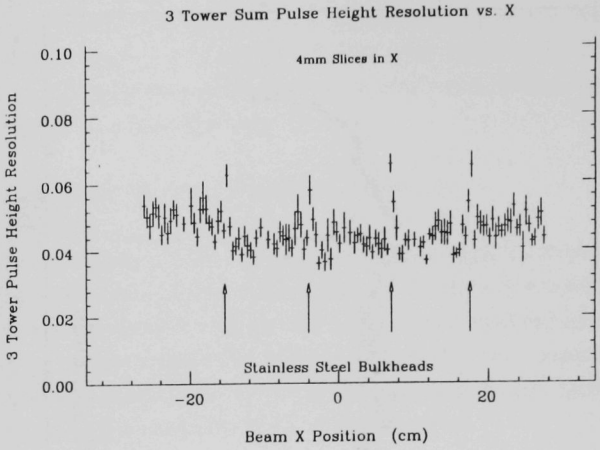

Fig. 38a. Uncorrected resolution in a scan across bulkheads.

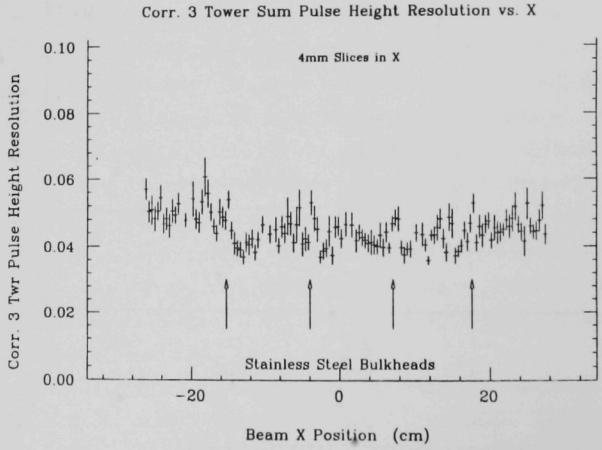

Fig. 38b. Resolution in a scan across bulkheads for the position corrected response, using the fit function shown in Fig. 37.

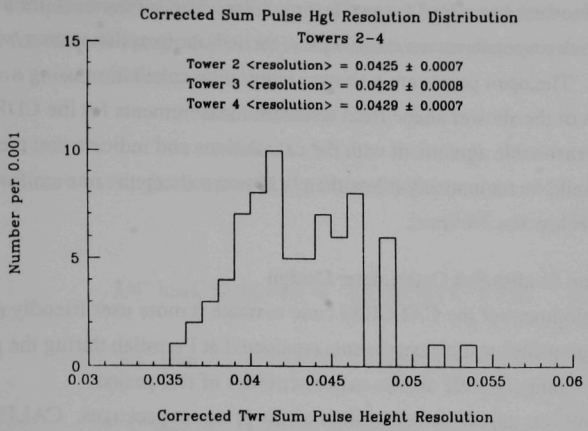

Fig. 39. The distribution of corrected resolution for the three central towers in the test module.

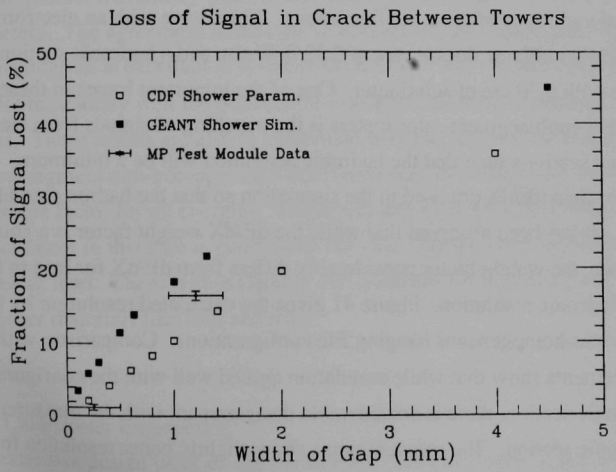

Fig. 40. The measured, and calculated loss of signal as a function of crack size for the bare crack between tiles, which is used to form towers in the ϕ direction.

between pairs of towers in each of the two test modules. The solid points are a GEANT simulation of crack response versus crack width (carried out in collaboration with Dr. J. Yarba at SSCL). The open points are a shower integration calculation using a parameterisation of the shower shape from testbeam measurements for the CDF detector. The data are in reasonable agreement with the calculations and indicate that the gap between tiles should be maintained at less than 0.35 mm to keep the non-uniformity in signal response below the 3% level.

3. Simulation Studies For Calorimeter Design

The development of the CALOR89 code to make it more user friendly and the analysis of "hanging file" test measurements conducted at Fermilab during the period September 1991 - January 1992 are the major activities of this period.

CALOR89 was supplemented with two new program packages. CALPREP is a program for the preparation of the input files for CALOR89 in general geometry and ANALYZ is an analysis package to extract the final result from CALOR89 relevant to calorimeters. Two script programs, LCALOR and PCALOR, were also implemented. LCALOR runs a CALOR89 sequence of programs and EGS4 for a given configuration sequentially on a single processor. PCALOR runs concurrently on a multiprocessor workstation.

Two hanging file non-homogeneous configurations were simulated first along with several variations of these configurations. These were with an electromagnetic section of Pb/scintillator thicknesses of 0.32/0.30 cm, and a hadronic section of 2.54 cm of Pb or Fe with 0.30 cm of scintillator. One of the important issues in these multiabsorber-multisegment calorimeters is the matching of signals from electromagnetic and hadronic sections such that the hadronic resolution will be a minimum. Weight factors other than dE/dX are used in the simulation so that the hadron resolution can be minimized. It has been observed that while the dE/dX weight factor is a good choice for lead absorber, the weight factor considerably differs from dE/dX for iron to have the minimum hadronic resolution. Figure 41 gives the calculated resolution by CALOR89 for the two non-homogeneous hanging file configurations. Comparison with the hanging file measurements show that while simulation agreed well with the configuration with Pb in the hadronic section, there is considerable disagreement with the measurement with Fe in the hadronic section. The measurements show slightly better resolution for the Fe hadronic calorimeter than Pb whereas the simulation results show the opposite.

Several other hanging file homogeneous configurations were analysed to solve this discrepancy. Altogether we have analysed ten hanging file configurations and the

results are compared with the measurements. Figure 42 gives the hadronic resolution values as a function of energy for the three homogeneous configurations. The resolutions are fitted to a functional form

$$(\sigma/E)^2 = (a^2/E) + b^2$$

The fitted values are compared with the test beam results.

3/4" lead, $52.44/\sqrt{E} \oplus 0.6$ ($51.7/\sqrt{E} \oplus 3.2$)

3/4" iron, $62.02/\sqrt{E} \oplus 3.8$ ($45.4/\sqrt{E} \oplus 3.9$)

1" iron, $63.43/\sqrt{E} \oplus 4.2$ ($57.3/\sqrt{E} \oplus 3.0$)

The number in parenthesis are the measured resolutions. Figure 43 gives the e/π and e/h ratios calculated by CALOR89. These test beam measurements are also given for comparison.

Our analysis of the hanging file experiments with CALOR89 shows that, CALOR89 can predict reasonably well the test beam measurements with the scintillating plate calorimeters. The agreement in the case of lead-scintillator homogeneous (single segment) configuration is excellent in terms of the e/π ratio and the hadronic resolution. It could predict reasonably well the outcome of iron-scintillator homogeneous configurations. These results are also in agreement with the previous measurements. In the case of two segment non-homogeneous configurations, the resolutions were optimised by a single weight factor for all energies. The agreement between CALOR89 simulation and the measurement in this case is good when both the segments consist of the same absorber material, lead. There is considerable disagreement for the configuration with different absorber materials like lead and iron.

4. SDC Calorimeter Engineering

The extensive design work on the barrel EMC and other parts of the SDC calorimeter system are described in the section on Mechanical Support (III.A.1).

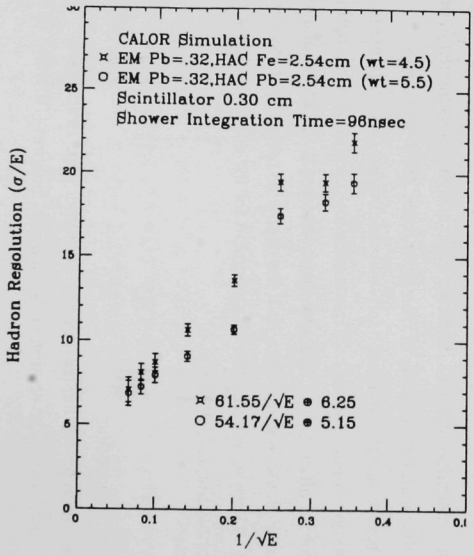

Fig. 41. Hadronic resolution for the two hanging file non-homogeneous configurations.

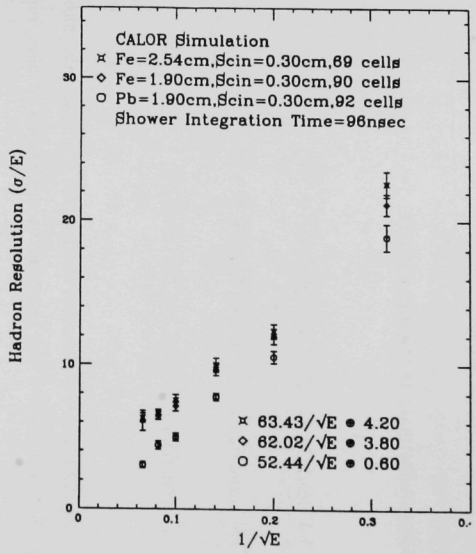

Fig. 42. Hadronic resolution for the three homogeneous hanging file configurations.

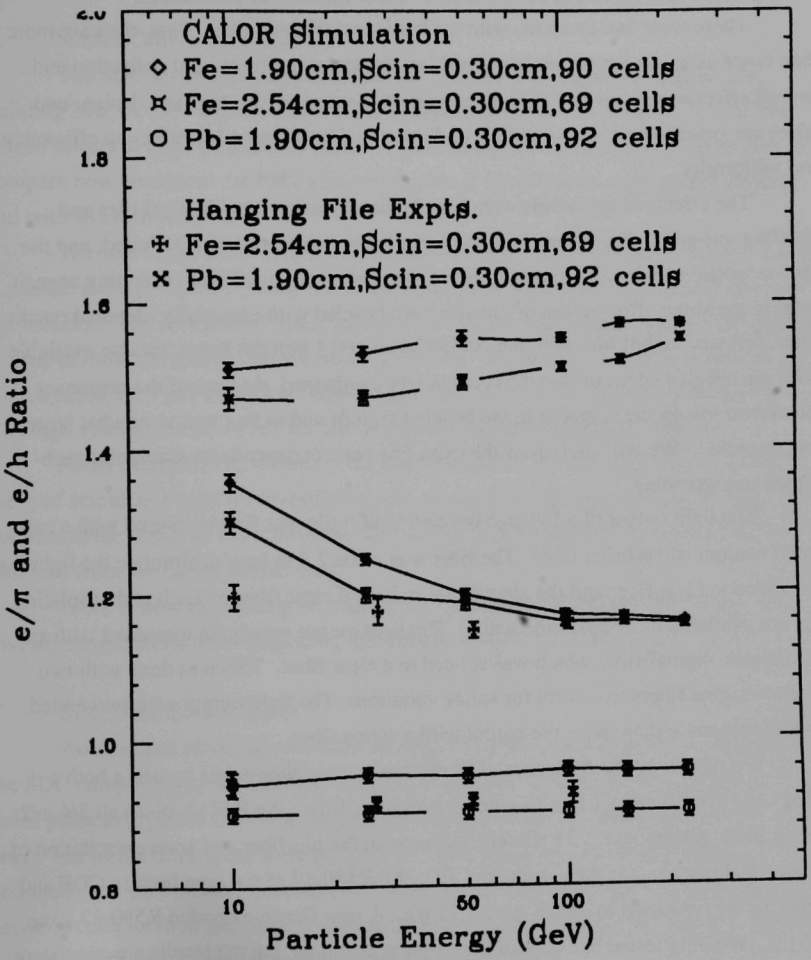

Fig. 43. e/π and e/h ratio for the three homogeneous hanging file configurations.

5. Optical System R&D

The main emphasis of the work in this period was the response of high η EM calorimeter tiles. There was also some study of light coupling from large tiles and a comparison of photocathode efficiencies of a few varieties of phototubes.

There were two concerns with the high η calorimeter tiles. First, they are more than twice as big as the previously tested low η tiles, so uniform light collection and overall effectiveness needed to be investigated. Second, in the Argonne design, two edges are beveled very sharply (28°), and this could also have a big effect on efficiency and uniformity.

The effects of the bevels were first studied by using two identical tiles and beveling one edge. No change in light output in the central region was found, and the edge response was roughly proportional to the amount of scintillator remaining at each point in the slope. Both edges of one tile were beveled with essentially identical results. Later, full size high η tiles with the correct bevel and 4 mm thickness became available. With the beveled edges of two tiles completely overlapped, the sum of the responses showed no loss in the response in the beveled regions and in fact was somewhat larger than expected. We will study how the extra few percent depends on machining techniques and wrapping.

The light output of a full size beveled high η tile was first measured with a two-ended readout waveshifter fiber. The fiber was made 2.3 m long to simulate the light loss of a splice to clear fiber and the attenuation in 2 m of clear fiber on each end. (Splicing was not available on a short time scale.) The light output was again measured with an aluminized "sigma" fiber which was spliced to a clear fiber. This was done with two different sigma fibers to control for splice variations. The light output with two-ended readout was more than twice the output with a sigma fiber.

We compared the responses of three Hamamatsu phototubes by using both a green LED system and a tile with green waveshifter fiber. An R1213, bi-alkali 3/4 inch tube of older design gave 1.31 photoelectrons with the tile-fiber and source excitation of the tile. Calibration was done with the LED. An R580-12 of the type used in CDF and similar to the type used in ZEUS gave 1.71 p.e. A new Green-extended R580-17 gave 2.06 p.e. We only tested one tube of each type at this time, but the results are consistent with a previous test of a Philips Green extended tube.

We did some tests of the efficiency and uniformity of light collection from large tiles. Such tests might be useful for Hadron Calorimeter tiles. Fibers with aluminized ends were placed along two edges of the tile. No glue was used. The aluminized mylar wrapping formed an approximately parabolic concentrator to transport the scintillator

light to the shifter fiber for a tile thickness of 2.5 mm and fiber diameter of 1 mm. Light output of 2 p.e. was obtained from a tile of Bicron bc408 about 25 cm square. The uniformity was approximately 5% , with effects of this magnitude clearly coming from imperfections in the tile as well as from the light collection and attenuation.

5. Source Calibration Studies

The SDC testbeam calorimeter is in the process of being source scanned in building 366. A Cs^{137} source driver from Purdue University is now set up to scan the fifteen towers at eight positions in depth. One of the goals of this set up is to be able to compare how consistent the PMT gain settings are if the HV is set with source current and with an electron beam.

The source system is driven with an IBM-PC based CAMAC system. The source is pushed through flexible plastic tubes, each connected to one of the 32 source tubes in the detector. The selection of tubes is done via software, and a gattling gun-type selector is used to route the source into the respective tower. As the source is drawn through the source tubes, the PMT current is recorded as a function of time for each of the towers. The high voltage can be varied via one of the ANL-designed CAMAC DACs.

As an example, Fig. 44 shows the PMT output for two separate runs of a test piece of scintillator used for investigating the effects of Pb casting tolerances. The mean currents in the center of the scintillator tiles will be compared with the mean pulse height obtained from the earlier FNAL tests.

Work is now proceeding on making the scan more automated, as well as investigating the effects of displacing the source from the scintillators.

C. SDC Data Systems R&D

An Argonne physicist continued as co-chair of the computing group. A workshop of the SDC computing group was held at SSCL in January. Among other planning actions, it made plans to organize the computing group into three task forces, with more to be added later. The initial three areas were (a) Core software definition, (b) Data modeling methods and tools, and (c) Software development tools. These task forces organized meetings between collaboration meetings, (many at times by video that allowed Japanese participation) and provided much of the focus at collaboration meetings.

The editing and much of the writing of the Computing chapter of the SDC TDR was focused at Argonne. The chapter described plans for computing that attempt to make use of developments in the computing industry and academia. Substantial computing power will provided by parallel farms, much as the SSCL has already started doing with

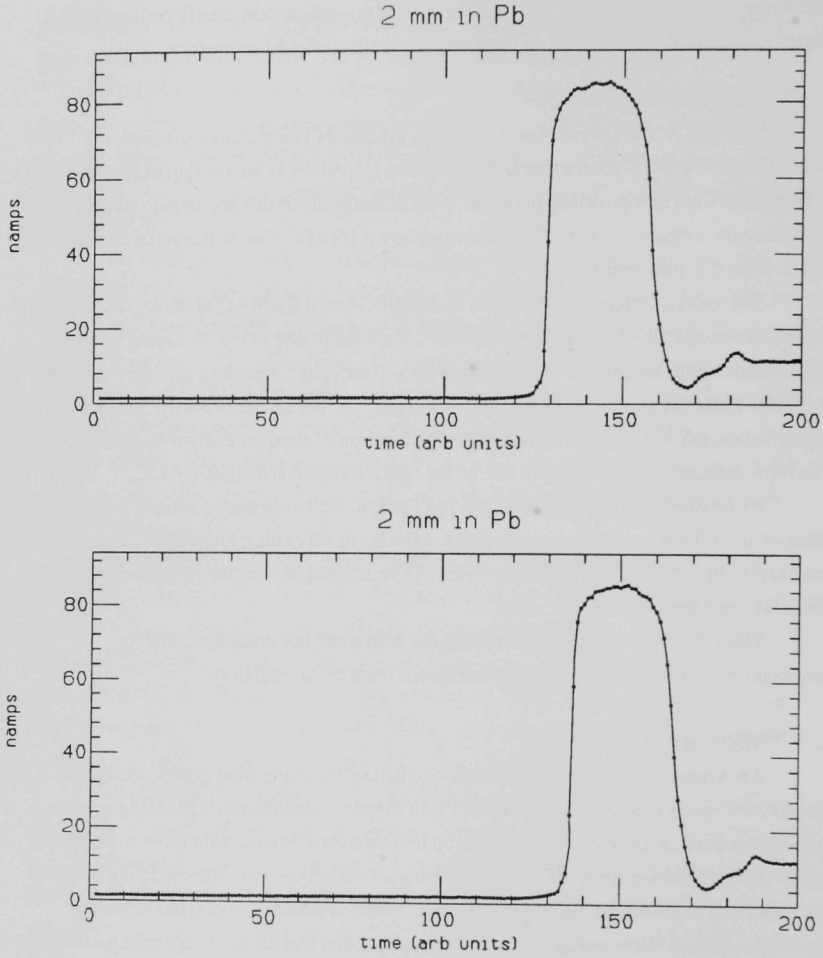

Fig. 44. Sample photomultiplier tube output for two separate runs of a test piece of scintillator used for investigating the effects of Pb casting tolerances..

their PDSF. Extensive use is planned of software design methodologies, data modeling, and graphical user interfaces.

The High Performance Computing and Communication (HPCC) initiative project led by Argonne was expanded to include LBL and SSCL, in addition to the original membership of Argonne, University of Illinois at Chicago, and University of Maryland, and was given a new name (PASS, for Petabyte Access and Storage Solutions). An updated proposal was approved as a five-year project in the DOE HPCC program.

Recent accomplishments of the PASS project include:

- Preliminary development of a scientific data model suitable for the database computing analysis of HEP data
- Implementation of the data model in Sybase and Object Store commercial database systems
- Preparation of a test bed of approximately 600 Mbyte of CDF psi data for performance analysis of the different prototype systems
- Completion of a psi analysis using a prototype database developed on top of Sybase, a commercial relational database
- Completion of a psi analysis using a prototype database developed on top of Object Store, a commercial object oriented database
- Preliminary results of the psi analysis using a proof of concept persistent event store developed by the project

As a result, we see the proof of concept phase as over and see results indicating that analyzing physics data using database computing is a competitive technology, with the ability to scale up to sizes required for next generation physics experiments.

The next steps for the project include first performance benchmarks on the existing data sets and database systems. Then work will begin on the "Mark I" system, which will combine our own code with commercial engines and aim to handle data set sizes up to 100 GB. This phase of the project will take the next 18 months. (L. Price)

VI. PUBLICATIONS

A. Journal Publications, Conference Proceedings, Books

Scalar Dilepton Production at TeV e^+e^- Colliders
T. Rizzo (ANL)
Phy. Rev. D45, 45 (1992)

Identifying the Origin of New Gauge Bosons at the Superconducting Super Collider
T. Rizzo (ANL) and J. Hewett (U. of Wisconsin)
Phy. Rev. D45, 161 (1992)

Lower Limit on Top-Quark Mass from Events with Two Leptons in $\bar{p}p$ Collisions at $\sqrt{s}$ = 1.8 TeV
L. Nodulman (ANL) & CDF Collaboration
Phys. Rev. Letters, 68, 447 (1992)

Determination of Pion Intranuclear Rescattering Rates in ν_μ-N_e Versus ν_μ-D Interactions for the Atmospheric ν Flux
M. Derrick (ANL)
Phys. Rev. D45, 743 (1992)

Inclusive Jet Cross Section in $\bar{p}p$ Collisions at $\sqrt{s}$ = 1.8 TeV
L. Nodulman (ANL) & CDF Collaboration
Phys. Rev. Letters, 68, 1104 (1992)

Topology of Three-Jet Events in $\bar{p}p$ Collisions at $\sqrt{s}$ = 1.8 TeV
L. Nodulman (ANL) & CDF Collaboration
Phys. Rev. D45, 1448 (1992)

Coincidences Between Extensive Air Showers and the Soudan 1 Underground Muon Detector
U. DasGupta, P. Border, K. Johns, N. Longley, M. Marshak, E. Peterson, K. Ruddick, and M. Shupe (U of Minnesota); D. Ayres, J. Dawson, T. Fields, M. Goodman, and E. May (ANL)
Phys. Rev. D45, 1459 (1992)

Semi-Inclusive Deeply Inelastic Scattering at Electron-Proton Colliders
R. Meng (ANL); F. Olness (U. of Oregon); D. Soper (CERN)
Nucl. Phys. B, 371, 79 (1992)

Search for New Gauge Bosons in $\bar{p}p$ Collisions at $\sqrt{s}$ = 1.8 TeV
L. Nodulman (ANL) & CDF Collaboration
Phys. Rev. Letters, 68, 1468 (1992)

Lepton Asymmetry in W-Boson Decays from $\bar{p}p$ Collisions at $\sqrt{s}$ = 1.8 TeV
L. Nodulman (ANL) & CDF Collaboration
Phys. Rev. Letters 68, 1458 (1992)

S-Matrix Bootstrap of a Scalar Higgs
D. Sivers and J. Uretsky (ANL/HEP)
Phys. Rev. Letters 68, 1649 (1992)

Properties of Events With Large Total Transverse Energy Produced in Proton-Antiproton Collisions at $\sqrt{s}$ = 1.8 TeV
L. Nodulman (ANL) & CDF Collaboration
Phy. Rev. D45, No. 7 p. 2249, (1 April 1992)

Leading Radiative Corrections in Two Scalar Doublet Models
C.D. Froggatt , R.G. Moorhouse (U. of Glasgow); and I.G. Knowles (ANL)
Phys. Rev. D45 p. 2471, (1 April 1992)

Measurement of the Isolated Prompt Photon Cross Section in $\bar{p}p$ Collisions at $\sqrt{s}$ = 1.8 TeV
L. Nodulman (ANL) & CDF Collaboration
Phys. Rev. Letters, V68, p. 2734, (4 May 1992)

Limit On The Top-Quark Mass From Proton-Antiproton Collisions at $\sqrt{s}$ = 1.8 Tev
L. Nodulman (ANL) & CDF Collaboration
Physical Review D45, 3921 (1992)

Desert Grand Unified Theories and New Light Degrees of Freedom
T. Rizzo
Phys. Rev. D45, 3903 (1992)

Study of Inclusive Λ Production in e^+e^- Annihilations at 29 GeV
S. Abachi, M. Derrick, P. Kooijman, B. Musgrave, L. Price, J. Repond, K. Sugano (ANL); T. Geld, H. Neal, C. Akerlof, J. Chapman, D. Errede, M. Ken, P. Kesten, D. Meyer, D. Nitz, R. Thun, R. Tschirhart (U. of Michigan); D. Blockus, B. Brabson, J Brom, C. Jung, H. Ogren, D. Rust, A. Snyder (Indiana U.); B. Cork (Lawrence Berkeley Lab); P. Baringer, B. Bylsma, R. Debonte, E. Low, R. McIlwain, D. Miller, C. Ng, K. Rangan, and E. Shibata (Purdue U.)
Phys. Rev. D45, 3949 (1992)

Measurement of the Ratio B ($W \rightarrow \tau\nu$)/B ($W \rightarrow e\nu$) in $\bar{p}p$ Collisions at $\sqrt{s}$ = 1.8 TeV
L. Nodulman (ANL) & CDF Collaboration
Phys. Rev. Letters 68, 3398 (1992)

Measurement of B-meson and b-quark Cross Sections at $\sqrt{s}$ = 1.8 TeV Using the Exclusive Decay $B^{\pm} \rightarrow J/\psi K^{\pm}$
L. Nodulman (ANL) & CDF Collaboration
Phys. Rev. Letters 68, 3403 (1992)

Altering the Symmetry of Wavefunctions in Quantum Algebras and Supersymmetry
C. Zachos
Mod. Phys. Lett. A7, 1595 (1992)

Design Considerations for a Scintillating Plate Calorimeter
P.K. Job, L.E. Price, J. Proudfoot, T. Handler, and T.A. Gabriel
Nucl. Instr. and Meth. A316, 174 (1992)

B. Papers Submitted for Publication and ANL Reports

Two Scalar Doublet Models with Softly Broken Symmetries
I. Knowles (ANL), C. Froggatt, R. Moorhouse (U. of Glasgow)
ANL-HEP-92-01
Submitted to Nucl. Phys. B

Indirect Dilepton Signatures in TeV e^+e^- and e^-e^- Collisions
T. Rizzo (ANL)
ANL-HEP-PR-92-02
Submitted to Phys. Rev. D

^2H (p,n)2p Spin Transfer from 305 to 788 MeV
H. Spinka (ANL), M. McNaughton, I. Supek (Los Alamos), K. McNaughton, K, Johnston, P. Riley, D. Ambrose, P. Coffey (U. of Texas), G. Glass, J. Hiebert, L. Northcliffe, A. Simon (Texas A&M U.), D. Mercer (U. of Colorado), D. Adams (Rice U.), R. Jeppesen (U. of Montana), G. Tripard (Washington State U.), H. Woolverton (U. of Central Arkansas)
ANL-HEP-CP-92-08
Submitted to Phys. Rev. Letters

Heavy Quark Cross Sections at Hadron Collider Energies
E. Berger and R. Meng (ANL)
ANL-HEP-PR-92-11
Submitted to Phys. Rev. D

Phenomenology of R-Parity Breaking in E_6 Models
T. Rizzo (ANL)
ANL-HEP-PR-92-26
Submitted to Phys. Rev. D

Contributions to the W-Boson Anomalous Moments in the Two-Higgs-Doublet Model at Collider Energies
T. Rizzo
ANL-HEP-PR-92-27
Submitted to Phys. Rev. D

Signals for Virtual Leptoquark Exchange at HERA
M. Doncheski, J. Hewett (ANL)
ANL-HEP-PR-92-28
Submitted to Zeit. fur Phys.

Rigorous QCD Predictions for Decays of P-Wave Quarkonia
G. Bodwin (ANL), E. Bratten (Northwestern U.), G. Lepage (Cornell)
ANL-HEP-PR-92-30
Submitted to Phys. Rev. Letters

Implications of Bottom Quark Cross Section Data at Hadron Collider Energies
E. Berger, R. Meng (ANL), W.-K. Tung (IIT)
ANL-HEP-PR-92-32
Submitted to Phys. Rev. D

Probing New Gauge Boson Couplings via Three-Body Decays
J. Hewett and T. Rizzo (ANL)
ANL-HEP-PR-92-33
Submitted to Nuclear Physics B

New Probes for Extended Gauge Structures at HERA
T. Rizzo (ANL)
ANL-HEP-PR-92-37
Submitted to Phys. Rev. D

Light Quarks and Small X Physics
A. White (ANL)
ANL-HEP-PR-92-40
Submitted to Nuclear Physics B

Neutron-Proton Elastic Scattering Spin-Spin Correlation Parameter Measurements Between 500 and 800 MeV: II. C_{SS} and C_{LS} at Forward c.m. Angles
T. Shima, D. Hill, K. Johnson, H. Shimizu, H. Spinka, R. Stanek, D. Underwood, and A. Yokosawa (ANL); G. Burleson, J. Faucett, R. Garnett, M. Rawoll-Sullivan (New Mexico State U.); G. Glass, J. Hiebert, R. Kenefick, S. Nath, L. Northcliff, (Texas A&M U.); R. Damjanovich, J. Jarmer, (Los Alamos); R. Jeppesen (U. of Montana); G. Tripard (Washington State U.)
ANL-HEP-PR-92-45
Submitted to Phys. Rev. D.

C. Papers or Abstracts Contributed to Conferences

Experimental Results with the Fermilab Polarized Beams
A. Yokosawa (ANL)
ANL-HEP-CP-92-29
Submitted to Proceedings of Adriatico Research Conference on Polarization Dynamics in Nuclear and Particle Physics, Trieste, Italy January 1992

Mechanical Design and Finite Element Analysis of the SDC Central Calorimeter
V. Guarino, N. Hill, J. Nasiatka (ANL); D. Hoecker, T. Hordubay,
D. Scherbarth, R. Swensrud (Westinghouse Electric Corp.)
ANL-HEP-CP-92-13
Submitted to Proceedings of 4th Annual International Industrial Symposium on the Super Collider, New Orleans, Louisiana March 1992

Search for AGN υ's with the Soudan 2 Detector
I. Ambats, D. Ayres, L. Balka, W. Barrett, T. Brock, W. Dawson, T. Fields, M. Goodman, N. Hill, J. Hoftiezer, D. Jankowski, F. Lopez, E. May, L. Price, J. Schlereth, J. Thron, H. Trost (ANL); P. Border, H. Courant, D. Demuth, R. Gray, K. Johns, S. Kasahara, N. Longley, M. Lowe, M. Marshak, D. Maxam, W. Miller, C. Minor, E. Peterson, D. Roback, D. Rosen, K. Ruddick, J. Schmid, M. Shupe, G. Villaume, J. Werkema (U. of MN); W. Allison, G. Barr, C. Brooks, J. Cobb, R. Giles, G. Giller, D. Perkins, P. Shield, M. Thomson, L. Tupper, N. West (U. of Oxford); G. Alner, D. Cockerill, V. Edwards, C. Garcia-Garcia, P. Litchfield, G. Pearce, C. Woods (Rutherford Appleton Lab); D. Benjamin, B. Ewen, T. Kafka, J. Kochocki, W. Leeson, W. Mann, L. McMaster, R. Milburn, A. Napier, W. Oliver, B. Saitta, J. Schneps, N. Sundaralingam (Tufts U.)
ANL-HEP-CP-92-39
Submitted toProceedings of the Workshop on High Energy Neutrino Astrophysics,. Honolulu, Hawaii March 1992

Conference Summary
J. Proudfoot
ANL-HEP-CP-92-46
Submitted to Proceedings of the International Conference on Radiation Tolerant Scintillator and Detectors, Tallahassee, Florida, April 1992

Probing New Gauge Boson Couplings at Hadron Supercolliders
T. Rizzo
ANL-HEP-CP-92-47
Submitted to Proceedings of the Physics Beyond the Standard Model III Conference, Ottawa, Canada, June 1992

D. Technical Notes

On the Scattering of Atmospheric Muons in the Rock Above Soudan 2
Hans-Jochen Trost (ANL)
ANL-HEP-TR-92-05, PDK 500

On the "Massless Gap" Adjustment of Detected Energy for Passive Material in Front of a Calorimeter
Hans-Jochen Trost (ANL)
ANL-HEP-TR-92-06, SDC-92-187

Finite Element Analysis of the SDC Barrel and Endcap Calorimeter
N. Hill (ANL)
ANL-HEP-TR-92-20

Simulation of Hanging File Experiments with CALOR89
P. Job, L. Price, J. Proudfoot (ANL); T. Handler (U. of Tennessee); T. Gabriel (Oak Ridge)
ANL-HEP-TR-92-22

High Energy Physics Division Semiannual Report of Research Activities; July 1-December 31, 1991
P. Schoessow, P. Moonier, R. Talaga, R. Wagner (ANL)
ANL-HEP-TR-93-24

Unix Version of CALOR89 for Calorimeter Applications
P. Job, L. Price (ANL)
ANL-HEP-TR-92-38

AGN-18 A Liquid Dielectric Option for a Dielectric Cavity
J. Simpson (ANL)

AGN-19 Tunnel Safety Interlock System
M. Rosing (ANL)

CDF-1688 A Search for Fourth Generation B' Quarks via Flavor Changing Neutral C
P. Maas

CDF-1689 A Search for Fourth Generation Quarks via FCNC Decays
P. Maas

CDF-1691 A Handy Guide to YMON (Updated)
L. Nodulman

CDF-1711 Monitoring SVX with YMON
L. Nodulman, J. Skarha

CDF-1717 The Chi_C Cross Section
R. Snider, R. Blair, A. Yagil

CDF-1731 Calorimetry Compression for Pads
K. Byrum, T. Rodrigo, A. Mukherjee

CDF-1770 The Cross Section for Production of Two Isolated Prompt Photons
M. Takano, R. Harris, S. Miyashita, R. Blair, S. Kuhlmann

CDF-1771 A Preconverter for the CDF Plug Upgrade
S. Kuhlmann

PDK-512 Quarterly Activity Report January - March 1992
D. Ayres (ANL)

PDK-518 Decisions of the Oxford Collaboration Meeting, May 19-22, 1992
D. Ayres (ANL)

PDK-519 Filter Scan Rules
M. Goodman, D. Roback (ANL); P. Litchfield (Rutherford Appleton Lab)

PDK-520 Summary of the Experimental Plant Facilities and Cavity Parameters for the Soudan Underground Physics Laboratory in Soudan, MN
D. Jankowski (ANL)

PDK-522 A Search for Magnetic Monopoles with the Soudan 2 Detector
J. Thron (ANL) and the Soudan 2 Collaboration

SDC-92-187 On the "Massless Gap" Adjustment of Detected Energy for Passive Material in Front of a Calorimeter
H.-J. Trost

SDC-92-919 Erratum/Addendum to: On the "Massless Gap" Adjustment of Detected Energy for Passive Material in Front of a Calorimeter
H.-J. Trost

SDC-92-222 Finite Element Analysis of the SDC Barrel and Endcap Calorimeters
V. Guarino, N. Hill, J. Nasiatka

WF-164 Feasibility of a Dielectric Loaded rf Gun Cavity
J. Simpson (ANL)

WF-165 Causality and Space Charge
J. Norem (ANL)

WF-166 High Power Tests of the Gun Cavity
C. Ho, E. Chojnacki, R. Konecny, and J. Power (ANL)

WF-167 Comment on the CLIC Note "Beam Loading of RF-Gun by Dark Current"
C. Ho (ANL)

VII. COLLOQUIA AND CONFERENCE TALKS

E. Berger

"Bottom Quark Production at Collider Energies"
SSC Laboratory (January 1992)

"Implications of Bottom Quark Cross Section Data at Collider Energies"
Fermilab (April 1992)

"Bottom Quark Cross Sections at SSC Fixed Target and Collider Energies"
SSC Laboratory (June 1992)

"Heavy Quark Production in Proton-Antiproton Collisions"
Aachen Conference (June 1992)

"Constraints on the Gluon Density from Heavy Quark Production"
Aachen Conference (June 1992)

T. Fields

"The Soudan Proton Decay Experiment"
ANL Physics Colloquium (May 1992)

M. Goodman

"Prospects for Long Baseline Neutrino Oscillations"
U. of Maryland (February 1992)

"Neutrino Astronomy with Soudan 2"
High Energy Neutrino Astronomy Workshop, Honolulu, Hawaii (March 1992)

"Neutrinos from Active Galactic Nuclei"
Fermilab (June 1992)

J. Hewett

"The Search for Top: A Status Report"
IIT (February 1992)

"The Physics Potential of the SSC"
U. of Iowa (March 1992)

"Probing the Flavor Changing Vertex of Heavy Quarks"
U. of Wisconsin (April 1992)

"Discovering and Identifying New Gauge Bosons at the SSC"
Purdue Univ. (April 1992)

"Discovering and Identifying New Gauge Bosons at the SSC"
Michigan State Univ. (May 1992)

"Signals for New Physics at HERA"
Carleton Univ. Ottawa, Canada (June 1992)

"Topics in Top Physics"
Northwestern Univ. (June 1992)

S. Kim

"Hadron Spectrum of Quenched QCD on the Touchstone Delta"
Caltech (February 1992)

T. Kirk

"The Supercollider and Argonne's Role in It"
NALCO Corporation (February 1992)

I. Knowles

"Properties of Two Scalar Doublet Models"
Purdue Univ. (March 1992)

"Leading Radiative Corrections in Two Scalar Doublet Models"
SSC Workshop, Madison, WI (April 1992)

"A History of Pythia Ancient and Modern"
Fermilab (April 1992)

"Radiative Corrections in Two Scalar Doublet Models"
Northwestern Univ. (May 1992)

S. Kuhlmann

"Hadron Collider Physics"
Aachen, Germany (June 1992)

E. May

"The PASS Project: Petabyte Databases for HEP"
Conference on High Speed Computing, Salisban, OR (May 1992)

R. Meng

"Order α_s^3 QCD Heavy Quark Cross Sections at Collider Energies"
U. of Illinois at Chicago (March 1992)

"Implications of Bottom Quark Cross Section Data at Collider Energies"
SSC Physics Symposium, Madison, WI (April 1992)

"Gluon Distribution functions at Relative Small X"
U. of Wisconsin (May 1992)

J. Proudfoot

"Conference Summary, Raddan '92"
International Conference on Radiation Tolerant Scintillators & Detectors,
Florida State Univ. (April 1992)

T. Rizzo

"Finding and Identifying the Origin of New Gauge Bosons at the SSC and LHC"
U. of Wisconsin, (April 1992)

"Finding and Identifying the Origin of New Gauge Bosons at Hadron Supercolliders"
U. of Hawaii (May 1992)
Northwestern Univ. (May 1992)

"Probing the Couplings of New Gauge Bosons at Hadron Supercolliders"
Carleton Univ. Ottawa, Canada (June 1992)

"Probing New Gauge Boson Couplings via Rare Decays at Hadron supercolliders"
SSC Physics Symposium, Madison, WI (April 1992)

D. Underwood

"Observation of Polarization Effects at 200 GeV"
Fermilab (May 1992)

S. Vokos

"Resolving the Unitary Gauge Puzzle in Thermal Phase Transitions"
U. of Oregon at Eugene (January 1992)

Instability of Hot Electroweak Theory: Bounds on M_{top} and M_{Higgs}
SLAC (January 1992)
CERN (January 1992)
Max Planck Inst. (January 1992)
Erole Normale, Paris (January 1992)
U. of Athens (January 1992)

R. Wagner

"The Tile/Fiber Prototype for the SDC Central E-M Calorimeter"
3rd Int. Conf. on Advanced Technology and Particle Physics, Como, Italy (June 1992)

A. White

"Light Quarks and Small n Physics"
Teupitz, Germany (April 1992)

"Massive Photon Pairs as a Signal for New Physics"
Fermilab (May 1992)

"Color Sextet Quarks and New High Energy Interactions"
U. of Michigan (June 1992)

A. B. Wicklund

"b Physics at Hadron Colliders"
La Thiuile (March 1992)
U. of Chicago (April 1992)

A. Yokosawa

"The Fermilab Polarized Beam: Results and Plans"
Trieste, Italy (January 1992)

C. Zachos

"Quantum Algebras, q-Planes, and Q-Oscillators"
Purdue Univ. (January 1992)

"Symmetry of Wavefunctions in Quantum Algebras and Graded Systems"
XXI International DGMTP Conference, Tianjin, China (June 1992)

"Altered Perturbation Symmetries in Quantum Algebras and Supersymmetry"
Academia Sinica, Institute of Theoretical Physics, Beijing, China (June 1992)

"Overview of Particle Physics"
Student Research Participation Seminar, ANL (February 1992)

VIII. HIGH ENERGY PHYSICS COMMUNITY ACTIVITIES

D. Ayres
Co-convenor of Parallel Session on Non-Accelerator Physics, 1992 DPF Meeting (at FNAL)

E. Berger

Editor, Research Directions for the Decade, Proceedings of the 1990 DPF Summer Study on High Energy Physics, Snowmass, Colorado, June 15-July 13, 1990.

Member, High Energy Physics Advisory Panel (HEPAP), 1991 -

Member, Committee on Meetings, American Physical Society, 1991 -

Consultant, Department of Energy Review of the High Energy Physics Program at Brookhaven National Laboratory, April 1992

Session Organizer, Particle Physics in the '90's, 1992 Gordon Research Conference, July 13-17, 1992, Andover, N.H.

Member, U.S. Contact Person, Scientific Program Committee, XXVIII Recontre de Moriond, "QCD and High Energy Hadronic Interactions", Les Arcs, France, March 1992

International Advisory Committee, 7th Meeting of the Division of Particles and Fields of the American Physical Society, Fermilab, November 1992

Local Organizing Committee, 7th Meeting of the Division of Particles and Fields of the American Physical Society, Fermilab, November 1992

Organizing Committee, Fifth Conference on the Intersections between Particle and Nuclear Physics, May 1994

T. Fields

Fermilab DOE Review Consultant Member,
URA Visiting Committee, Fermilab

J. Hewett

Parallel Session Organizer, Beyond the Standard Model III Conference, Carleton University, Ottawa, ON, Canada, June 1992

E. May

Chairman, HEPNET Technical Coordinating Committee

L. Nodulman

IEEE NSS Program Committee, Orlando, Florida 1992

L. Price

Member, International Advisory Committee on Detector R&D for the SSC

Member, ESNET Steering Committee

Secretary, Users Organization for the SSC

Member, SDC Executive Board

Chairman, Program Committee, IEEE Mass Storage Symposium

Member, International Advisory Committee, International Conference on Monte-Carlo Simulation in High Energy and Nuclear Physics

A. White

Co-Chairman, Organizing Committee Workshop on Small-n and Diffractive Physics at the Tevatron, Fermilab, September 16-18, 1992

A. B. Wicklund

DPF '92 Local Organizing Committee

A. Yokosawa

RSC (RHIC Spin Collaboration) Workshop at Argonne, February 10, 1992

C. Zachos

HEP Division Seminar Organization

IX. HIGH ENERGY PHYSICS RESEARCH PERSONNEL

Administration

L. Price/T. Kirk
P. Moonier

Accelerator Physicists

W. Gai
J. Norem
M. Rosing
P. Schoessow
J. Simpson

Experimental Physicists

D. Ayres
R. Blair
M. Derrick
T. Fields
M. Goodman
D. Grosnick
R. Hagstrom
P. Job
S. Kuhlmann
D. Lopiano
S. Magill
E. May
B. Musgrave
L. Nodulman
Y. Ohashi
J. Proudfoot
J. Repond
H. Spinka
R. Stanek
K. Sugano
R. Talaga
J. Thron
D. Underwood
R. Wagner
A. B. Wicklund
A. Yokosawa

Theoretical Physicists

E. Berger
G. Bodwin
J. Hewett
S. Y. Kim
I. Knowles
R. Meng
T. Rizzo
D. Sinclair
S. Vokos
A. White
C. Zachos

Engineers, Computer Scientists and Applied Scientists

E. Chojnacki
J. Dawson
T. Ekenberg
V. Guarino
D. Hill
N. Hill
J. Nasiatka
R. Noland
H. Rhude
J. Schlereth

Technical Support Staff

I. Ambats
L. Balka
H. Blair
W. Haberichter
D. Jankowski
T. Kasprzyk
R. Konecny
R. Laird
R. Rezmer
J Sheppard

Laboratory Graduate Participants

C. Ho
J. Power
D. Roback

ARGONNE NATIONAL LAB WEST
3 4444 00016888 0